## INFORMATION TO USERS

This reproduction was made from a copy of a document sent to us for microfilming. While the most advanced technology has been used to photograph and reproduce this document, the quality of the reproduction is heavily dependent upon the quality of the material submitted.

The following explanation of techniques is provided to help clarify markings or notations which may appear on this reproduction.

1. The sign or "target" for pages apparently lacking from the document photographed is "Missing Page(s)". If it was possible to obtain the missing page(s) or section, they are spliced into the film along with adjacent pages. This may have necessitated cutting through an image and duplicating adjacent pages to assure complete continuity.

2. When an image on the film is obliterated with a round black mark, it is an indication of either blurred copy because of movement during exposure, duplicate copy, or copyrighted materials that should not have been filmed. For blurred pages, a good image of the page can be found in the adjacent frame. If copyrighted materials were deleted, a target note will appear listing the pages in the adjacent frame.

3. When a map, drawing or chart, etc., is part of the material being photographed, a definite method of "sectioning" the material has been followed. It is customary to begin filming at the upper left hand corner of a large sheet and to continue from left to right in equal sections with small overlaps. If necessary, sectioning is continued again—beginning below the first row and continuing on until complete.

4. For illustrations that cannot be satisfactorily reproduced by xerographic means, photographic prints can be purchased at additional cost and inserted into your xerographic copy. These prints are available upon request from the Dissertations Customer Services Department.

5. Some pages in any document may have indistinct print. In all cases the best available copy has been filmed.

University Microfilms International
300 N. Zeeb Road
Ann Arbor, MI 48106

**Jin, Myoung Gyou**

POST-BUCKLING BEHAVIOR OF ELASTIC FRAME STRUCTURES

*The University of Arizona* PH.D. 1983

PLEASE NOTE:

In all cases this material has been filmed in the best possible way from the available copy. Problems encountered with this document have been identified here with a check mark __✓__.

1. Glossy photographs or pages _____
2. Colored illustrations, paper or print _____
3. Photographs with dark background _____
4. Illustrations are poor copy _____
5. Pages with black marks, not original copy _____
6. Print shows through as there is text on both sides of page _____
7. Indistinct, broken or small print on several pages __✓__
8. Print exceeds margin requirements _____
9. Tightly bound copy with print lost in spine _____
10. Computer printout pages with indistinct print _____
11. Page(s) _____ lacking when material received, and not available from school or author.
12. Page(s) _____ seem to be missing in numbering only as text follows.
13. Two pages numbered _____. Text follows.
14. Curling and wrinkled pages _____
15. Other _____

# POST-BUCKLING BEHAVIOR OF ELASTIC FRAME STRUCTURES

by

Myoung Gyou Jin

---

A Dissertation Submitted to the Faculty of the

DEPARTMENT OF CIVIL ENGINEERING AND ENGINEERING MECHANICS

In Partial Fulfillment of the Requirements
for the Degree of

DOCTOR OF PHILOSOPHY
WITH A MAJOR IN CIVIL ENGINEERING

In the Graduate College

THE UNIVERSITY OF ARIZONA

1 9 8 3

THE UNIVERSITY OF ARIZONA
GRADUATE COLLEGE

As members of the Final Examination Committee, we certify that we have read the dissertation prepared by Myoung Gyou Jin

entitled Post-buckling Behavior of Elastic Frame Structures

and recommend that it be accepted as fulfilling the dissertation requirement for the Degree of Doctor of Philosophy, Civil Engineering.

| | |
|---|---|
| Ralph M. Richard | 19 Dec 83 |
| | Date |
| William G. Faris | Dec 14, 1983 |
| | Date |
| [signature] | Dec 14, '83 |
| | Date |
| Donald G. DeDoppo | Dec 14, 1983 |
| | Date |
| H. A. Kamel | Dec. 14, 1983 |
| | Date |

Final approval and acceptance of this dissertation is contingent upon the candidate's submission of the final copy of the dissertation to the Graduate College.

I hereby certify that I have read this dissertation prepared under my direction and recommend that it be accepted as fulfilling the dissertation requirement.

| | |
|---|---|
| Donald G. DeDoppo | Dec 14, 1983 |
| Dissertation Director | Date |

STATEMENT BY AUTHOR

This dissertation has been submitted in partial fulfillment of requirements for an advanced degree at The University of Arizona and is deposited in the University Library to be made available to borrowers under rules of the Library.

Brief quotations from this dissertation are allowable without special permission, provided that accurate acknowledgment of source is made. Requests for permission for extended quotation from or reproduction of this manuscript in whole or in part may be granted by the head of the major department or the Dean of the Graduate College when in his judgment the proposed use of the material is in the interests of scholarship. In all other instances, however, permission must be obtained from the author.

SIGNED: Myoung Gyon Jin

TO MY MOTHER

ACKNOWLEDGEMENTS

I wish to express my gratitude and appreciation to Dr. Hussein A. Kamel and Dr. Donald A. DaDeppo for their direction, encouragement, and time contributed to this research and for their guidance and provision of financial support throughout the course of my study at the University of Arizona.

I would like to extend my gratitude to my colleagues Mr. Sungmin Kim, Ms. Nesrin Sarigül and Mr. Ramesh Kolar for their contribution to this research.

This research has been supported by the Office of Naval Research under contract N0001475C0837 and the College of Engineering. The author gratefully acknowledges the support.

Last but not least, sincere thanks are due to my wife, Myoung-Hee, daughter Jee-Hyun, and son Jhong-In for their fullest support and patience without which this effort could not have been achieved.

TABLE OF CONTENTS

LIST OF ILLUSTRATIONS

LIST OF ILLUSTRATIONS--continued

LIST OF TABLES

ABSTRACT

This study intends to develop a useful tool for the investigation of the behavior of three-dimensional elastic frame structures undergoing large deformations and large rotations, using a mini-computer with an attached array processor. An updated Lagrangian finite element formulation is established by employing conventional two node-twelve degree of freedom beam elements. In order to trace the pre- and post-buckling equilibrium path, an improved nonlinear solution procedure is proposed. The software is designed to make it possible to solve large-scale problems on a mini-computer by adopting a hypermatrix scheme and the segmentation into a number of processors which are independent programs. The software is simulated to estimate the performance of the software on a combined mini-computer/array processor system. By using the simulator time measurements are performed for three different cases of large-scale three-dimensional frame structure models, which verify the usefulness of the array processor in the solution of nonlinear finite element structural problems. With the use of the hypermatrix scheme, an alternative solution algorithm for system of linear equations is proposed. The accuracy of the finite element formulation and the effectiveness of the solution algorithms implemented are demonstrated by carefully selected two- and three-dimensional frame examples. Finally, directions for further research are discussed.

NOMENCLATURE

| | |
|---|---|
| $t_0, t_1, t_2, t, t+\Delta t$ | Discrete time points |
| $\delta u_k$ | Variation of incremental displacement components at time $t + \Delta t$ |
| ${}^t u_k$ , ${}^t F_k$ , ${}^t T_k$ | Displacement, body force, and surface traction components at time t |
| ${}^t A$ , ${}^t V$, ${}^t \rho$ | Area, volume, and mass density at time t |
| $x_1, x_2, x_3$ | Cartesian global coordinate axes |
| ${}_t x_1$ , ${}_t x_2$, ${}_t x_3$ | Convected Cartesian beam element coordinate axes at time t |
| $u_i$ | Incremental displacements at time $t + \Delta t$ |
| ${}^t x_1$, ${}^t x_2$, ${}^t x_3$ | Cartesian coordinates at time t referred to global coordinate axes |
| ${}^t_{t_0} x_1$, ${}^t_{t_0} x_2$, ${}^t_{t_0} x_3$ | Cartesian coordinates at time t referred to beam element coordinate axes at time $t_0$ |
| $\delta W_i$ , $\delta W_e$ | Internal and external virtual works |
| ${}^t \tau_{ij}$ , ${}^t e_{ij}$ | Cartesian components of Cauchy stress tensor and Cauchy's infinitesimal strain tensor at time t |
| ${}^{t+\Delta t}_{\ t} S_{ij}$ , ${}^{t+\Delta t}_{\ t} \varepsilon_{ij}$ | Cartesian components of 2nd Piola-kirchhoff stress tensor and Green strain tensor at time $t + \Delta t$ but referred to the configuration at time t. |
| ${}_t S_{ij}$ , ${}_t \varepsilon_{ij}$ | Cartesian components of incremental 2nd Piola-Kirchhoff stress tensor and Green strain tensor at time $t + \Delta t$ but referred to the configuration at time t. |
| ${}_t e_{ij}$ , ${}_t \eta_{ij}$ | Linear and nonlinear parts of ${}_t \varepsilon_{ij}$ |
| ${}_t C_{ijrs}$ | Constitutive tensor |

| | |
|---|---|
| ${}^{t}_{t+\Delta t}X_{i,k}$ | $= \partial\, {}^{t}X_i / \partial\, {}^{t+\Delta t}X_k$ |
| ${}^{t+\Delta t}_{t}U_{i,j}$ | $= \partial\, {}^{t+\Delta t}U_i / \partial\, {}^{t}X_j$ |
| $p, q, r\ (=\bar{X}_1, \bar{X}_2, \bar{X}_3)$ | Local beam element coordinate axes |
| $\bar{u}_k$ | Components of local nodal point displacement increments |
| $H, D, L$ | Width, depth, and length of beam element |
| $\bar{u}_i$ | Local incremental displacement field |
| $N_k^i$ | Interpolation functions corresponding to the local axes $\bar{x}_i$ at time t |
| $\bar{u}_{i,j}$ , $N^i_{k,j}$ | $= \partial \bar{u}_i / \partial \bar{x}_j$ and $\partial N_k^i / \partial x_j$ |
| $\bar{\varepsilon}_{ij}$ | Local incremental strain tensor |
| $\bar{e}_{ij}$ , $\bar{\eta}_{ij}$ | Linear and nonlinear parts of $\varepsilon_{ij}$ |
| $\bar{\sigma}_p\ (=\bar{\tau}_{11})$ | Local axial stress |
| $\tau_{pq}\ (=\tau_{12})$, $\bar{\tau}_{pr}\ (=\bar{\tau}_{13})$ | Local shear stresses |
| $E, G, \nu$ | Young's modulus, shear modulus, and Poisson's ratio |
| $\{\bar{e}\}$, $\{\bar{\eta}\}$ | Element linear and nonlinear strain vectors |
| $\{\bar{u}\}$ | Element incremental nodal point displacement vector |
| $\{\bar{\tau}\}$ | Element Cauchy stress vector |
| $\{\bar{R}\}, \{\bar{F}\}, \{\Delta\bar{R}\}$ | Element nodal load, internal force, and residual force vectors |

| | |
|---|---|
| $\{R\}, \{S\}, \{\Delta R\}$ | Global nodal load, internal force, and residual force vectors |
| $\{u\} (= \{\Delta D\})$ | Global incremental displacement vector |
| $[B_L], [B_N]$ | Linear and nonlinear strain-displacement transformation matrices |
| $[\bar{\tau}]$ | Element Cauchy stress matrix |
| $[\bar{C}]$ | Incremental stress-strain material property matrix |
| $[\bar{K}]$ | Element incremental stiffness matrix |
| $[\bar{K}_L], [\bar{K}_N]$ | Linear and nonlinear parts of $[\bar{K}]$ |
| $[{}^{\circ}\underset{\sim}{T}], [\bar{\underset{\sim}{T}}], [\underset{\sim}{T}]$ | Global to initial, initial to current, and global to current beam element coordinate transformation matrices |
| $[T]$ | Transformation matrix relating displacements measured in global coordinate system to those measured in current beam element coordinate system |
| $[K]$ | Global incremental stiffness matrix |
| $[T], [\bar{T}]$ | Upper triangular hypermatrices |
| $[D], [\bar{D}]$ | Diagonal hypermatrices |
| $\{D\}$ | Displacement vector |

| | |
|---|---|
| $\lambda$ | Load factor |
| ${}^{m}l$ | Generalized "arc-length" at increment step m |
| $\vec{t}_i$ | Tangent vector |
| s | Scale factor for displacement vector |
| w | Balance factor for modified constant-arc-length method |
| ${}^{m}l_s$ | Scaled "arc-length" at increment step m |

# CHAPTER 1

## INTRODUCTION

Over the last two decades the rapid advances in computer technology and a better understanding of the physical principles involved have resulted in significant improvements in the development and application of theory in solving difficult structural problems involving complicated geometry, large deflections and inelastic material behavior. In spite of these improvements, and because of the complex nature of nonlinear structural analysis, it is still desirable to develop more efficient formulations and solution procedures in order to reduce computational cost and to analyze more complicated structural models in a more complex environment.

The persisting architectural need to cover larger spans without intermediate supports and the development and use of more economical structural materials have made the buckling problem of spatial structure more important. Even though it is not allowed in practical structural design to have a design load larger than the buckling load, the tracing of the postbuckling behavior provides useful insights and helps to locate buckling modes and to predict the response of the structure under unexpectedly large accidental loads. This study is concerned with the postbuckling analysis of elastic space frames under static loading.

In the past many researchers have engaged in the nonlinear analysis of frame structures. In surveying the literature, it is noted that the methods which have been adopted in deriving the governing nonlinear equations are either based on the finite element concept (40, 46, 47, 48, 50, 51, 52, 53, 60, 64) or on the use of the so-called beam-column approach, or direct consideration of forces (49, 54, 55, 65, 66, 68). Recently the rapidly increasing advances in finite element research have made the method the most powerful tool in developing general purpose nonlinear structural analysis programs (56). Most finite element techniques for postbuckling analysis are based on using either the asymptotic (perturbation) method or the incremental/iterative (step-by-step) approach. The former method is an adaptation of Koiter's perturbation procedure for the study of the immediate postbuckling response and the sensitivity of the structure to initial imperfections (31, 33, 34, 39). Although many papers have been devoted to this method (32, 39-45), very few papers (32, 40) have addressed the application of the method to framed structures. At this time the conventional incremental/iterative method appears to be computationally more effective, and it will be employed in this study.

While many publications have treated nonlinear finite element analysis of plane or space frames, relatively few of them have included postbuckling analysis. The large number of publications on nonlinear analysis of framed structures

is, at least partially, due to the fact that various kinematic nonlinear formulations can be employed, and that at this time it is not clear which formulation is most effective (47). For plane frame problems, Wood and Zienkiwicz (51) used the total Lagrangian formulation and employed a paralinear isoparametric element associated with straight and curved beams. A study of nonlinear static, pre- and postbuckling response of elastic plane frame using the updated Lagrangian formulation and curved beam elements was presented by Karamanlidis et al (52). Bagci (53) used a planar flexural finite element for determining the buckling load and the corresponding mode vectors. Problems of material nonlinearity for plane frame were presented by Bagchi (37) using a beam element with four degrees of freedom and allowing transverse shear, while Banovec (36) used a mixed type element with three degrees of freedom at each end and with n ( n = 1, 2, 3,...) internal degrees of freedom along the element. For space frames Remseth (50) presented a geometrically nonlinear static and dynamic analysis employing the total Lagrangian formulation and curved beam elements. Bathe and Bolourchi (47) presented a large displacement analysis of three dimensional beam structures using straight beam elements and conventional beam displacement functions. For the postbuckling analysis Papadrakakis (60) applied two vector iteration methods, dynamic relaxation and first order conjugate gradient, to the investigation of the large deflection behavior of elastic spatial

structures. While most authors have dealt with geometric nonlinearities for space frames, Uzgider (38) analyzed the inelastic response of space frames to dynamic loads under the assumption of small displacements. Argyris et al (64) proposed a finite element analysis procedure for large deformations in arbitrary three-dimensional elasto-plastic frames by employing the so-called natural formulation (30) which seems to be effective in the provision of numerical solutions for a broad class of nonlinear problems.

Because of the complex nature of nonlinear structural problems, various simplifying assumptions are imposed on the magnitude of deformations, rotations and strains, the material properties, the type of loadings, etc., which limits the practical usage of the solution method developed. Also the limitations on computer hardware resources restrict the size of the problem and the effectiveness of the solution schemes implemented. This research aims to develop a nonlinear finite element program compatible with a mini-computer/array processor system and applicable to a large variety of spatial frame structures with few restrictions on geometry and problem sizes, and to investigate the postbuckling behavior of these structures.

By considering large displacements, large rotations, and small strains, only geometric nonlinearities are taken into account. However, provided with proper constitutive material laws and time integration schemes, it may be extended to

include material nonlinearities and dynamic loadings. The beam element and the finite element formulation employed here are rather conventional, but special emphasis is placed on the selection of efficient linear and nonlinear solution techniques to trace out the complete solution path, including the postbuckling range, and the design of software to handle large problems efficiently by introducing a hypermatrix scheme, vectorization, and potential use of an array processor attached to a host mini-computer. Accordingly, this study should constitute a solid basis for the investigation of the postbuckling behavior of various structures and for the development of a general purpose nonlinear finite element package.

# CHAPTER 2

## FINITE ELEMENT FORMULATIONS

For a large displacement formulation of describing the motion of a structural body, essentially two distinct approaches exist, namely the Lagrangian ( material) description in which the initial configuration is taken as the reference state, and the Eulerian ( spatial) description, in which the final deformed configuration is taken as a moving reference state. Computationally an Eulerian formulation is strictly an updated Lagrangian approach where the initial position becomes the current equilibrium state prior to some incremental change (51). Therefore, the formulations are termed total Lagrangian and updated Lagrangian formulations. Under consistent material laws, both formulations are theoretically equivalent because they use the same equilibrium principles. Therefore the choice between the formulations depends on the relative ease of application and efficiency of the formulations.

Even though the total Lagrangian formulation has successfully been used for both geometrical and material nonlinearities while the updated Lagrangian formulation has been less successful until recent years, it is now recognized that the updated formulation often presents more simplicity than the total formulation, especially for large displacement-small

strain problems (3, 47, 52, 67). In this study convected (or moving) coordinates attached to beam elements are employed and all of the static and kinematic variables are referred to an updated configuration in each load step.

(1) Incremental Equilibrium Equation of Continua

Let us consider the motion of a body in a moving Cartesian co-ordinate system, as shown in Figure 2.1. Now, we want to evaluate the equilibrium positions of the body at the discrete time points $t_o$, $t_1$, $t_2$,.... Assume that the solution for the kinematic and static variables for time steps in the range of time $t_o$ to time t have been reached. It is now required to solve for the unknown variables in the configuration at time $t + \Delta t$. The static equilibrium and incremental equations at time $t + \Delta t$ can be derived from the principle of virtual work (1, 3, 50, 68, 69). Corresponding to the virtual variation $\delta u_k$ in the current displacement components ${}^{t+\Delta t}u_k$, the total external virtual work expression due to the body forces with components ${}^{t+\Delta t}F_k$ and surface tractions with components ${}^{t+\Delta t}T_k$ is

$$\delta W_e = \int_{t+\Delta t_V} {}^{t+\Delta t}\rho \; {}^{t+\Delta t}F_k \; \delta u_k \; {}^{t+\Delta t}dV + \int_{t+\Delta t_A} {}^{t+\Delta t}T_k \; \delta u_k \; {}^{t+\Delta t}dA \qquad (2.1)$$

where V, $\rho$ and A are the volume, mass density and surface area respectively, and the left superscript $t+\Delta t$ indicates

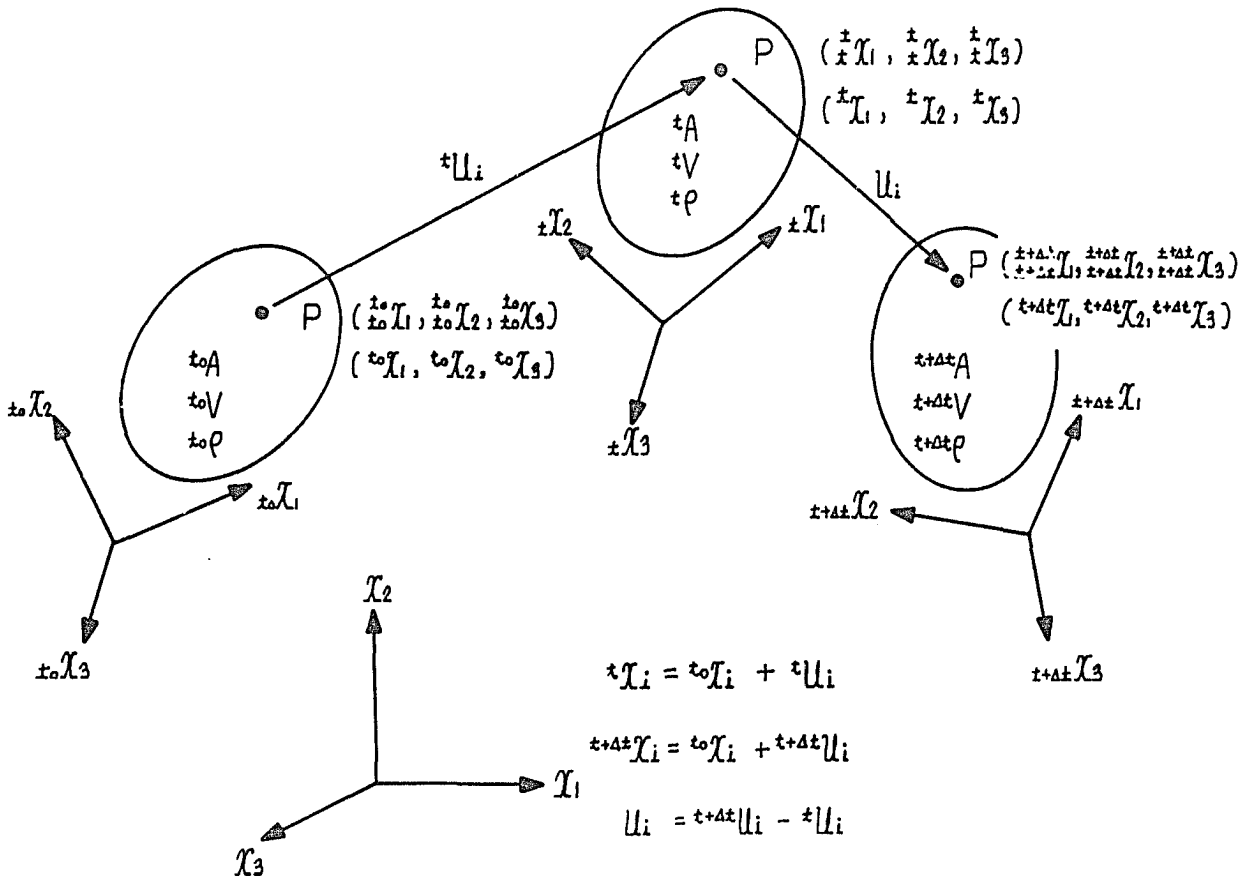


Figure 2.1. Motion of a body

the quantities in the configuration at the current time $t+\Delta t$. The internal virtual work expression is

$$\delta W_i = \int_{t+\Delta t_V} {}^{t+\Delta t}\tau_{ij}\, \delta\, {}^{t+\Delta t}e_{ij}\, {}^{t+\Delta t}dV \qquad (2.2)$$

where $\tau_{ij}$ is the Cartesian components of the Cauchy (true or Euler) stress tensor referred to the current configuration and $\delta e_{ij}$ is the variations in the Cartesian components of Cauchy's infinitesimal strain tensor referred to the current configuration (3, 67). Combined with Equations (2.1) and (2.2), the requirement of $\delta W_i = \delta W_e$ yields the incremental equilibrium equation

$$\int_{t+\Delta t_V} {}^{t+\Delta t}\tau_{ij}\, \delta\, {}^{t+\Delta t}e_{ij}\, {}^{t+\Delta t}dV = \int_{t+\Delta t_V} {}^{t+\Delta t}\rho\, {}^{t+\Delta t}F_k\, \delta u_k\, {}^{t+\Delta t}dV + \int_{t+\Delta t_A} {}^{t+\Delta t}T_k\, \delta u_k\, {}^{t+\Delta t}dA \qquad (2.3)$$

In the preceding equations and the equations to follow the Einstein's summation convention of tensor notation (72) is adopted.

To solve Equation (2.3) for the current unknown configuration at time $t+\Delta t$, all of the variables referred to the current configuration should be changed to the variables referred to a previously known configuration. In the updated Lagrangian formulation, all of the variables are referred to the configuration at time t. Then Equation (2.3) is transformed to

$$\int_{t_V} {}^{t+\Delta t}_{t}S_{ij}\,\delta\,{}^{t+\Delta t}_{t}\varepsilon_{ij}\,{}^{t}dV = \int_{t_V} {}^{t}\rho\,{}^{t+\Delta t}_{t}F_k\,\delta u_k\,{}^{t}dV + \int_{t_A} {}^{t+\Delta t}_{t}T_k\,\delta u_k\,{}^{t}dA \qquad (2.4)$$

where ${}^{t+\Delta t}_{t}S_{ij}$ = Cartesian components of the 2nd Piola-Kirchhoff stress tensor corresponding to the configuration at time $t+\Delta t$ but measured in the configuration at time t, and $\delta\,{}^{t+\Delta t}_{t}\varepsilon_{ij}$ = variations in the Cartesian components of the Green strain tensor in the configuration at time $t+\Delta t$ and referred to the configuration at time t. The left superscript t denotes the quantitites in the configuration at time t, and the left subscript t denotes the quantities measured in the coordinate axes at time t. The stress and strain tensors are defined as

$${}^{t+\Delta t}_{t}S_{ij} = \frac{{}^{t}\rho}{{}^{t+\Delta t}\rho}\;{}^{t}_{t+\Delta t}X_{i,k}\;{}^{t+\Delta t}\tau_{kl}\;{}^{t}_{t+\Delta t}X_{j,l} \qquad (2.5)$$

and

$${}^{t+\Delta t}_{t}\varepsilon_{ij} = \frac{1}{2}\left({}^{t+\Delta t}_{t}u_{i,j} + {}^{t+\Delta t}_{t}u_{j,i} + {}^{t+\Delta t}_{t}u_{k,i}\;{}^{t+\Delta t}_{t}u_{k,j}\right) \qquad (2.6)$$

where ${}^{t}_{t+\Delta t}X_{i,k} = \partial {}^{t}x_i / \partial {}^{t+\Delta t}x_j$, ${}^{t+\Delta t}_{t}u_{i,j} = \partial\,{}^{t+\Delta t}u_i / \partial {}^{t}x_j$, and the displacements $u_i$ are measured from the configuration at time t (5,68).

Since the stresses ${}^{t+\Delta t}_{t}S_{ij}$ and strains ${}^{t+\Delta t}_{t}\varepsilon_{ij}$ are unknown, for solution the following incremental decompositions are employed.

$$ {}^{t+\Delta t}_{t}S_{ij} = {}^{t}_{t}S_{ij} + {}_{t}S_{ij} \quad , \tag{2.7} $$

and

$$ {}^{t+\Delta t}_{t}\varepsilon_{ij} = {}^{t}_{t}\varepsilon_{ij} + {}_{t}\varepsilon_{ij} \quad . \tag{2.8} $$

By noting that ${}^{t}_{t}S_{ij} \equiv {}^{t}\tau_{ij}$ and ${}^{t}_{t}\varepsilon_{ij} \equiv 0$ , Equations (2.7) and (2.8) become

$$ {}^{t+\Delta t}_{t}S_{ij} = {}^{t}\tau_{ij} + {}_{t}S_{ij} \quad , \tag{2.9} $$

and

$$ {}^{t+\Delta t}_{t}\varepsilon_{ij} = {}_{t}\varepsilon_{ij} \quad . \tag{2.10} $$

Since the displacements at time t and referred to the coordinate axes at time t, ${}^{t}u_{i}$ , are zero, the displacements at time t+ $\Delta t$, ${}^{t+\Delta t}u_{i}$ , are reduced to

$$ {}^{t+\Delta t}u_i = {}^{t}u_i + u_i \equiv u_i \quad . \qquad (2.11) $$

Therefore, Equations (2.6), (2.10) and (2.11) yield

$$ {}_t\varepsilon_{ij} = \frac{1}{2}\left( {}_t u_{i,j} + {}_t u_{j,i} + {}_t u_{k,i}\ {}_t u_{k,j} \right) \quad . \qquad (2.12) $$

Equivalently

$$ {}_t\varepsilon_{ij} = {}_t e_{ij} + {}_t\eta_{ij} \quad , \qquad (2.13) $$

where

$$ {}_t e_{ij} = \frac{1}{2}\left( {}_t u_{i,j} + {}_t u_{j,i} \right) \quad , \qquad (2.14) $$

and

$$ {}_t\eta_{ij} = \frac{1}{2}\ {}_t u_{k,i}\ {}_t u_{k,j} \quad . \qquad (2.15) $$

With the constitutive tensor ${}_tC_{ijrs}$, the incremental 2nd Piola-Kirchhoff stresses and the incremental Green strains are related as

$$ {}_t S_{ij} = {}_t C_{ijrs}\ {}_t\varepsilon_{rs} \quad . \qquad (2.16) $$

From Equation (2.10),

$$\delta\, {}^{t+\Delta t}_{t}\varepsilon_{ij} = \delta_t \varepsilon_{ij} \quad . \tag{2.17}$$

Substituting Equations (2.9), (2.13), (2.16), and (2.17) into Equation (2.4) gives

$$\int_{t_V} {}_t C_{ijrs}\, {}_t\varepsilon_{rs}\, \delta_t \varepsilon_{ij}\, {}^t dV + \int_{t_V} {}^t\tau_{ij}\, \delta_t \eta_{ij}\, {}^t dV = \delta W_e - \int_{t_V} {}^t\tau_{ij}\, \delta_t e_{ij}\, {}^t dV \quad , \tag{2.18}$$

where

$$\delta W_e = \int_{t_V} {}^t\rho\, {}^{t+\Delta t}_{t}F_k\, \delta u_k\, {}^t dV + \int_{t_A} {}^{t+\Delta t}_{t}T_k\, \delta u_k\, {}^t dA \quad . \tag{2.19}$$

This Equation (2.19) is nonlinear in the incremental displacements $u_i$, and can be linearized by using the approximations

$${}_t S_{ij} \simeq {}_t C_{ijrs}\, {}_t e_{rs} \tag{2.20}$$

and

$$\delta_t \varepsilon_{ij} \simeq \delta_t e_{ij} \tag{2.21}$$

Now, the approximate linear incremental equilibrium equation

to be solved is

$$\int_{t_V} {}_tC_{ijrs}\, {}_te_{rs}\, \delta_t e_{ij}\, {}^t dV + \int_{t_V} {}^t\tau_{ij}\, \delta_t \eta_{ij}\, {}^t dV$$

$$= \delta W_e - \int_{t_V} {}^t\tau_{ij}\, \delta_t e_{ij}\, {}^t dV \quad . \tag{2.22}$$

(2) Beam Element

As shown in Figure 2.2, a conventional three-dimensional prismatic beam element which has two nodes with 6 degrees of freedom per node is used in this study. The element is assumed to be straight and of constant rectangular cross-section in the undeformed state. The element can transmit an axial force, two shear forces, two bending moments, and a torque.

It is assumed that plane cross-sections of the beam element remain plane during deformation, and perpendicular to the centroidal axis. Thus the effect of shear is neglected. The element can undergo large deflections and large rotations, but small strains are assumed. Therefore changes in the cross-sectional area and the length of the beam element during deformation are negligibly small.

The three principal moment of inertia axes of the beam element define the local co-ordinate system, p, q, r as in Figure 2.2. The two end nodes of the beam element and a reference node in the p-q plane are used in these local axes. In the development that follows, a bar over a character indicates that the corresponding quantity is defined locally.

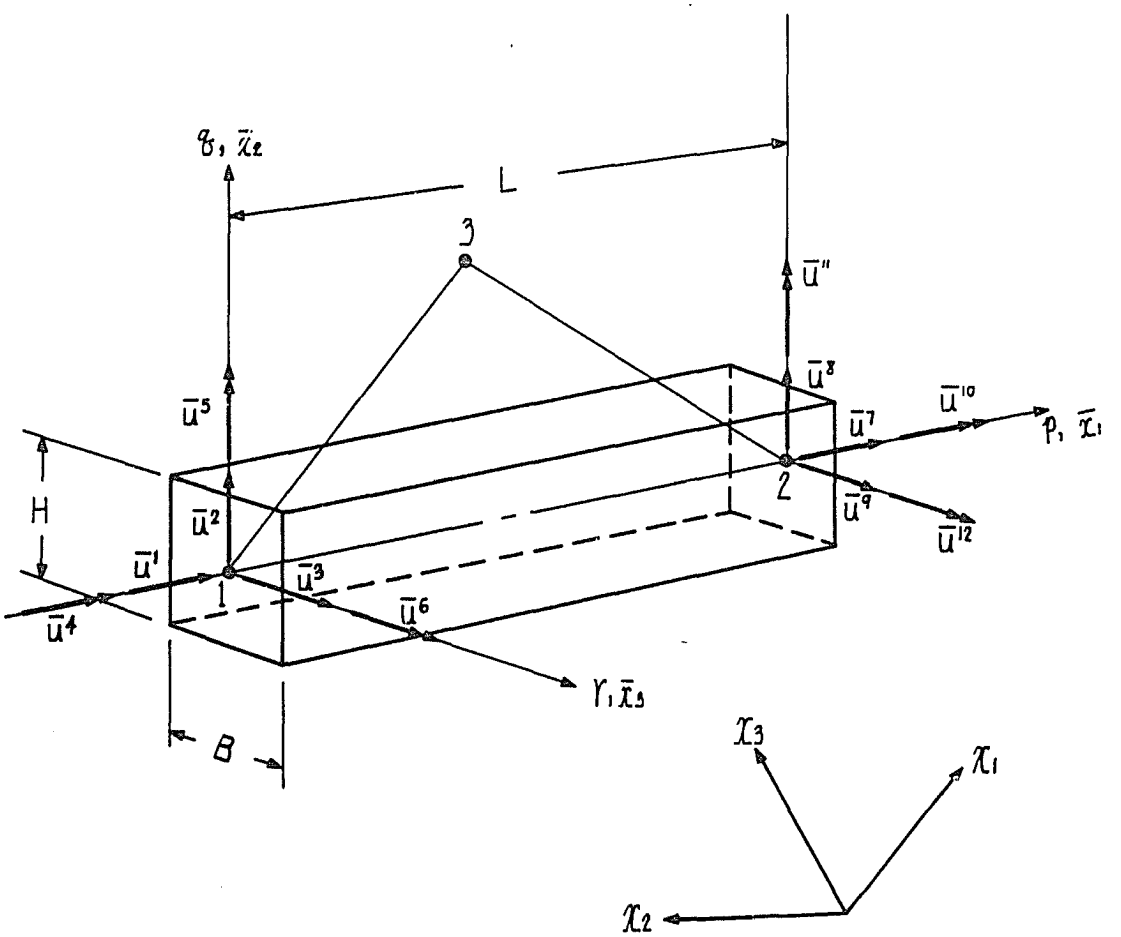


Figure 2.2. Three-dimensional beam element

(3) Interpolation Functions

In finite element analysis the equilibrium equations in incremental displacements are discretized by employing appropriate displacement interpolation functions. For a beam of constant cross-section in small displacement analysis it is conventional to use cubic Hermitian interpolation functions for the transverse bending displacements, and linear interpolation functions for the torsional and longitudinal displacements (47). By introducing the moving convected co-ordinate system and referring the interpolation functions to the coordinate axes, we can employ the same functions for our case, namely large displacements.

Figure 2.3 shows the linear and cubic Hermitian interpolation functions. In the linear interpolation

$$f(x) = N_1(x) f(x_1) + N_2(x) f(x_2) \quad , \tag{2.23}$$

$$N_1(x) = (x_2 - x) / (x_2 - x_1)$$

and

$$N_2(x) = (x - x_1) / (x_2 - x_1) \quad .$$

The cubic Hermitian interpolation function is expressed as (4,70).

$$f(x) = N_1(x) f(x_1) + N_2(x) f'(x_1) + N_3(x) f(x_2) + N_4(x) f'(x_2) \tag{2.24}$$

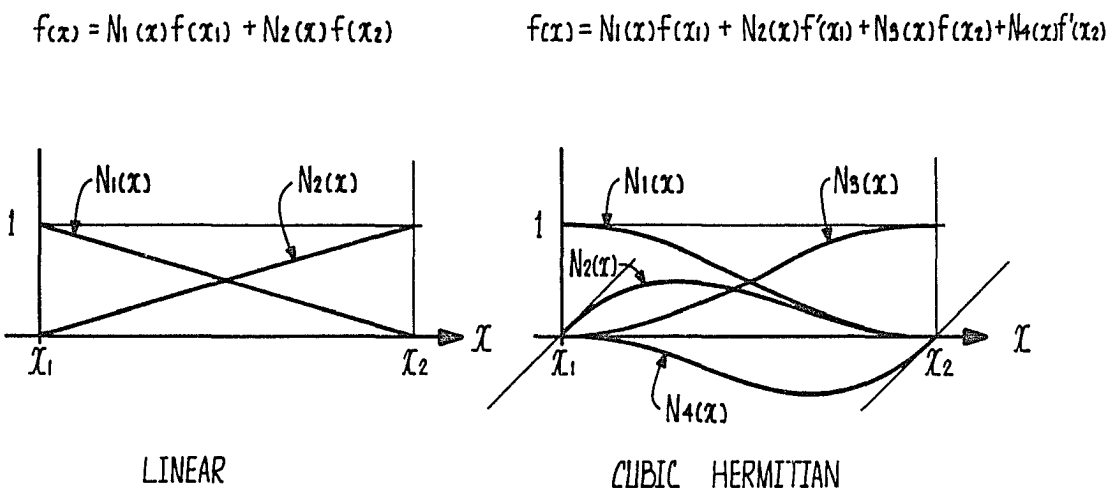


Figure 2.3. Linear and cubic Hermitian interpolation functions

where

$$N_1(x) = \left(1 + 2\,\frac{X - X_1}{X_2 - X_1}\right)\left(\frac{X_2 - X}{X_2 - X_1}\right)^2$$

$$N_2(x) = \frac{(X - X_1)\,(X_2 - X)^2}{(X_2 - X_1)^2}$$

$$N_3(x) = \left(1 + 2\,\frac{X_2 - X}{X_2 - X_1}\right)\left(\frac{X - X_1}{X_2 - X_1}\right)^2$$

and

$$N_4(x) = -\frac{(X - X_1)^2\,(X_2 - X)}{(X_2 - X_1)^2}$$

Now, the incremental displacement field in the beam element are interpolated as a function of the incremental nodal point displacement components, i.e.,

$$\bar{u}_i = \sum_{k=1}^{12} N_k^i\,\bar{u}^k \qquad (2.25)$$

where the $N_k^i$ are the interpolation functions corresponding to the local axes $\bar{x}_i$ at time t, and the $\bar{u}^k$ are the nodal point displacement increments measured in the local axes at time t. The interpolation functions are

$$N_1' = 1 - \frac{P}{L}$$

$$N_2' = \frac{6pq}{L^2} - \frac{6p^2q}{L^3}$$

$$N_3' = \frac{6pr}{L^2} - \frac{6p^2r}{L^3}$$

$$N_4' = 0$$

$$N_5' = r - \frac{4pr}{L} + \frac{3p^2r}{L^2}$$

$$
\begin{aligned}
N_6^1 &= -q + \frac{4pq}{L} - \frac{3p^2q}{L^2} \\
N_7^1 &= \frac{p}{L} \\
N_8^1 &= -\frac{6pq}{L^2} + \frac{6p^2q}{L^3} \\
N_9^1 &= -\frac{6pr}{L^2} + \frac{6p^2r}{L^3} \\
N_{10}^1 &= 0 \\
N_{11}^1 &= -\frac{2pr}{L} + \frac{3p^2r}{L^2} \\
N_{12}^1 &= \frac{2pq}{L} - \frac{3p^2q}{L^2} \\
N_1^2 &= 0 \\
N_2^2 &= 1 - \frac{3p^2}{L^2} + \frac{2p^3}{L^3} \\
N_3^2 &= 0 \\
N_4^2 &= -r + \frac{pr}{L} \\
N_5^2 &= 0 \\
N_6^2 &= p - \frac{2p^2}{L} + \frac{p^3}{L^2} \\
N_7^2 &= 0 \\
N_8^2 &= \frac{3p^2}{L^2} - \frac{2p^3}{L^3} \\
N_9^2 &= 0 \\
N_{10}^2 &= -\frac{pr}{L} \\
N_{11}^2 &= 0 \\
N_{12}^2 &= -\frac{p^2}{L} + \frac{p^3}{L^2} \\
N_1^3 &= N_2^3 = 0 \\
N_3^3 &= 1 - \frac{3p^2}{L^2} + \frac{2p^3}{L^3} \\
N_4^3 &= q - \frac{pq}{L} \\
N_5^3 &= -p + \frac{2p^2}{L} - \frac{p^3}{L^2}
\end{aligned}
\qquad (2.26)
$$

$$N_6^3 = N_7^3 = N_8^3 = 0$$

$$N_9^3 = \frac{3p^2}{L^2} - \frac{2p^3}{L^3}$$

$$N_{10}^3 = \frac{pq}{L}$$

$$N_{11}^3 = \frac{p^2}{L} - \frac{p^3}{L^2}$$

$$N_{12}^3 = 0$$

where L is the length of the beam element, and the coordinates p, q, and r are defined as in Figure 2.2.

(4) Strain-displacement Transformation Matrix

From Equation (2.25), we get

$$\bar{u}_{i,j} = \sum_{k=1}^{12} N_{k,j}^i \bar{u}^k , \qquad j = 1, 2, 3 \tag{2.27}$$

where $\bar{u}_{i,j} = \partial \bar{u}_i / \partial \bar{x}_j$ and $N_{k,j}^i = \partial N_k^i / \partial \bar{x}_j$ . By using Equation (2.12), for a beam element referred to the local coordinate axes at time t, we get the following expressions for the incremental strains.

$$\bar{\varepsilon}_{11} = \bar{u}_{1,1} + \tfrac{1}{2}\left[(\bar{u}_{1,1})^2 + (\bar{u}_{2,1})^2 + (\bar{u}_{3,1})^2\right] \tag{2.28}$$

$$\bar{\varepsilon}_{12} = \tfrac{1}{2}\left[\bar{u}_{1,2} + \bar{u}_{2,1}\right] + \tfrac{1}{2}\left[\bar{u}_{1,1}\bar{u}_{1,2} + \bar{u}_{3,1}\bar{u}_{3,2}\right] \tag{2.29}$$

$$\bar{\varepsilon}_{13} = \tfrac{1}{2}\left[\bar{u}_{1,3} + \bar{u}_{3,1}\right] + \tfrac{1}{2}\left[\bar{u}_{1,1}\bar{u}_{1,3} + \bar{u}_{2,1}\bar{u}_{2,3}\right] \tag{2.30}$$

Thus, the linear portion of the strains decomposed as in Equation (2.13) becomes

$$\bar{e}_{11} = \bar{u}_{1,1} \tag{2.31}$$

$$\bar{e}_{12} = \frac{1}{2}\left[\bar{u}_{1,2} + \bar{u}_{2,1}\right] \tag{2.32}$$

$$\bar{e}_{13} = \frac{1}{2}\left[\bar{u}_{1,3} + \bar{u}_{3,1}\right] . \tag{2.33}$$

By taking the strain vector $\{\bar{e}\}$ defined as

$$\{\bar{e}\}^T = \left[\bar{e}_{11} \quad 2\bar{e}_{12} \quad \bar{e}_{13}\right] \tag{2.34}$$

we have the equation

$$\{\bar{e}\} = [B_L]\{\bar{u}\} \tag{2.35}$$

where $[B_L]$ is the 3 x 12 linear strain-displacement transformation matrix and $\{\bar{u}\}$ is the incremental nodal point displacement vector. From Equation (2.27) with Equations (2.31) to (2.34), we get

$$[B_L] = \begin{bmatrix} N^1_{1,1} & N^1_{2,1} & \cdots & N^1_{12,1} \\ (N^1_{1,2} + N^2_{1,1}) & (N^1_{2,2} + N^2_{2,1}) & \cdots & (N^1_{12,2} + N^2_{12,1}) \\ (N^1_{1,3} + N^3_{1,1}) & (N^1_{2,3} + N^3_{2,1}) & \cdots & (N^1_{12,3} + N^3_{12,1}) \end{bmatrix} \tag{2.36}$$

The evaluation of the linear strain-displacement transformation matrix is performed by using Equation (2.26), and is listed in Table 2.1.

As presented in (71), from Equations (2.13), (2.28), (2.29) and (2.30) we can express the nonlinear portion of the incremental strains as

$$\{\bar{\eta}\} = \begin{bmatrix} \frac{1}{2}\bar{u}_{1,1} & \frac{1}{2}\bar{u}_{2,1} & \frac{1}{2}\bar{u}_{3,1} & 0 & 0 & 0 & 0 \\ 0 & 0 & 0 & \bar{u}_{1,1} & \bar{u}_{3,1} & 0 & 0 \\ 0 & 0 & 0 & 0 & 0 & \bar{u}_{1,1} & \bar{u}_{2,1} \end{bmatrix} \begin{Bmatrix} \bar{u}_{1,1} \\ \bar{u}_{2,1} \\ \bar{u}_{3,1} \\ \bar{u}_{1,2} \\ \bar{u}_{3,2} \\ \bar{u}_{1,3} \\ \bar{u}_{2,3} \end{Bmatrix} \tag{2.37}$$

or

$$\{\bar{\eta}\} = [A]\{\alpha\} \tag{2.38}$$

where $\{\bar{\eta}\}^T = [\bar{\eta}_{11} \quad 2\bar{\eta}_{12} \quad 2\bar{\eta}_{13}]$ . Again, by using Equation (2.27) the vector $\{\alpha\}$ can be related to the nodal incremental displacements as

$$\{\alpha\} = [B_N]\{\bar{u}\} \tag{2.39}$$

where we have for the nonlinear strain-displacement transformation matrix $B_N$.

$$[B_N] = \begin{bmatrix} N^1_{1,1} & N^1_{2,1} & N^1_{3,1} & \cdots & N^1_{12,1} \\ N^2_{1,1} & N^2_{2,1} & N^2_{3,1} & \cdots & N^2_{12,1} \\ N^3_{1,1} & N^3_{2,1} & N^3_{3,1} & \cdots & N^3_{12,1} \\ N^1_{1,2} & N^1_{2,2} & N^1_{3,2} & \cdots & N^1_{12,2} \\ N^3_{1,2} & N^3_{2,2} & N^3_{3,2} & \cdots & N^3_{12,2} \\ N^1_{1,3} & N^1_{2,3} & N^1_{3,3} & \cdots & N^1_{12,3} \\ N^2_{1,3} & N^2_{2,3} & N^2_{3,3} & \cdots & N^2_{12,3} \end{bmatrix} \tag{2.40}$$

Table 2.1. Linear strain-displacement transformation matrix

$$\left[B_L\right] = \begin{bmatrix} -\frac{1}{L} & \left(\frac{6q}{L^2} - \frac{12pq}{L^3}\right) & \left(\frac{6r}{L^2} - \frac{12pr}{L^3}\right) & 0 & \left(-\frac{4r}{L} + \frac{6pr}{L^2}\right) & \left(\frac{4q}{L} - \frac{6pq}{L^2}\right) & \frac{1}{L} & \left(-\frac{6q}{L^2} + \frac{12pq}{L^3}\right) & \left(-\frac{6r}{L^2} + \frac{12pr}{L^3}\right) & 0 & \left(-\frac{2r}{L} + \frac{6pr}{L^2}\right) & \left(\frac{2q}{L} - \frac{6pq}{L^2}\right) \\ 0 & 0 & 0 & \frac{r}{L} & 0 & 0 & 0 & 0 & 0 & -\frac{r}{L} & 0 & 0 \\ 0 & 0 & 0 & -\frac{q}{L} & 0 & 0 & 0 & 0 & 0 & \frac{q}{L} & 0 & 0 \end{bmatrix}$$

The elements in the nonlinear strain-displacement transformation matrix are listed in Table 2.2.

From Equation (2.13) the variations of the incremental strains are

$$\delta\varepsilon_{ij} = \delta e_{ij} + \delta\eta_{ij} \quad . \tag{2.41}$$

For the beam element Equation (2.35) gives

$$\{\delta\bar{e}\} = [B_L]\{\delta\bar{u}\} \tag{2.42}$$

where $\{\delta\bar{u}\}$ is the variation of the incremental nodal point displacement vector. From Equation (2.38) we have

$$\{\delta\bar{\eta}\} = [\delta A]\{\alpha\} + [A]\{\delta\alpha\} \quad . \tag{2.43}$$

Here, an interesting property of the matrix $[A]$ and the vector $\{\alpha\}$ is observed, i.e.,

$$[\delta A]\{\alpha\} = \begin{bmatrix} \frac{1}{2}\delta\bar{u}_{1,1} & \frac{1}{2}\delta\bar{u}_{2,1} & \frac{1}{2}\delta\bar{u}_{3,1} & 0 & 0 & 0 & 0 \\ 0 & 0 & 0 & \delta\bar{u}_{1,1} & \delta\bar{u}_{3,1} & 0 & 0 \\ 0 & 0 & 0 & 0 & 0 & \delta\bar{u}_{1,1} & \delta\bar{u}_{2,1} \end{bmatrix} \begin{Bmatrix} \bar{u}_{1,1} \\ \bar{u}_{2,1} \\ \bar{u}_{3,1} \\ \bar{u}_{1,2} \\ \bar{u}_{3,2} \\ \bar{u}_{1,3} \\ \bar{u}_{2,3} \end{Bmatrix}$$

$$= \begin{bmatrix} \frac{1}{2}\bar{u}_{1,1} & \frac{1}{2}\bar{u}_{2,1} & \frac{1}{2}\bar{u}_{3,1} & 0 & 0 & 0 & 0 \\ \bar{u}_{1,2} & 0 & \bar{u}_{3,2} & 0 & 0 & 0 & 0 \\ \bar{u}_{1,3} & \bar{u}_{2,3} & 0 & 0 & 0 & 0 & 0 \end{bmatrix} \begin{Bmatrix} \delta\bar{u}_{1,1} \\ \delta\bar{u}_{2,1} \\ \delta\bar{u}_{3,1} \\ \delta\bar{u}_{1,2} \\ \delta\bar{u}_{3,2} \\ \delta\bar{u}_{1,3} \\ \delta\bar{u}_{2,3} \end{Bmatrix} , \tag{2.44}$$

Table 2.2. Nonlinear strain-displacement transformation matrix

$$
[B_N] = \begin{bmatrix}
-\frac{1}{L} & (\frac{6q}{L^2} - \frac{12pq}{L^3}) & (\frac{6r}{L^2} - \frac{12pr}{L^3}) & 0 & (-\frac{4r}{L} + \frac{6pr}{L^2}) & (\frac{4q}{L} - \frac{6pq}{L^2}) & \frac{1}{L} & (-\frac{6q}{L^2} + \frac{12pq}{L^3}) & (-\frac{6r}{L^2} + \frac{12pr}{L^3}) & 0 & (-\frac{2r}{L} + \frac{6pr}{L^2}) & (\frac{2q}{L} - \frac{6pq}{L^2}) \\
0 & (-\frac{6p}{L^2} + \frac{6p^2}{L^3}) & 0 & \frac{r}{L} & 0 & (1 - \frac{4p}{L} + \frac{3p^2}{L^2}) & 0 & (\frac{6p}{L^2} - \frac{6p^2}{L^3}) & 0 & -\frac{r}{L} & 0 & (-\frac{2p}{L} + \frac{3p^2}{L^2}) \\
0 & 0 & (-\frac{6p}{L^2} + \frac{6p^2}{L^3}) & -\frac{q}{L} & (-1 + \frac{4p}{L} - \frac{3p^2}{L^2}) & 0 & 0 & 0 & (\frac{6p}{L^2} - \frac{6p^2}{L^3}) & \frac{q}{L} & (\frac{2p}{L} - \frac{3p^2}{L^2}) & 0 \\
0 & (\frac{6p}{L^2} - \frac{6p^2}{L^3}) & 0 & 0 & 0 & (-1 + \frac{4p}{L} - \frac{3p^2}{L^2}) & 0 & (-\frac{6p}{L^2} + \frac{6p^2}{L^3}) & 0 & 0 & 0 & (\frac{2p}{L} - \frac{3p^2}{L^2}) \\
0 & 0 & 0 & (1 - \frac{p}{L}) & 0 & 0 & 0 & 0 & 0 & \frac{p}{L} & 0 & 0 \\
0 & 0 & (\frac{6p}{L^2} - \frac{6p^2}{L^3}) & 0 & (1 - \frac{4p}{L} + \frac{3p^2}{L^2}) & 0 & 0 & 0 & (-\frac{6p}{L^2} + \frac{6p^2}{L^3}) & 0 & (-\frac{2p}{L} + \frac{3p^2}{L^2}) & 0 \\
0 & 0 & 0 & (-1 + \frac{p}{L}) & 0 & 0 & 0 & 0 & 0 & -\frac{p}{L} & 0 & 0
\end{bmatrix}
$$

or

$$[\delta A]\{\alpha\} = [H]\{\delta\alpha\} \quad , \tag{2.45}$$

where

$$[H] = \begin{bmatrix} \frac{1}{2}\bar{u}_{1,1} & \frac{1}{2}\bar{u}_{2,1} & \frac{1}{2}\bar{u}_{3,1} & 0 & 0 & 0 & 0 \\ \bar{u}_{1,2} & 0 & \bar{u}_{3,2} & 0 & 0 & 0 & 0 \\ \bar{u}_{1,3} & \bar{u}_{2,3} & 0 & 0 & 0 & 0 & 0 \end{bmatrix} \quad . \tag{2.46}$$

Thus, Equation (2.43) becomes

$$\{\delta\bar{\eta}\} = ([H] + [A])\{\delta\alpha\} \tag{2.47}$$

or

$$\{\delta\bar{\eta}\} = [G]\{\delta\alpha\} \quad , \tag{2.48}$$

where

$$[G] = [H] + [A]$$

$$= \begin{bmatrix} u_{1,1} & u_{2,1} & u_{3,1} & 0 & 0 & 0 & 0 \\ u_{1,2} & 0 & u_{3,2} & u_{1,1} & u_{3,1} & 0 & 0 \\ u_{1,3} & u_{2,3} & 0 & 0 & 0 & u_{1,1} & u_{2,1} \end{bmatrix} \quad . \tag{2.49}$$

From Equation (2.39), we have

$$\{\delta\alpha\} = [B_N]\{\delta\bar{u}\} \quad . \tag{2.50}$$

Finally, substituting Equation (2.50) into Equation (2.48) gives

$$\{\delta\bar{\eta}\} = [G][B_N]\{\delta\bar{u}\} \quad . \tag{2.51}$$

(5) Stresses and Stress-strain Relationship

For the beam element considered, three stress components, an axial stress ($\bar{\sigma}_p$) and two shear stresses ($\bar{\tau}_{pq}$ and $\bar{\tau}_{pr}$), exist. The Cauchy stress vector at time t is defined as

$$\{\bar{\tau}\}^T = [\,\bar{\tau}_{11}\ \bar{\tau}_{12}\ \bar{\tau}_{13}\,] = [\,\bar{\sigma}_p\ \bar{\tau}_{pq}\ \bar{\tau}_{pr}\,] \quad , \tag{2.52}$$

and the Cauchy stress matrix at time t (derived later) is

$$[\bar{\tau}] = \begin{bmatrix} \bar{\tau}_{11} & 0 & 0 & \bar{\tau}_{12} & 0 & \bar{\tau}_{13} & 0 \\ 0 & \bar{\tau}_{11} & 0 & 0 & 0 & 0 & \bar{\tau}_{13} \\ 0 & 0 & \bar{\tau}_{11} & 0 & \bar{\tau}_{12} & 0 & 0 \\ \bar{\tau}_{12} & 0 & 0 & 0 & 0 & 0 & 0 \\ 0 & 0 & \bar{\tau}_{12} & 0 & 0 & 0 & 0 \\ \bar{\tau}_{13} & 0 & 0 & 0 & 0 & 0 & 0 \\ 0 & \bar{\tau}_{13} & 0 & 0 & 0 & 0 & 0 \end{bmatrix} \quad . \tag{2.53}$$

Applying the generalized Hooke's law to the beam element we have the relationship between the incremental stresses and the incremental strains, referred to the coordinate axes at time t, i.e.

$$\{\bar{S}\} = [\bar{C}]\{\bar{\varepsilon}\} \tag{2.54}$$

where $\{\bar{S}\}$ and $\{\bar{\varepsilon}\}$ are the incremental stress and strain vectors, and $[\bar{C}]$ is the incremental stress-strain material property matrix. The $[\bar{C}]$ is expressed as

$$[C] = \begin{bmatrix} E & 0 & 0 \\ 0 & G & 0 \\ 0 & 0 & G \end{bmatrix} \tag{2.55}$$

or

$$[C] = \begin{bmatrix} E & 0 & 0 \\ 0 & \frac{E}{2(1+\nu)} & 0 \\ 0 & 0 & \frac{E}{2(1+\nu)} \end{bmatrix} , \qquad (2.56)$$

where E = Young's modulus,

G = shear modulus,

and $\nu$ = Poisson's ratio.

(6) Incremental Equilibrium Equations of Beam Element

Now we have to construct the finite element formulation equivalent to the incremental equilibrium equation, Equation (2.22),

$$\int_{{}^tV} {}_tC_{ijrs}\, {}_te_{rs}\, \delta_t e_{ij}\, {}^tdV + \int_{{}^tV} {}^t\tau_{ij}\, \delta_t \eta_{ij}\, {}^tdV = \delta W_e - \int_{{}^tV} {}^t\tau_{ij}\, \delta_t e_{ij}\, {}^tdV \qquad (2.57)$$

where

$$\delta W_e = \int_{{}^tV} {}^t\rho\, {}^{t+\Delta t}_{\ t}F_k\, \delta u_k\, {}^tdV + \int_{{}^tA} {}^{t+\Delta t}_{\ t}T_k\, \delta u_k\, {}^tdA \quad . \qquad (2.58)$$

For a beam element, with the notations defined before, the first and last terms of Equation (2.57) are transformed easily as

$$\int_{{}^tV} {}_tC_{ijrs}\, {}_te_{rs}\, \delta_t e_{ij}\, {}^tdV = \{\delta\bar{u}\}^T \left( \int_V [B_L]^T [C] [B_L] dV \right) \{\bar{u}\} , \qquad (2.59)$$

and

$$\int_{t_V} {}^{t}\tau_{ij}\ \delta\, {}_{t}e_{ij}\, {}^{t}dV \;=\; \{\delta\bar{u}\}^{T} \int_{V} [B_L]^{T}\{\bar{\tau}\}\, dV \qquad . \tag{2.60}$$

By using Equation (2.51), the second term of Equation (2.57) becomes

$$\int_{t_V} {}^{t}\tau_{ij}\ \delta\, {}_{t}\eta_{ij}\, {}^{t}dV \;=\; \int_{V} \{\delta\bar{u}\}^{T}[B_N]^{T}[G]^{T}\{\bar{\tau}\}\, dV \qquad . \tag{2.61}$$

From Equations (2.49) and (2.52),

$$[G]^{T}\{\bar{\tau}\} = \begin{bmatrix} \bar{u}_{1,1} & \bar{u}_{1,2} & \bar{u}_{1,3} \\ \bar{u}_{2,1} & 0 & \bar{u}_{2,3} \\ \bar{u}_{3,1} & \bar{u}_{3,2} & 0 \\ 0 & \bar{u}_{1,1} & 0 \\ 0 & \bar{u}_{3,1} & 0 \\ 0 & 0 & \bar{u}_{1,1} \\ 0 & 0 & \bar{u}_{2,1} \end{bmatrix} \begin{Bmatrix} \bar{\tau}_{11} \\ \bar{\tau}_{12} \\ \bar{\tau}_{13} \end{Bmatrix}$$

$$= \begin{bmatrix} \bar{\tau}_{11} & 0 & 0 & \bar{\tau}_{12} & 0 & \bar{\tau}_{13} & 0 \\ 0 & \bar{\tau}_{11} & 0 & 0 & 0 & 0 & \bar{\tau}_{13} \\ 0 & 0 & \bar{\tau}_{11} & 0 & \bar{\tau}_{12} & 0 & 0 \\ \bar{\tau}_{12} & 0 & 0 & 0 & 0 & 0 & 0 \\ 0 & 0 & \bar{\tau}_{12} & 0 & 0 & 0 & 0 \\ \bar{\tau}_{13} & 0 & 0 & 0 & 0 & 0 & 0 \\ 0 & \bar{\tau}_{13} & 0 & 0 & 0 & 0 & 0 \end{bmatrix} \begin{Bmatrix} \bar{u}_{1,1} \\ \bar{u}_{2,1} \\ \bar{u}_{3,1} \\ \bar{u}_{1,2} \\ \bar{u}_{3,2} \\ \bar{u}_{1,3} \\ \bar{u}_{2,3} \end{Bmatrix} \tag{2.67}$$

or

$$[G]^{T}\{\bar{\tau}\} \;=\; [\bar{\tau}]\{\alpha\} \qquad . \tag{2.68}$$

Substituting Equations (2.68) and (2.39) into Equation (2.61) yields

$$\int_{t_v} {}^{t}\tau_{ij}\, \delta_t \eta_{ij}\, {}^{t}dV = \{\delta\bar{u}\}^T \left( \int_V [B_N]^T [\bar{\tau}] [B_N]\, dV \right) \{\bar{u}\} \quad . \tag{2.69}$$

The external virtual work expression is transformed in the usual way (71) as

$$\delta W_e = \{\delta\bar{u}\}^T \{\bar{R}\} \quad , \tag{2.70}$$

where $\{\bar{R}\}$ is the vector of externally applied element nodal loads at time $t+\Delta t$.

Thus, Equation (2.57) becomes

$$\{\delta\bar{u}\}^T \left( \int_V [B_L]^T [C] [B_L]\, dV \right) \{\bar{u}\} + \{\delta\bar{u}\}^T \left( \int_V [B_N]^T [\bar{\tau}] [B_N]\, dV \right) \{\bar{u}\} = \{\delta\bar{u}\}^T \{\bar{R}\} - \{\delta\bar{u}\}^T \int_V [B_L]^T \{\tau\}\, dV \tag{2.80}$$

Now, Equation (2.80) yields the incremental force equilibrium equations

$$\left( \int_V [B_L]^T [C] [B_L]\, dV + \int_V [B_N]^T [\bar{\tau}] [B_N]\, dV \right) \{\bar{u}\} = \{\bar{R}\} - \int_V [B_L]^T \{\bar{\tau}\}\, dV \quad . \tag{2.81}$$

Equivalently Equation (2.81) can be expressed as

$$\left( [\bar{K}_L] + [\bar{K}_N] \right) \{\bar{u}\} = \{\bar{R}\} - \{\bar{F}\} \tag{2.82}$$

where
$$[\bar{K}_L] = \int_V [B_L]^T [C] [B_L] \, dV \tag{2.83}$$

$$[\bar{K}_N] = \int_V [B_N]^T [\bar{\tau}] [B_N] \, dV \quad , \tag{2.84}$$

and
$$\{\bar{F}\} = \int_V [B_L]^T \{\bar{\tau}\} \tag{2.85}$$

Furthermore, by denoting

$$[\bar{K}] = [\bar{K}_L] + [\bar{K}_N] \tag{2.86}$$

and
$$\{\Delta\bar{R}\} = \{\bar{R}\} - \{\bar{F}\} \tag{2.87}$$

Equation (2.82) is reduced to

$$[\bar{K}] \{\bar{u}\} = \{\Delta\bar{R}\} \tag{2.88}$$

where $[\bar{K}]$ is termed as the incremental (tangential) stiffness matrix, and $\{\Delta\bar{R}\}$ is termed as the residual (out-of-balance) force vector. The matrices $[\bar{K}_L]$ and $[\bar{K}_N]$ are called the linear and nonlinear strain incremental stiffness matrices.

(7) Incremental Stiffness Matrices

The use of Table 2.1 and Equation (2.56) and the integration over the beam element in Equation (2.83) gives

Table 2.3. Linear strain incremental stiffness matrix of beam element

$$[K_L] = \begin{bmatrix}
\frac{AE}{L} & 0 & 0 & 0 & 0 & 0 & -\frac{AE}{L} & 0 & 0 & 0 & 0 & 0 \\
0 & \frac{12EI_1}{L^3} & 0 & 0 & 0 & \frac{6EI_1}{L^2} & 0 & -\frac{12EI_1}{L^3} & 0 & 0 & 0 & \frac{6EI_1}{L^2} \\
0 & 0 & \frac{12EI_2}{L^3} & 0 & -\frac{6EI_2}{L^2} & 0 & 0 & 0 & -\frac{12EI_2}{L^3} & 0 & -\frac{6EI_2}{L^2} & 0 \\
0 & 0 & 0 & \frac{G(I_1+I_2)}{L} & 0 & 0 & 0 & 0 & 0 & -\frac{G(I_1+I_2)}{L} & 0 & 0 \\
0 & 0 & -\frac{6EI_2}{L^2} & 0 & \frac{4EI_2}{L} & 0 & 0 & 0 & \frac{6EI_2}{L^2} & 0 & \frac{2EI_2}{L} & 0 \\
0 & \frac{6EI_1}{L^2} & 0 & 0 & 0 & \frac{4EI_1}{L} & 0 & -\frac{6EI_1}{L^2} & 0 & 0 & 0 & \frac{2EI_1}{L} \\
-\frac{AE}{L} & 0 & 0 & 0 & 0 & 0 & \frac{AE}{L} & 0 & 0 & 0 & 0 & 0 \\
0 & -\frac{12EI_1}{L^3} & 0 & 0 & 0 & -\frac{6EI_1}{L^2} & 0 & \frac{12EI_1}{L^3} & 0 & 0 & 0 & -\frac{6EI_1}{L^2} \\
0 & 0 & -\frac{12EI_2}{L^3} & 0 & \frac{6EI_2}{L^2} & 0 & 0 & 0 & \frac{12EI_2}{L^3} & 0 & \frac{6EI_2}{L^2} & 0 \\
0 & 0 & 0 & -\frac{G(I_1+I_2)}{L} & 0 & 0 & 0 & 0 & 0 & \frac{G(I_1+I_2)}{L} & 0 & 0 \\
0 & 0 & -\frac{6EI_2}{L^2} & 0 & \frac{2EI_2}{L} & 0 & 0 & 0 & \frac{6EI_2}{L^2} & 0 & \frac{4EI_2}{L} & 0 \\
0 & \frac{6EI_1}{L^2} & 0 & 0 & 0 & \frac{2EI_1}{L} & 0 & -\frac{6EI_1}{L^2} & 0 & 0 & 0 & \frac{4EI_1}{L}
\end{bmatrix}$$

where $I_1 = \frac{BH^3}{12}$, $I_2 = \frac{\overset{3}{B}H}{12}$, E = Young's modulus, G = shear modulus, and A, B, H and L are defined as shown in Figure 2.2.

the evaluation of the linear strain incremental stiffness matrix in closed form as listed in Table 2.3.

By using Table 2.2 and Equation (2.53), the nonlinear strain incremental stiffness matrix expression in Equation (2.84) is simplified as the following:

$$\bar{K}_N(1,1) = \int_V (BL11)(\sigma_1)(BL11)\, dV$$

$$\bar{K}_N(1,2) = \int_V (BL11)\{(\sigma_1)(BL12)-(\sigma_2)(BN22)\}\, dV$$

$$\bar{K}_N(1,3) = \int_V (BL11)\{(\sigma_1)(BL13)-(\sigma_3)(BN22)\}\, dV$$

$$\bar{K}_N(1,4) = 0$$

$$\bar{K}_N(1,5) = \int_V (BL11)\{(\sigma_1)(BL15)+(\sigma_3)(BN26)\}\, dV$$

$$\bar{K}_N(1,6) = \int_V (BL11)\{(\sigma_1)(BL16)-(\sigma_2)(BN26)\}\, dV$$

$$\bar{K}_N(1,7) = -\int_V (BL11)(\sigma_1)(BL11)\, dV$$

$$\bar{K}_N(1,8) = -\int_V (BL11)\{(\sigma_1)(BL12)-(\sigma_2)(BN22)\}\, dV$$

$$\bar{K}_N(1,9) = -\int_V (BL11)\{(\sigma_1)(BL13)-(\sigma_3)(BN22)\}\, dV$$

$$\bar{K}_N(1,10) = 0$$

$$\bar{K}_N(1,11) = \int_V (BL11)\{(\sigma_1)(BL111) + (\sigma_3)(BN212)\}\, dV$$

$$\bar{K}_N(1,12) = \int_V (BL11)\{(\sigma_1)(BL112) - (\sigma_2)(BN212)\}\, dV$$

$$\bar{K}_N(2,2) = \int_V [(BL12)\{(\sigma_1)(BL12) - 2(\sigma_2)(BN22)\} + (BN22)(\sigma_1)(BN22)]\, dV$$

$$\bar{K}_N(2,3) = \int_V [(BL12)\{(\sigma_1)(BL13) - (\sigma_3)(BN22)\} - (BN22)(\sigma_2)(BL13)]\, dV$$

$$\bar{K}_N(2,4) = \int_V (BN22)\{(\sigma_1)(BL24) - (\sigma_3)(BN54)\}\, dV$$

$$\bar{K}_N(2,5) = \int_V [(BL12)\{(\sigma_1)(BL15) + (\sigma_3)(BN26)\} - (BN22)(\sigma_2)(BL15)]\, dV$$

$$\bar{K}_N(2,6) = \int_V [(BL12)\{(\sigma_1)(BL16) - (\sigma_2)(BN26)\} + (BN22)(\sigma_1)(BN26) - (BN22)(\sigma_2)(BL16)]\, dV$$

$$\bar{K}_N(2,7) = -\int_V (BL11)\{(\sigma_1)(BL12) - (\sigma_2)(BN22)\}\, dV$$

$$\bar{K}_N(2,8) = -\int_V [(BL12)\{(\sigma_1)(BL12) - 2(\sigma_2)(BN22)\} + (BN22)(\sigma_1)(BN22)]\, dV$$

$$\bar{K}_N(2,9) = -\int_V [(BL12)\{(\sigma_1)(BL13) - (\sigma_3)(BN22)\} + (BN22)(\sigma_2)(BL13)]\, dV$$

$$\bar{K}_N(2,10) = -\int_V (BN22)\{(\sigma_1)(BL24) + (\sigma_3)(BN510)\}\, dV$$

$$\bar{K}_N(2,11) = \int_V [(BL12)\{(\sigma_1)(BL111) + (\sigma_3)(BN212)\} - (BN22)(\sigma_2)(BL111)]\, dV$$

$$\bar{K}_N(2,12) = \int_V [(BL12)\{(\sigma_1)(BL112) - (\sigma_2)(BN212)\} + (BN22)\{(\sigma_1)(BN212) - (\sigma_2)(BL112)\}]\, dV$$

$$\bar{K}_N(3,3) = \int_V [(BL13)\{(\sigma_1)(BL13) - 2(\sigma_3)(BN22)\} + (BN22)(\sigma_1)(BN22)]\, dV$$

$$\bar{K}_N(3,4) = \int_V (BN22)\{(\sigma_1)(BL34) + (\sigma_2)(BN54)\}\, dV$$

$$\bar{K}_N(3,5) = \int_V [(BL13)\{(\sigma_1)(BL15) + (\sigma_3)(BN26)\} - (BN22)\{(\sigma_1)(BN26) + (\sigma_3)(BL15)\}]\, dV$$

$$\bar{K}_N(3,6) = \int_V [(BL13)\{(\sigma_1)(BL16) - (\sigma_2)(BN26)\} - (BN22)(\sigma_3)(BL16)]\, dV$$

$$\bar{K}_N(3,7) = \int_V (BL11)\{(\sigma_3)(BN22) - (\sigma_1)(BL13)\}\, dV$$

$$\bar{K}_N(3,8) = \int_V [(BL13)\{(\sigma_2)(BN22) - (\sigma_1)(BL12)\} + (BN22)(\sigma_3)(BL12)]\, dV$$

$$\bar{K}_N(3,9) = \int_V [(BL13)\{(\sigma_3)(BN22) - (\sigma_1)(BL13)\} - (BN22)\{(\sigma_1)(BN22) - (\sigma_3)(BL13)\}]\, dV$$

$$\bar{K}_N(3,10) = -\int_V (BN22)\{(\sigma_1)(BL34) - (\sigma_2)(BN510)\}\, dV$$

$$\bar{K}_N(3,11) = \int_V [(BL13)\{(\sigma_1)(BL111) + (\sigma_3)(BN212)\} - (BN22)\{(\sigma_1)(BN212) + (\sigma_3)(BL111)\}]\, dV$$

$$\bar{K}_N(3,12) = \int_V [(BL13)\{(\sigma_1)(BL112) - (\sigma_2)(BN212)\} - (BN22)(\sigma_3)(BL112)]\, dV$$

$$\bar{K}_N(4,4) = \int_V [(BL24)\{(\sigma_1)(BL24) - 2(\sigma_3)(BN54)\} + (BL34)\{(\sigma_1)(BL34) + 2(\sigma_2)(BN54)\}]\, dV$$

$$\bar{K}_N(4,5) = -\int_V (BN26)\{(\sigma_1)(BL34) + (\sigma_2)(BN54)\}\, dV$$

$$\bar{K}_N(4,6) = \int_V (BN26)\{(\sigma_1)(BL24) - (\sigma_3)(BN54)\}\, dV$$

$$\bar{K}_N(4,7) = 0$$

$$\bar{K}_N(4,8) = -\int_V (BN22)\{(\sigma_1)(BL24) - (\sigma_3)(BN54)\}\,dV$$

$$\bar{K}_N(4,9) = -\int_V (BN22)\{(\sigma_1)(BL34) + (\sigma_2)(BN54)\}\,dV$$

$$\bar{K}_N(4,10) = -\int_V [(BL24)\{(\sigma_1)(BL24) + (\sigma_3)(BN510) - (\sigma_3)(BN54)\} + (BL34)\{(\sigma_1)(BL34) - (\sigma_2)(BN510) + (\sigma_2)(BN54)\}]\,dV$$

$$\bar{K}_N(4,11) = -\int_V (BN212)\{(\sigma_1)(BL34) - (\sigma_2)(BN54)\}\,dV$$

$$\bar{K}_N(4,12) = \int_V (BN212)\{(\sigma_1)(BL24) - (\sigma_3)(BN54)\}\,dV$$

$$\bar{K}_N(5,5) = \int_V [(BL15)\{(\sigma_1)(BL15) - 2(\sigma_3)(BN26)\} + (BN26)(\sigma_1)(BN26)]\,dV$$

$$\bar{K}_N(5,6) = \int_V [(BL15)\{(\sigma_1)(BL16) - (\sigma_2)(BN26)\} + (BN26)(\sigma_3)(BL16)]\,dV$$

$$\bar{K}_N(5,7) = -\int_V (BL11)\{(\sigma_1)(BL15) + (\sigma_3)(BN26)\}\,dV$$

$$\bar{K}_N(5,8) = -\int_V [(BL15)\{(\sigma_1)(BL12) - (\sigma_2)(BN22)\} + (BN26)(\sigma_3)(BL12)]\,dV$$

$$\bar{K}_N(5,9) = -\int_V [(BL15)\{(\sigma_1)(BL13) - (\sigma_3)(BN22)\} + (BN26)\{(\sigma_3)(BL13) - (\sigma_1)(BN22)\}]\, dV$$

$$\bar{K}_N(5,10) = \int_V (BN26)\{(\sigma_1)(BL34) - (\sigma_2)(BN510)\}\, dV$$

$$\bar{K}_N(5,11) = \int_V [(BL15)\{(\sigma_1)(BL111) + (\sigma_3)(BN212)\} + (BN26)\{(\sigma_1)(BN212) + (\sigma_3)(BL111)\}]\, dV$$

$$\bar{K}_N(5,12) = \int_V [(BL15)\{(\sigma_1)(BL112) - (\sigma_2)(BN212)\} + (BN26)(\sigma_3)(BL112)]\, dV$$

$$\bar{K}_N(6,6) = \int_V [(BL16)\{(\sigma_1)(BL16) - 2(\sigma_2)(BN26)\} + (BN26)(\sigma_1)(BN26)]\, dV$$

$$\bar{K}_N(6,7) = -\int_V (BL11)\{(\sigma_1)(BL16) - (\sigma_2)(BN26)\}\, dV$$

$$\bar{K}_N(6,8) = -\int_V [(BL16)\{(\sigma_1)(BL12) - (\sigma_2)(BN22)\} + (BN26)\{(\sigma_1)(BN22) - (\sigma_2)(BL12)\}]\, dV$$

$$\bar{K}_N(6,9) = -\int_V [(BL16)\{(\sigma_1)(BL13) - (\sigma_3)(BN22)\} - (BN26)(\sigma_2)(BL13)]\, dV$$

$$\bar{K}_N(6,10) = -\int_V (BN26)\{(\sigma_1)(BL24) + (\sigma_3)(BN510)\}\, dV$$

$$\bar{K}_N(6,11) = \int_V [(BL16)\{(\sigma_1)(BL111) + (\sigma_3)(BN212)\} - (BN26)(\sigma_2)(BL111)]\, dV$$

$$\bar{K}_N(6,12) = \int_V [(BL16)\{(\sigma_1)(BL112) - (\sigma_2)(BN212)\} + (BN26)\{(\sigma_1)(BN212) - (\sigma_2)(BL112)\}]\, dV$$

$$\bar{K}_N(7,7) = \int_V (BL11)(\sigma_1)(BL11)\, dV$$

$$\bar{K}_N(7,8) = \int_V (BL11)\{(\sigma_1)(BL12) - (\sigma_2)(BN22)\}\, dV$$

$$\bar{K}_N(7,9) = \int_V (BL11)\{(\sigma_1)(BL13) - (\sigma_3)(BN22)\}\, dV$$

$$\bar{K}_N(7,10) = 0$$

$$\bar{K}_N(7,11) = -\int_V (BL11)\{(\sigma_1)(BL111) + (\sigma_3)(BN212)\}\, dV$$

$$\bar{K}_N(7,12) = -\int_V (BL11)\{(\sigma_1)(BL112) - (\sigma_2)(BN212)\}\, dV$$

$$\bar{K}_N(8,8) = \int_V [(BL12)\{(\sigma_1)(BL12) - 2(\sigma_2)(BN22)\} + (BN22)(\sigma_1)(BN22)]\, dV$$

$$\bar{K}_N(8,9) = \int_V [(BL12)\{(\sigma_1)(BL13) - (\sigma_3)(BN22)\} - (BN22)(\sigma_2)(BL13)]\, dV$$

$$\bar{K}_N(8,10) = \int_V (BN22)\{(\sigma_1)(BL24) + (\sigma_3)(BN510)\}\, dV$$

$$\bar{K}_N(8,11) = -\int_V [(BL12)\{(\sigma_1)(BL111) - (\sigma_3)(BN212)\} - (BN22)(\sigma_2)(BL111)]\, dV$$

$$\bar{K}_N(8,12) = -\int_V [(BL12)\{(\sigma_1)(BL112) + (\sigma_2)(BN212)\} + (BN22)\{(\sigma_1)(BN212) - (\sigma_2)(BL112)\}]\, dV$$

$$\bar{K}_N(9,9) = \int_V [(BL13)\{(\sigma_1)(BL13) - (\sigma_3)(BN22)\} + (BN22)\{(\sigma_1)(BN22) - (\sigma_3)(BL13)\}]\, dV$$

$$\bar{K}_N(9,10) = \int_V (BN22)\{(\sigma_1)(BL34) - (\sigma_2)(BN510)\}\, dV$$

$$\bar{K}_N(9,11) = -\int_V [(BL13)\{(\sigma_1)(BL111) - (\sigma_3)(BN212)\} - (BN22)\{(\sigma_1)(BN212) + (\sigma_3)(BL111)\}]\, dV$$

$$\bar{K}_N(9,12) = -\int_V [(BL13)\{(\sigma_1)(BL112) - (\sigma_2)(BN212)\} - (BN22)(\sigma_3)(BL112)]\, dV$$

$$\bar{K}_N(10,10) = \int_V [(BL24)\{(\sigma_1)(BL24) + 2(\sigma_3)(BN510)\} + (BL34)\{(\sigma_1)(BL34) - 2(\sigma_2)(BN510)\}]\, dV$$

$$\bar{K}_N(10,11) = \int_V (BN212)\{(\sigma_1)(BL34) - (\sigma_2)(BN510)\}\, dV$$

$$\bar{K}_N(10,12) = -\int_V (BN212)\{(\sigma_1)(BL24) + (\sigma_3)(BN510)\}\, dV$$

$$\bar{K}_N(11,11) = \int_V [(BL111)\{(\sigma_1)(BL111) + 2(\sigma_3)(BN212)\} + (BN212)(\sigma_1)(BN212)]\, dV$$

$$\bar{K}_N(11,12) = \int_V [(BL111)\{(\sigma_1)(BL112) - (\sigma_2)(BN212)\} + (BN212)(\sigma_3)(BL12)]\, dV$$

$$\bar{K}_N(12,12) = \int_V [(BL112)\{(\sigma_1)(BL112) - 2(\sigma_2)(BN212)\} + (BN212)(\sigma_1)(BN212)]\, dV$$

where $BL\ 11 = -\frac{1}{L}$,

$BL\ 12 = \frac{6q}{L^2} - \frac{12pq}{L^3}$,

$BL\ 13 = \frac{6r}{L^2} - \frac{12pq}{L^3}$,

$BL\ 15 = -\frac{4r}{L} + \frac{6pr}{L^2}$,

$BL\ 16 = \frac{4q}{L} - \frac{6pq}{L^2}$,

$BL111 = -\frac{2r}{L} + \frac{6pr}{L^2}$,

$BL112 = \frac{2q}{L} - \frac{6pq}{L^2}$,

$BL\ 24 = \frac{r}{L}$, (2.89)

$BL\ 34 = -\frac{q}{L}$,

$BN\ 22 = -\frac{6p}{L^2} + \frac{6p^2}{L^3}$,

$BN\ 26 = 1 - \frac{4p}{L} + \frac{3p^2}{L^2}$,

$BN212 = -\frac{2p}{L} + \frac{3p^2}{L^2}$,

$BN\ 54 = 1 - \frac{p}{L}$,

$BN510 = \frac{p}{L}$,

$\sigma_1 = \bar{\tau}_{11} = \bar{\sigma}_p$,

$\sigma_2 = \bar{\tau}_{12} = \bar{\tau}_{pq}$,

and $\sigma_3 = \bar{\tau}_{13} = \bar{\tau}_{yz}$

The nonlinear strain incremental stiffness matrix is symmetric, and only the diagonal and upper off-diagonal components are listed above. The final evaluation of the nonlinear strain incremental stiffness matrix is performed by using an appropriate numerical integration scheme which will be described later.

(8) Internal Force Vector

The internal force vector F of Equation (2.85) is evaluated by using Table 2.1 and Equation (2.53). The simplified form is

$$\bar{F}(1) = \int_V (BL\ 11)(\sigma_1)\, dV$$

$$\bar{F}(2) = \int_V (BL\ 12)(\sigma_1)\, dV$$

$$\bar{F}(3) = \int_V (BL\ 13)(\sigma_1)\, dV$$

$$\bar{F}(4) = \int_V \{(BL\ 24)(\sigma_2) + (BL\ 34)(\sigma_3)\}\, dV$$

$$\bar{F}(5) = \int_V (BL\ 15)(\sigma_1)\, dV$$

$$\bar{F}(6) = \int_V (BL\ 16)(\sigma_1)\, dV$$

$$\bar{F}(7) = -\int_V (BL\ 11)(\sigma_1)\, dV$$

$$\bar{F}(8) = -\int_V (BL\ 12)(\sigma_1)\, dV$$

$$\bar{F}\ (9) = -\int_V (BL\ 13)(\sigma_1)\, dV$$

$$\bar{F}\ (10) = -\int_V \{(BL\ 24)(\sigma_2) + (BL\ 34)(\sigma_3)\}\, dV$$

$$\bar{F}\ (11) = \int_V (BL111)(\sigma_1)\, dV$$

$$\bar{F}\ (12) = \int_V (BL112)(\sigma_1)\, dV$$

where the variables are the same as defined in Equation (2.89). The final evaluation is performed by using a numerical integration scheme.

(9) Computation of Stresses

Under the assumption that the stress components correspond to the beam element configuration at time t, we get the nodal point displacement increments by solving the incremental equation, Equation (2.88). Then we compute the corresponding strain increments, which yield the stress increments by using Equation (2.54). The addition of these stress increments to the stress components at time t yields the stress components corresponding to the configuration at time $t+\Delta t$.

For large displacement analysis, in order to evaluate the stress increments accurately the contribution to the extension of the beam element due to transverse deflection must be taken into account in evaluation of the normal strain increment (47). Thus, the strain increments are evaluated by using

$$\bar{\varepsilon}_{ii} = \sum_{\substack{j=2 \\ j\neq 7}}^{12} B_L(i,j)\,\bar{u}^j + ({}^t\bar{e}_{ii} - {}^{t-\Delta t}\bar{e}_{ii})\,\delta_{ii} \qquad (2.90)$$

where the $B_L$ (i,j) are the components of the linear strain-displacement matrix given in Table 2.1, $\delta_{ij}$ is the Kronecker delta, and

$${}^t\bar{e}_{ii} = ({}^tL - {}^0L)/{}^0L \qquad (2.91)$$

in which ${}^0L$ is the original length of the beam element, and ${}^tL$ is the length at time t.

By using Table 2.1 and Equation (2.54) we have the following expressions for the stress increments

$$\begin{aligned}
\bar{S}(1) &= E\{(BL12)(\bar{u}^2-\bar{u}^8)+(BL13)(\bar{u}^3-\bar{u}^9)+(BL15)\bar{u}^5 \\
&\quad +(BL16)\bar{u}^6+(BL111)\bar{u}^{11}+(BL112)\bar{u}^{12}+\frac{{}^tL-{}^{t-\Delta t}L}{{}^0L} \\
\bar{S}(2) &= G\,(BL24)(\bar{u}^4-\bar{u}^{10}) \qquad (2.92) \\
\bar{S}(3) &= G\,(BL34)(\bar{u}^4-\bar{u}^{10})
\end{aligned}$$

where E = Young's modulus, G = Shear modules, and other variables are the same as defined in Equations (2.89) and (2.91).

(10) Transformation to Global Coordinates

To solve for entire structure, the incremental stiffness matrix and the internal force vector of each beam element evaluated in the moving coordinate system of the element at the current time t should be transformed to a fixed global coordinate system. The transformation can be accomplished in two steps, transformation from current to initial beam coordinate axes and transformation from initial beam coordinate axes to global coordinate axes.

The global to initial beam element coordinate transformation matrix, denoted by $[{}^{\circ}\underset{\sim}{T}]$, is constructed from the direction cosines of the beam element coordinate axes with respect to the global coordinate axes. With the three global coordinates corresponding to two nodal points of the beam element and a reference point as shown in Figure 2.2, the direction cosines are easily computed.

The initial to current beam element coordinate transformation matrix, denoted by $[\bar{\underset{\sim}{T}}]$, is evaluated using Euler angles which define the rotations of the beam (47). These angles are shown in Figure 2.4. In the figure

$\alpha$ = rotation of coordinate axes about ${}_{t_0}\bar{X}_2$ axis
$({}_{t_0}\bar{X}_1, {}_{t_0}\bar{X}_2, {}_{t_0}\bar{X}_3)$ to $(\bar{\bar{I}}\bar{J}_1, {}_{t_0}\bar{X}_2, \tilde{r})$

$\beta$ = rotation of coordinate axes about $\tilde{r}$ axis
$(\bar{\bar{I}}\bar{J}_1, {}_{t_0}\bar{X}_2, \tilde{r})$ to $(\tilde{p}, \tilde{q}, \tilde{r})$

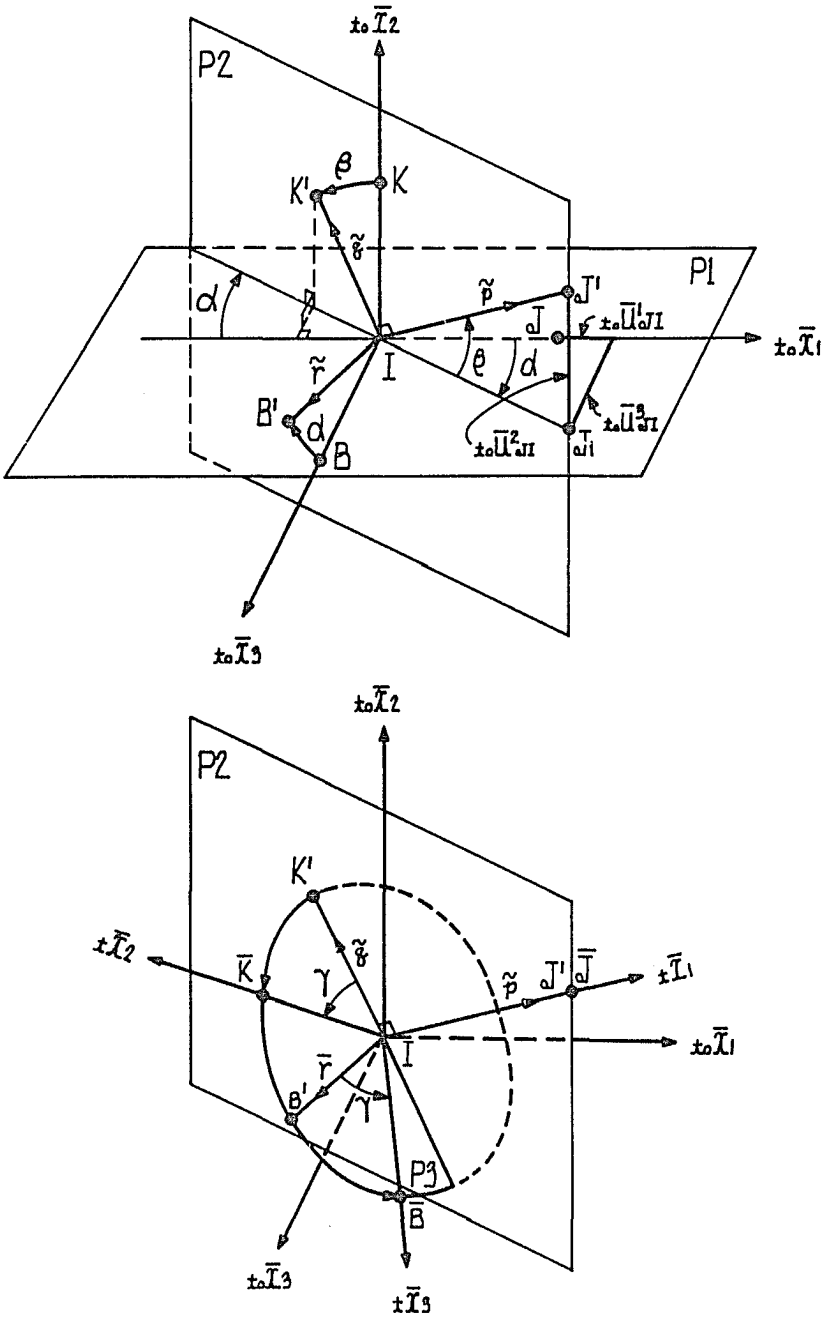


Figure 2.4. Rotation of beam element coordinate axes

$\gamma$ = rotation of coordinate axes about $\tilde{p}$ axis,

and the plane P1 is perpendicular to the plane P2 while the plane P3 is perpendicular to $\tilde{p}$ axis.

First, the relative translational displacements of node 1 and 2 (I and J in Figure 2.4) measured in the initial beam coordinate system are evaluated as

$$ {}_{t_o}\bar{U}^i_{JI} = {}^{o}\underset{\sim}{T}\,( u^{j+6} - {}^{t}u^{j} ) \qquad (i=1,2,3,\ \text{sum on } j=1,2,3) $$

where the ${}^{t}u^{k}$ are the element nodal point displacements measured in the global coordinate system, and the ${}^{o}T_{ij}$ are components of the matrix $[{}^{o}T]$ which transforms the global nodal point displacements to the element local axes at time $t_o$. Then the components of the matrix $[\bar{\underset{\sim}{T}}]$ are derived from the direction cosines of the axes ${}_{t}\bar{x}_i$ (i=1,2,3) with respect to the axes ${}_{t_o}\bar{x}_i$ (i=1,2,3). We begin with evaluating the transformation matrix $[\bar{\underset{\sim}{T}}^d]$ due to the relative displacements of nodes J and I whose components are the direction cosines of the axes $\tilde{p}$, $\tilde{q}$, $\tilde{r}$ with respect to ${}_{t_o}\bar{x}_i$ (i=1,2,3). These components are

$$ [\bar{\underset{\sim}{T}}^d] = \begin{bmatrix} \cos\alpha\cos\beta & \sin\beta & \sin\alpha\cos\beta \\ -\cos\alpha\sin\beta & \cos\beta & -\sin\alpha\sin\beta \\ -\sin\alpha & 0 & \cos\alpha \end{bmatrix} \qquad (2.93) $$

where the angle $\alpha$ represents the rotation about the negative ${}_{t_o}\bar{x}_3$ axis, and the angle $\beta$ represents the rotation about

the positive $\tilde{r}$ direction. With the initial length of the beam element ${}^{o}L$,

$$\cos\alpha = \frac{{}^{o}L + {}_{t_o}\bar{U}^{1}_{JI}}{\overline{IJ}_1} \tag{2.94}$$

and

$$\sin\beta = \frac{{}_{t_o}\bar{U}^{2}_{JI}}{{}^{t}L} \tag{2.95}$$

where $$\overline{I\,J}_1 = \left\{({}^{o}L + {}_{t_o}\bar{U}^{1}_{JI})^2 + ({}_{t_o}\bar{U}^{3}_{JI})^2\right\}^{1/2} \tag{2.96}$$

and the length of the beam element at time t

$${}^{t}L = \left\{(\overline{IJ}_1)^2 + ({}_{t_o}\bar{U}^{2}_{JI})^2\right\}^{1/2} \tag{2.97}$$

Next, consider the transformation matrix $[\bar{\underset{\sim}{T}}^{a}]$ that takes into account the axial rotation of the beam element. The components of the matrix $[\bar{\underset{\sim}{T}}^{a}]$ are the direction cosines between ${}_{t}\bar{X}_i$ $(i = 1,2,3)$ and the $\tilde{p}$, $\tilde{q}$, $\tilde{r}$ axes. They are evaluated as

$$[\bar{\underset{\sim}{T}}^{a}] = \begin{bmatrix} 1 & 0 & 0 \\ 0 & \cos\gamma & \sin\gamma \\ 0 & -\sin\gamma & \cos\gamma \end{bmatrix} \tag{2.98}$$

where $\gamma$ is the rigid body rotation of the beam element about $\tilde{p}$ - axis at time t. This angle is calculated using the increment

$$\Delta\gamma = \frac{1}{2}\left\{\bar{u}^{4} + \bar{u}^{10}\right\}$$

$$= \frac{1}{2}\left\{ \bar{\underset{\sim}{T}}^{d}_{11} \left( {}_{t_o}\bar{u}^{4} - {}_{t_o}\bar{u}^{10} \right) + \bar{\underset{\sim}{T}}^{d}_{12} \left( {}_{t_o}\bar{u}^{5} + {}_{t_o}\bar{u}^{11} \right) + \bar{\underset{\sim}{T}}^{d}_{13} \left( {}_{t_o}\bar{u}^{6} + {}_{t_o}\bar{u}^{12} \right) \right\} \qquad (2.99)$$

where ${}_{t_o}\bar{u}^{i}$ are the current incremental nodal point displacements measured in the initial beam element coordinate axes.

With the matrices $[\bar{\underset{\sim}{T}}^{d}]$ and $[\bar{\underset{\sim}{T}}^{a}]$, the initial to current beam element coordinate transformation matrix is evaluated by using

$$[\bar{\underset{\sim}{T}}] = [\bar{\underset{\sim}{T}}^{a}] \, [\bar{\underset{\sim}{T}}^{d}] \qquad (2.100)$$

Finally the matrix $[\underset{\sim}{T}]$ which transforms the global coordinate axes to the current beam element axes becomes

$$[\underset{\sim}{T}] = [\bar{\underset{\sim}{T}}] \, [{}^{*}\underset{\sim}{T}] \qquad (2.101)$$

For the beam element having twelve degrees of freedom as shown in Figure 2.2, the transformation matrix [T] that relates displacements measured in the global coordinate system to displacements measured in current beam element coordinate system can be constructed in the form

$$[T] = \begin{bmatrix} [\underset{\sim}{T}] & [\underset{\sim}{0}] & [\underset{\sim}{0}] & [\underset{\sim}{0}] \\ [\underset{\sim}{0}] & [\underset{\sim}{T}] & [\underset{\sim}{0}] & [\underset{\sim}{0}] \\ [\underset{\sim}{0}] & [\underset{\sim}{0}] & [\underset{\sim}{T}] & [\underset{\sim}{0}] \\ [\underset{\sim}{0}] & [\underset{\sim}{0}] & [\underset{\sim}{0}] & [\underset{\sim}{T}] \end{bmatrix} \qquad (2.102)$$

where $[\underset{\sim}{T}]$ is the 3 x 3 matrix defined above, and $[\underset{\sim}{0}]$ is the 3 x 3 matrix whose components are zeros. The matrix $[T]$ is symmetric and orthogonal, which gives the property

$$[T]^{-1} = [T]^{T} \tag{2.103}$$

Now the incremental equation for a beam element expressed in the beam element coordinate system at time t, Equation(2.88) can be expressed in the global coordinate system as

$$[K]\ \{u\} = \{\Delta R\} \tag{2.104}$$

where $[K] = [T]^{T}\ [\bar{K}]\ [T]$ (2.105)

$$\{u\} = [T]^{T}\ \{\bar{u}\} \tag{2.106}$$

and $$\{\Delta R\} = [T]^{T}\{\Delta \bar{R}\} \tag{2.107}$$

The contributions of each beam element for the $[K]$, $\{u\}$ and $\{\Delta R\}$ are assembled in the usual manner (71, 73, 74) to yield the incremental equation for the entire structural model

$$[K]_{T}\ \{u\}_{T} = \{\Delta R\}_{T} \tag{2.108}$$

The subscript T indicates the expression is for the entire structural model. Now our task is to solve Equation (2.108) by employing appropriate solution techniques. From now on, for simplicity the expressions in Equation (2.108) will be used without the subscript T. Thus Equation (2.108) will be equivalent to

$$[K]\{u\} = \{\Delta R\} \tag{2.109}$$

however, Equation (2.109) is different from Equation (2.104).

# CHAPTER 3

## SOLUTION SCHEMES

Most solution procedures for nonlinear finite element equations can be classified as either step-by-step or iterative. Both procedures have been widely used and frequently they are employed at the same time. Even though many different kinds of nonlinear solution techniques such as Newton-like, conjugate gradient (21, 60), static perturbation (41, 45), dynamic relaxation (58, 60) methods have been used successfully for many different structural problems, Newton-like methods seem to be most popular (9).

In geometrically nonlinear analysis, Newton-Raphson method has proved itself as one of the best methods of solution available, particularly for large displacement and stability analysis (1). To reduce the amount of computational effort, many analysts use a modified Newton-Raphson procedure wherein the coefficient matrix is held constant for several iterations and is updated only when the rate of convergence begins to deteriorate. Also to accelerate the convergence rate of the modified Newton-Raphson method, various iterative schemes have been introduced (2, 15, 16, 17, 19, 24). Furthermore, to replace the costly evaluation of the effective stiffness matrix by some economically obtained approximations, various quasi-Newton and secant Newton methods (6, 11, 12, 13, 14, 26, 57) have been developed. Recently an application of the

Lanczos algorithm to the Newton-Raphson method has been presented (63). In addition, various schemes that introduce constraint equations in load-displacement space at each incremental step have been developed mainly in order to effectively pass the limit points of the solution path (10, 25, 52, 59, 61, 62).

In postbuckling analysis it is required to find a solution technique which is not only efficient but also effective in passing the limit points.

(1) Incremental/Iterative Solution Procedure

In general, a nonlinear finite element analysis is accomplished most effectively by using an incremental formulation as described in Chapter 2. The relevant variables are updated incrementally at successive load or time steps in order to trace out the complete solution path.

By introducing the new notation $\{\Delta D\}$ for $\{u\}$ in order to indicate that they are incremental quantities, the governing incremental equations of the discretized model, Equation (2.109), can be expressed in the form

$$[K]\{\Delta D\} = \{\Delta R\} \tag{3.1}$$

or

$$[K]\{\Delta D\} = \{R\} - \{S\} \tag{3.2}$$

where $[K]$ is the incremental or tangent stiffness matrix corresponding to the configuration of the system at the current

load level; $\{\Delta D\}$ is the vector of nodal point incremental displacements; $\{R\}$ is the vector of externally applied nodal point loads; and $\{S\}$ is the vector of nodal point forces equivalent to the internal stresses at the given load level. For nodal equilibrium the residual forces $\{\Delta R\}$ must vanish. However, since an approximate solution is used, the $\{\Delta R\}$ vector is nonzero. Therefore, in most cases, to ensure sufficiently accurate solutions, equilibrium iterations are performed for each load step.

By employing the well known Newton-Raphson method as a representative solution scheme, the iterative solution procedure (Steps 4, 5, 6 and 7 in Figure 3.1) may be more accurately described by the equations:

$$[K]_i\{\Delta D\}_{i+1} = \{R\} - \{S\}_i \tag{3.3}$$

$$\{D\}_{i+1} = \{D\}_i + \{\Delta D\}_{i+1} \tag{3.4}$$

where $[K]_i$ and $\{S\}_i$ are based on the current displacements $\{D\}_i$ and $[K]_i, \{S\}_i$ and $\{D\}_i$ are updated after each cycle. Therefore, each iterative cycle involves the assembly and factorization of the tangent stiffness matrix, the computation of the residual forces, and the solution of a system of linear algebraic equations to find the displacement increments. After convergence at a given load level, external loads are estimated again to find the new equilibrium configuration.

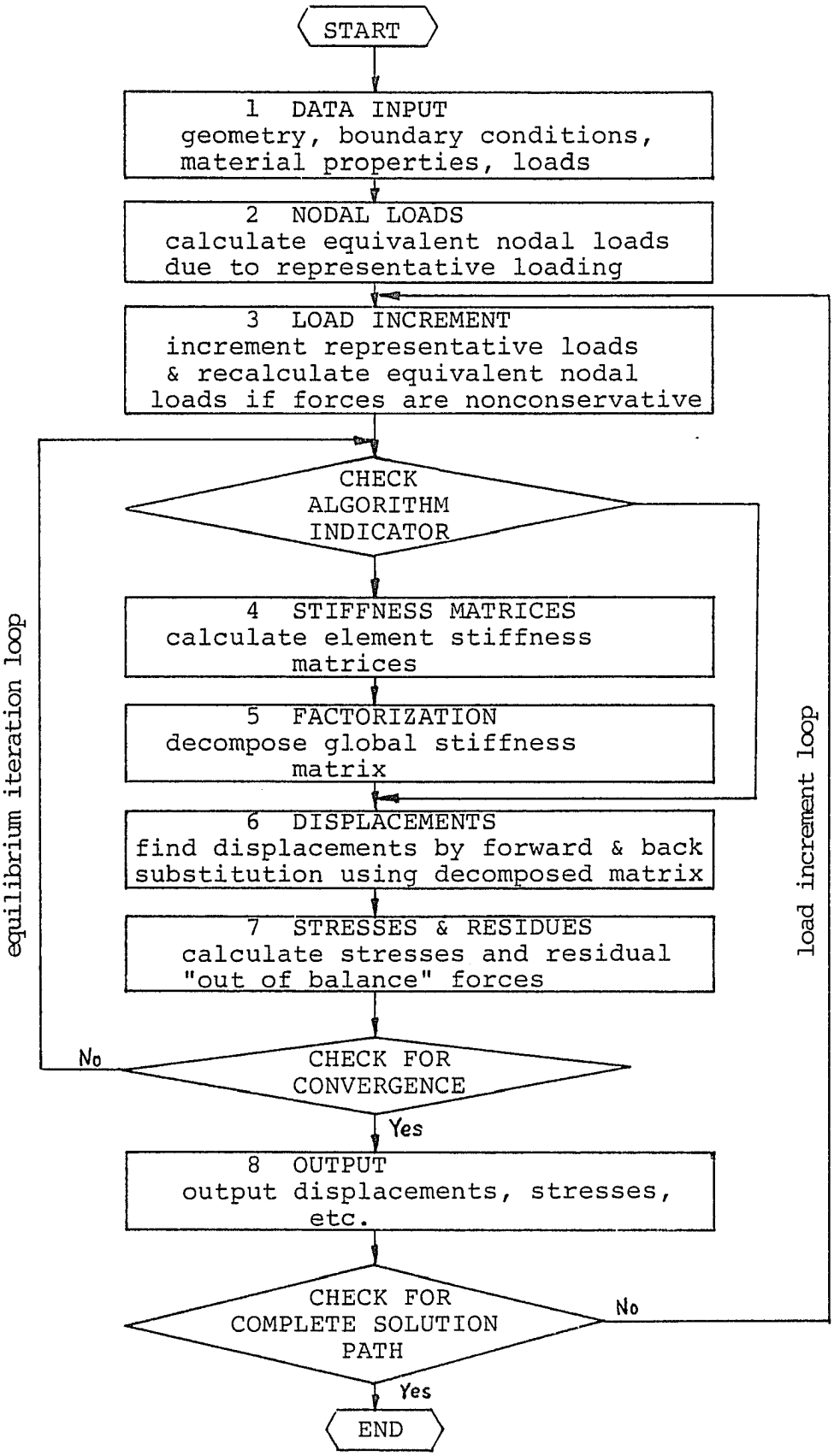


Figure 3.1. General flow-chart of nonlinear finite element structural analysis

Figure 3.1 is a general flow-chart that illustrates the basic computational scheme.

(2) Solution Schemes for tracing Postbuckling Path

While the Newton-Raphson method is a powerful iterative solution technique, it has two important short-comings.

a) inefficiencies associated with update requirements; and

b) convergence difficulties or failures in the neighborhood of limit points.

To improve the first problem many schemes, including quasi-Newton methods, have been developed.

In the past, several schemes have been suggested to overcome the second problem. The most popular procedures can be categorized as

a) introduction of fictious springs to make the tangent stiffness matrix positive definite (76),

b) use of displacement increments (75),

c) suppression of equilibrium iterations in the neighborhood of the critical point (15, 16, 17), and

d) use of constraints to control successive dependent iteration excursions (10, 25, 52, 59, 61, 62).

A possible load-displacement curve in postbuckling analysis is shown in Figure 3.2. It includes "snap-through" and "snap-back", and two horizontal limit points A and D and two vertical limit points B and C. The load incrementation at point A will yield a jump to point $A'$ while the displace-

ment incrementation at point B will produce a jump to point B'. In solution of practical problem, an algorithm for tracing the complete deformation path should satisfy the following requirements (52).

a) The method should not fail in the case of load-displacement curves having vertical tangents,

b) The method should be capable of detecting a bifurcation point to trace the second equilibrium path,

c) The symmetry and banded nature of the tangent stiffness matrix should be preserved, and

d) The load steps should be varied automatically according to the local curvature of the load-deflection curve.

The most important disadvantages of the fictious spring scheme are the trial and error often involved in the selection of the appropriate springs and the inadequateness in application to structures with local buckling or bifurcation problems. The displacement control method fails at the points of vertical tangents, and without some knowledge of the failure mode it is hard to select the appropriate displacement variables. The method of suppressing equilibrium iterations is mainly due to Bergan et al. They use the so called "current stiffness parameter" to monitor the local curvature and predict the position of the local maximum and minimum. In the neighborhood of the limit point, the iterations are suppressed and pure incrementation is used. The major setback of this scheme is that it requires very

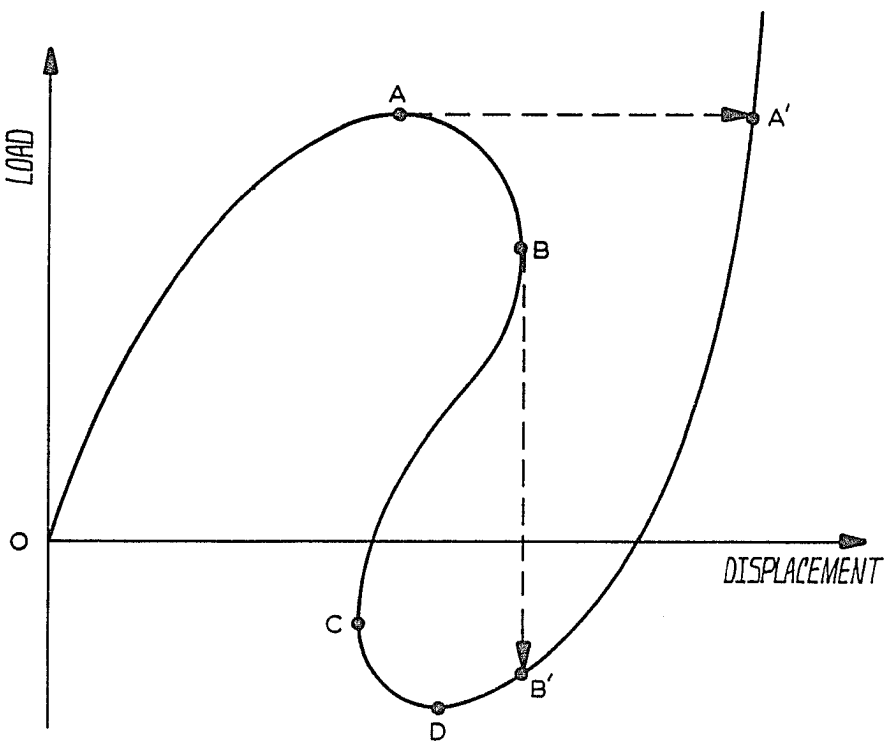


Figure 3.2. Load-displacement curve including snap-through and snap-back phenomena

small load increments to avoid drifting away from the equilibrium path near the limit points. On the other hand, the methods using constraints to control the increment step sizes and the iteration excursions appear to be most promising to be implemented for a general purpose nonlinear finite element code.

Riks (25) proposed a technique using the arc-length of the equilibrium path as control parameter. However, the addition of a constraint equation to the system of equilibrium equations destroys the property of symmetry and banded nature of the system of equations. Crisfield (10) and Ramm (61) modified this method respectively to make it easy to use with the finite element method. In computing the load increment at each iteration step, both authors use a technique similar to that suggested by Batoz and Dhatt (75) for standard displacement control. While Crisfield uses the Euclidean norm of displacement vector as the arc-length of the equilibrium path, Ramm includes load parameter in computing the arc-length. In the arc-length methods which can be associated with the Newton-Raphson, modified Newton-Raphson, or quasi-Newton methods, both displacements and loads vary during the iterations. This is achieved by constraining the iterative solutions to lie either:

a) on a plane normal to the tangent vector through the last converged point on the equilibrium path ( (2) in Fig. 3.3),

b) on a plane normal to the arc vector radiating from the last converged solution point on the equilibrium path to the last iterative solution point ( (3) in Figure 3.3), or

c) on a sphere having a radius given by the tangent vector in a) ( (4) in Figure 3.3). In each load step, Karamanlidis et al (52) use external work increments rather than load or displacements. In (61) Bergan suggests a technique that allows for incrementation of either loads or suitable displacement pattern, but constrains the load intensity and the displacements to minimize the residual force during the equilibrium iterations. Recently, Padovan and Tovichakchaikul proposed a predictor-corrector algorithm. In the predictor phase they use what they call a warpable hyper-elliptic constraint surface during the equilibrium iterations. The second corrector phase lies in the use of an energy constraint to scale the generation of the successive iterations so as to maintain the appropriate form of convergence behavior associated with the type of curvature of the zone of solution space.

While all of the constraining techniques have been used with success in tracing the postbuckling paths, the Ramm's method seems to be easiest to be implemented and still more, or at least equally, effective compared with the other techniques. In this study some improvements to the Ramm's method are made in order to make it more efficient and easier to be implemented by general users.

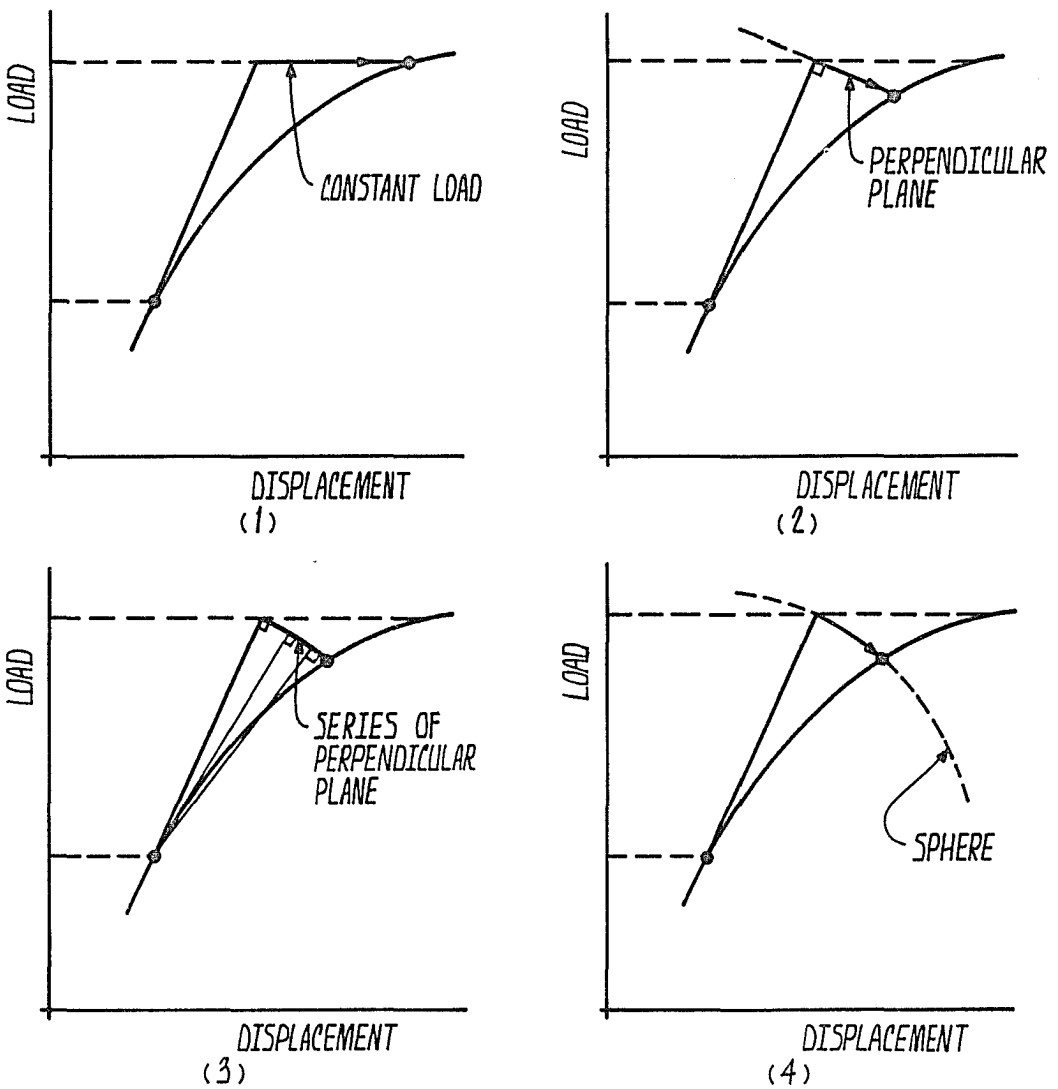


Figure 3.3 Constraints on iterative solution path

Let us assume that we have an equilibrium configuration at point m of the load-displacement path as shown in Figure 3.4. We have the total displacement vector ${}^m\{D\}$, the load vector ${}^m\{R\}$, the internal force vector ${}^m\{S\}$, and the residual force vector ${}^m\{\Delta R\}$. For proportional loading, the loads can be expressed by one load factor ${}^m\lambda$ using

$$ {}^m\{R\} = {}^m\lambda \{R_o\} \tag{3.5} $$

where $\{R_o\}$ is a vector of reference loads. Within one increment from configuration m to m + 1, consider the position i corresponding to the ith iterative cycle. The total of the increments between positions m and i are denoted by $\{\Delta D\}_i$, $\{\Delta R\}_i$ and $\Delta\lambda_i$, and the changes in increments from i to j (j = i + 1) are denoted by $\{\delta D\}_j$, $\{\delta R\}_j$ and $\delta\lambda_j$, respectively. Now we have

$$ \{D\}_j = {}^m\{D\} + \{\Delta D\}_j = {}^m\{D\} + \{\Delta D\}_i + \{\delta D\}_j \ , \tag{3.6} $$

$$ \{R\}_j = {}^m\{R\} + \{\Delta R\}_j = {}^m\{R\} + \{\Delta R\}_i + \{\delta R\}_j \ , \tag{3.7} $$

$$ \lambda_j = {}^m\lambda + \Delta\lambda_j = {}^m\lambda + \Delta\lambda_i + \delta\lambda_j \ . \tag{3.8} $$

In the constant-arc-length method, the load step $\Delta\lambda_1$ is controlled by the constraint equation:

$$ \{\Delta D\}_1^T \{\Delta D\}_1 + (\Delta\lambda_1)^2 = ({}^m l)^2 \tag{3.9} $$

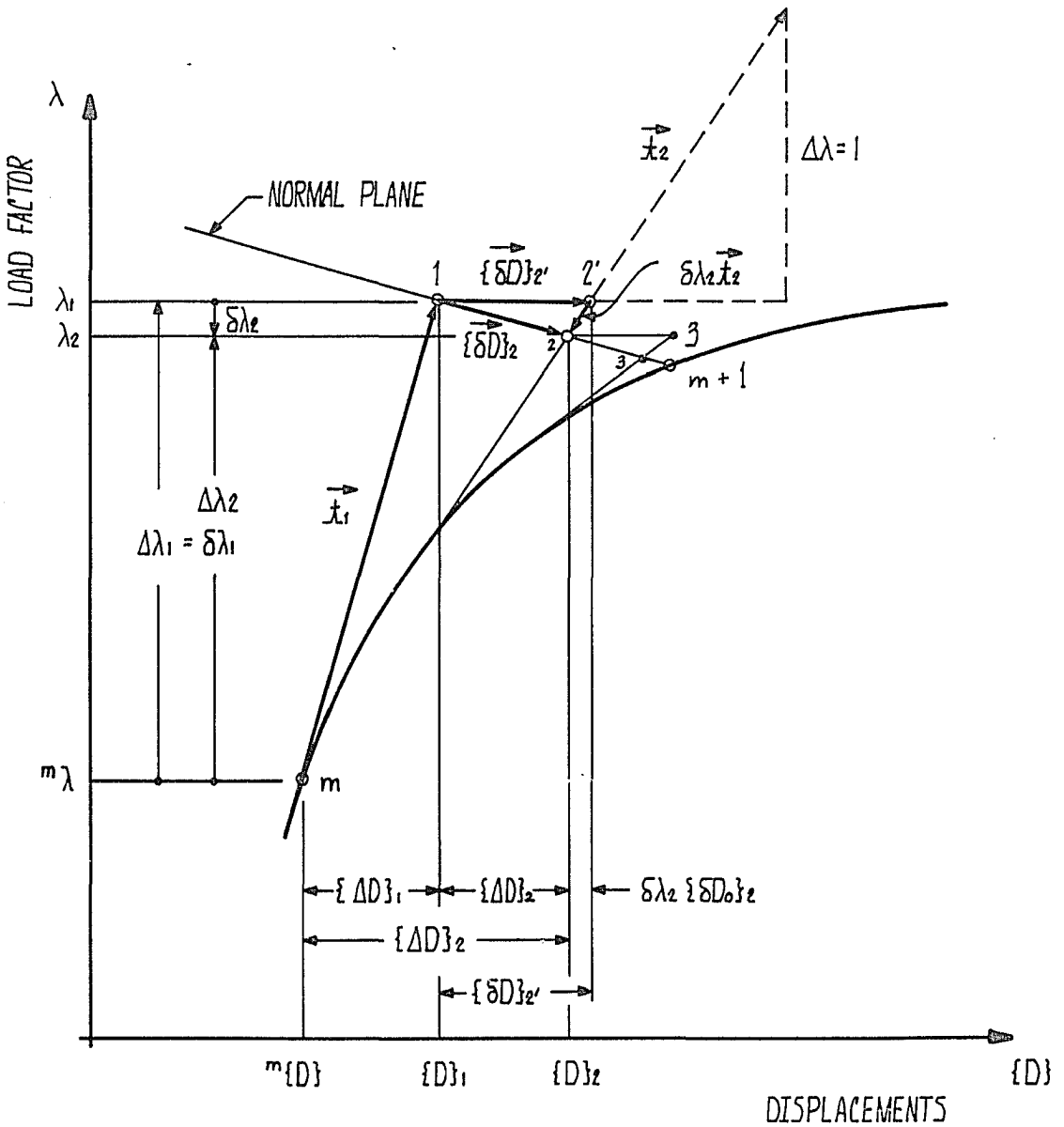


Figure 3.4. Constant-arc-length method

where $^{m}l$ is the generalized "arc-length" of the tangent at m, and should be prescribed. With the vector notation

$$\vec{t}_1 = \begin{Bmatrix} \{\Delta D\}_1 \\ \Delta\lambda_1 \end{Bmatrix} , \qquad (3.10)$$

the arc-length can be written as

$$^{m}l = |\vec{t}_1| . \qquad (3.11)$$

Of the several different kinds of constraint schemes during iteration, the normal plane method (Figure 3.3, (2)) appears to be simplest and still effective. In this study only the normal plane method is considered. The iteration path is constrained to follow a plane normal to the tangent (see Figure 3.4). The dot (scalar) product of the tangent vector $\vec{t}_1$ and the vector $\{\delta\vec{D}\}_2$ containing the unknown incremental load factor $\delta\lambda_2$ and displacements $\{\delta D\}_2$ should vanish:

$$\vec{t}_1 \cdot \{\delta D\}_2 = 0 , \qquad (3.12)$$

or

$$\{\Delta D\}_1^T \{\delta D\}_2 + \Delta\lambda_1 \delta\lambda_2 = 0 . \qquad (3.13)$$

Generally, for the jth iteration Equation (3.13) can be expressed as

$$\vec{t}_1 \cdot \{\delta\vec{D}\}_j = 0 \qquad (3.14)$$

or

$$\{\Delta D_1\}^T \{\delta D\}_j + \Delta\lambda_1 \delta\lambda_j = 0 \quad . \qquad (3.15)$$

The unknown vector $\{\delta\vec{D}\}_j$ is decomposed into two parts:

$$\{\delta\vec{D}\}_j = \{\delta\vec{D}\}_{j'} + \delta\lambda_j \vec{t}_j \quad , \qquad (3.16)$$

or

$$\{\delta D\}_j = \{\delta D\}_{j'} + \delta\lambda_j \{\delta D_o\}_j \quad . \qquad (3.17)$$

where $\{\delta D\}_{j'}$ and $\{\delta D_o\}_j$ are obtained by the equations using either the residual force vector $\{\Delta R\}_i$ or the reference load vector $\{R_o\}$ as right-hand sides. Namely,

$$[K]_i \{\delta D\}_{j'} = \{\Delta R\}_i \quad , \qquad (3.18)$$

$$[K]_i \{\delta D_o\}_j = \{R_o\} \quad . \qquad (3.19)$$

Substituting Equation (3.17) into Equation (3.15) yields

$$\delta\lambda_j = -\frac{\{\Delta D\}_1^T \{\delta D\}_{j'}}{\{\Delta D\}_1^T \{\delta D_o\}_j + \Delta\lambda_1} \quad . \qquad (3.20)$$

With the $\delta\lambda_j$ known, the corresponding displacement increments $\{\delta D\}_j$ are computed by using Equation (3.17). Then the itera-

tive solution point j is obtained by

$$\{D\}_j = \{D\}_i + \{\delta D\}_j \quad , \qquad (3.21)$$

$$\lambda_j = \lambda_i + \delta\lambda_j \quad . \qquad (3.22)$$

The above iteration procedure is repeated until the point on the iteration path converges to the point m + 1 on the equilibrium path.

(3) Modified Constant-arc-length Method

In Equation (3.9), two different kinds of variables, which have different dimensions, are employed in the computation of the "arc-length". For the problem where the incremental load factor is large compared to the displacement increments, the incremental step sizes around the limit points may be too large, which makes it difficult to locate the limit points. On the other hand, if the displacement increments are large compared to the incremental load factor, an excessively large number of incremental steps may be required in a region of severe nonlinearity, which results in unnecessarily high computing costs and sometimes even in failure to pass the limit points. Even for identical problems having the same geometry, loading conditions and initial incremental loads, the size of each incremental step will be different for different reference load levels. The user selecting a

specific reference load level and an initial load increment can predict neither the total number of incremental steps for the complete solution path nor the density of the incremental steps in specific regions, even though the characteristic of the solution path may be known from the results obtained by other investigators. Therefore, to have favorable incremental step sizes throughout the complete solution path, it is essential to have a balance between the displacement increments and the incremental load factor.

An experienced user may solve this problem by adjusting the reference load level. However, without knowing the displacement increments corresponding to the load increments in advance, it is impossible to select the right reference load level. An idea developed in this study is to scale the displacement vector to achieve a balance between the displacement increments and the incremental load factors. In this method, a user can choose the reference load level arbitrarily and take the initial load increment to define the initial incremental load factor. From the linear solution corresponding to the initial load increment, a scaling factor and a scaled "arc-length" are computed. Then the successive incremental step sizes are determined automatically.

In this scheme, Equation (3.9) is changed to

$$\{s\Delta D\}_1^T \{s\Delta D\}_1 + (\Delta\lambda_1)^2 = ({}^m l_s)^2 \quad , \qquad (3.23)$$

or

$$s^2 \{\Delta D\}_1^T \{\Delta D\}_1 + (\Delta\lambda_1)^2 = ({}^m l_s)^2 \qquad (3.24)$$

where s is the factor scaling the displacement vector, and ${}^{m}l_s$ is the scaled arc-length at incremental step m.

For the initial incremental step, Equation (3.24) becomes

$$s^2\{\Delta D\}_1^T\{\Delta D\}_1 + (\Delta\lambda_1)^2 = ({}^{\circ}l_s)^2 \qquad (3.25)$$

where $\{\Delta D\}_1$ and $\Delta\lambda_1$ are known, and s and ${}^{\circ}l_s$ are unknown. Here, we need to compute the scale factor s which produces the desired balance between the initial incremental load factor $\Delta\lambda_1$ and the scaled incremental displacement vector ${}^{s}\{\Delta D\}_1$. Now, we define a "balance factor" w as:

$$w^2 = \frac{s^2\{\Delta D\}_1^T\{\Delta D\}_1}{(\Delta\lambda_1)^2} \quad ,$$

$$\text{or} \quad w = \frac{s\sqrt{\{\Delta D\}_1^T\{\Delta D\}_1}}{\Delta\lambda_1} \quad . \qquad (3.26)$$

The balance factor w may be given by the user. Some preliminary experiments show that if w is smaller than 0.1 the incremental step sizes near the critical points become too large (Figure 3.5, (1)) while if w is larger than 1.0 the incremental step sizes become extremely small in a region of severe nonlinearity (Figure 3.5, (2)). Therefore, the generally favorable range of w appears to be between 0.1 to 1.0. The user should select a larger w value for problems having sharp turning points and smaller w values for problems having smooth turning points. If the user has no information on the characteristics of the solution path of the structural

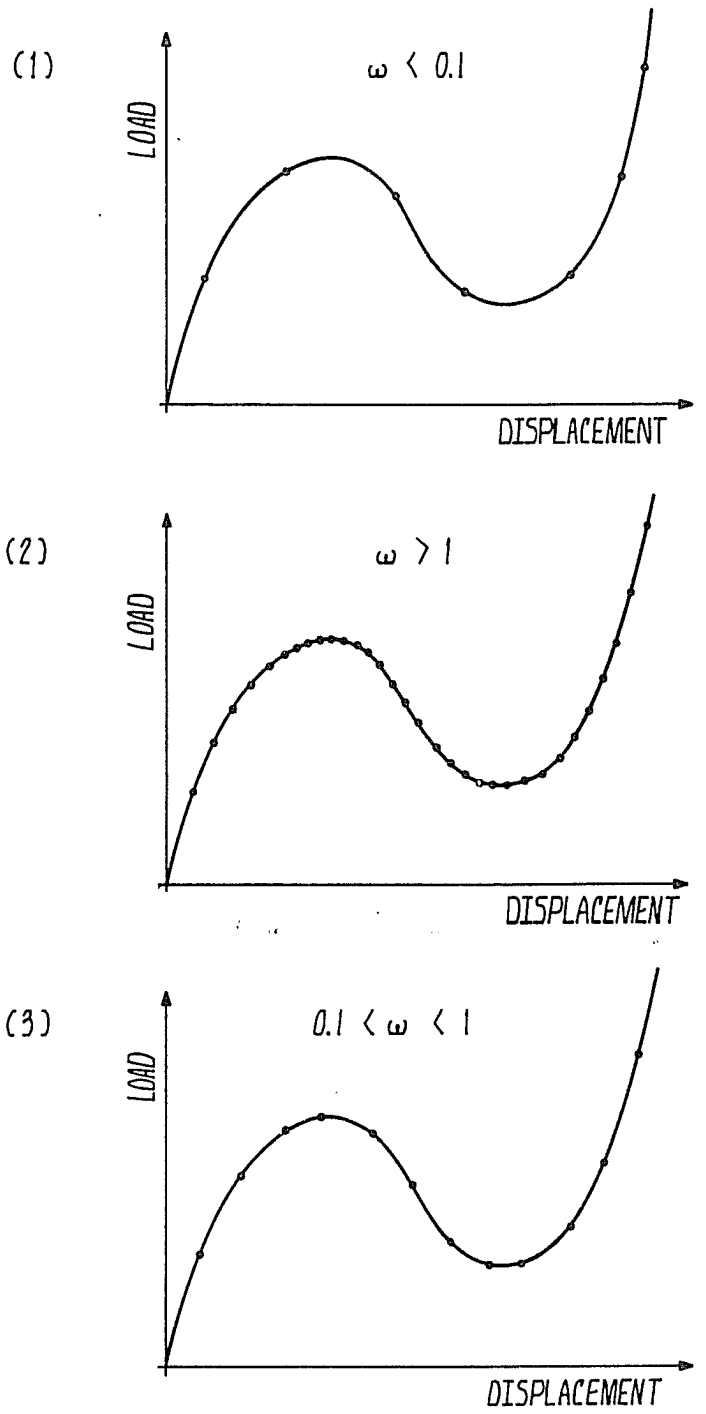


Figure 3.5. Effect of balance factor on increment steps

problem, w = 0.3 will be an adequate trial value. Even though s, w, and ${}^{m}l_s$ are kept constant through the entire set of incremental steps, the step size at each incremental step will vary because the contribution of the displacement increments in computing the scaled arc length varies according to the nonlinearity of the solution path in the region.

For a given w and a known $\{\Delta D\}_1$, which is the linear solution corresponding to the initial load factor increment $\Delta\lambda_1$, we compute the scale factor s by

$$s = \frac{w\Delta\lambda_1}{\sqrt{\{\Delta D\}_1^T \{\Delta D\}_1}} \quad . \qquad (3.27)$$

Next we compute the initial scaled arc-length ${}^{o}l_s$ by using either Equation (3.25) or

$${}^{o}l_s = \sqrt{1 + w^2}\ \Delta\lambda_1 \quad . \qquad (3.28)$$

The scaled arc-length may be kept constant for all incremental steps or may be varied according to

$${}^{m}l_s = {}^{m-1}l_s \sqrt{N_D / N_{m-1}} \qquad (3.29)$$

where ${}^{m-1}l_s$ = scaled arc-length at the previous increment step

$N_D$ = desired maximum number of iterations

$N_{m-1}$ = number of iterations required at previous increment step.

Numerical experiments performed in this study show that if we use the modified constant-arc-length method with the Newton-Raphson method, the number of iterations needed for each increment step is almost the same throughout the solution path. It excludes the need to update the scaled arc-length. However, for the modified constant-arc-length method associated with the modified Newton-Raphson method, the use of variable scaled arc-length is recommended.

For subsequent increments, we have

$$\{\Delta D\}_1 = [K]^{-1}(\Delta\lambda_1\{R_0\}) = \Delta\lambda_1\{\Delta D_0\}_1 \tag{3.30}$$

where $[K]$ is the tangent stiffness matrix corresponding to the current load level, and $\{\Delta D_0\}_1$ is computed by

$$[K]\{\Delta D_0\}_1 = \{R_0\} \tag{3.31}$$

Substituting Equation (3.30) into (3.24) yields

$$s^2(\Delta\lambda_1)^2\{\Delta D_0\}_1^T\{\Delta D_0\}_1 + (\Delta\lambda_1)^2 = (^m l_s)^2 \tag{3.32}$$

Equation (3.32) can be rewritten to give the equation for the load factor increment:

$$\Delta\lambda_1 = \pm\frac{^m l_s}{\sqrt{s^2\{\Delta D_0\}_1^T\{\Delta D_0\}_1 + 1}} \tag{3.33}$$

If a limit point is reached the determinant of [K] will change sign and a reversal of the sign of the load factor increment should be followed.

The constraints on the iteration path within an increment step are modified as shown in Figure 3.6. Now, Equation (3.15) is changed to

$$s^2 \{\Delta D_1\}^T \{\delta D\}_j + \Delta\lambda_1 \delta\lambda_j = 0 \quad . \qquad (3.34)$$

Accordingly, Equation (3.20) is also changed to

$$\delta\lambda_j = - \frac{s^2 \{\Delta D\}_1^T \{\delta D\}_{j'}}{s^2 \{\Delta D\}_1^T \{\delta D_0\}_j + \Delta\lambda_1} \qquad (3.35)$$

where $$\{\delta D\}_{j'} = [K]_i^{-1} \{\Delta R\}_i \quad , \qquad (3.36)$$

and $$\{\delta D_0\}_j = [K]_i^{-1} \{R_0\} \quad . \qquad (3.37)$$

If we use this method with the modified Newton-Raphson method which uses the tangent stiffness matrix [K] at the beginning of the increment step throughout the entire iteration steps, Equations (3.36) and (3.37) are replaced respectively by

$$\{\delta D\}_{j'} = [K]^{-1} \{\Delta R\}_i \quad , \qquad (3.38)$$

and $$\{\delta D_0\}_j = [K]^{-1} \{R_0\} = \{\Delta D_0\}_1 \quad . \qquad (3.39)$$

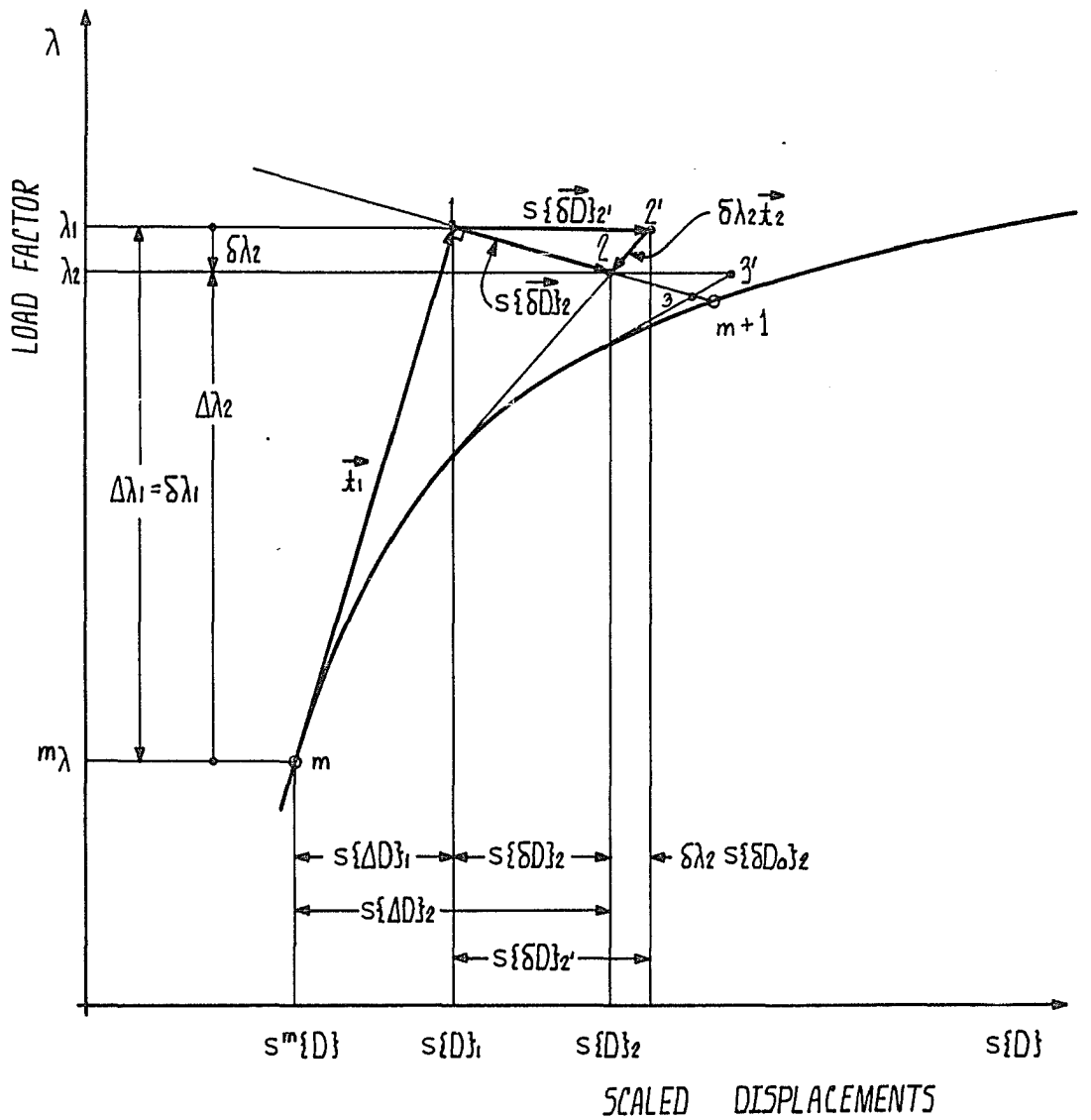


Figure 3.6. Modified constant-arc-length method

By using Equation (3.30), now Equation (3.35) becomes

$$\delta\lambda_j = - \frac{s^2 \Delta\lambda_1 \{\Delta D_0\}_1^T \{\delta D\}_j'}{s^2 \Delta\lambda_1 \{\Delta D_0\}_1^T \{\Delta D_0\}_1 + \Delta\lambda_1} \quad , \qquad (3.40)$$

or $$\delta\lambda_j = - \frac{s^2 \{\Delta D_0\}_1^T \{\delta D\}_j'}{s^2 \{\Delta D_0\}_1^T \{\Delta D_0\}_1 + 1} \quad . \qquad (3.41)$$

In this modified constant-arc-length method, compared with the Newton-Raphson method, the additional storage for the vectors $\{\Delta D\}_1$ and $\{\delta D_0\}_j$ are required if the tangent stiffness matrix is updated every iteration cycle. If the tangent stiffness matrix is updated only once at the beginning of each increment step, only additional storage for the vector $\{\Delta D_0\}_1$ is required. The performance of this algorithm is shown in Chapter 5.

(4) Solutions of Systems of Linear Equations

In every incremental or iterative step, we have to solve a system of linear equations to find the displacement increments corresponding to the load increments. In solving the system of linear equations, various schemes have been developed (77, 85). Of these the Gauss-Seidel procedure is a typical iterative solution method, and the Gauss Elimination and the Crout or Cholesky factorization procedures are representative of direct solution methods.

In solving a large-scale system of linear equations generated by the finite element solution procedure, many

algorithms including the banded, active column (profile or skyline) and frontal methods have been implemented in order to reduce both the time spent in performing the arithmetical operations as well as the required number of data transfers between core and external storage (18, 22, 23, 35, 85, 87). Also, with the use of powerful vector computers and multi-processing systems significant efforts have been devoted to vectorize the solution schemes in conjunction with parallel algorithms (88-92). In this study, the application of the direct solution procedure associated with the well-known $LDL^t$ decomposition procedure to the solution of very large system of equations using a hyper matrix scheme is employed.

To overcome the limitation of the core space of the given computer hardware, the tangent stiffness matrix is partitioned into smaller submatrices fitting the core restrictions. The details of the hypermatrix scheme employed are presented in Chapter 4.

The linearized system of equations to be solved is

$$[K]\{\Delta D\} = \{\Delta R\} \tag{3.42}$$

where the $[K]$, $\{\Delta D\}$ and $\{\Delta R\}$ are the same as defined previously. The hypermatrix $[K]$ is symmetric and divided into N partitions in each direction as shown in Figure 3.7. The submatrices have the relation

$$[K_{JI}] = [K_{IJ}]^T \tag{3.43}$$

$$
[K] = \begin{bmatrix}
[K_{11}] & [K_{12}] & [K_{13}] & & & & [K_{1N}] \\
[K_{21}] & [K_{22}] & [K_{23}] & & & & [K_{2N}] \\
[K_{31}] & [K_{32}] & [K_{33}] & & & & [K_{3N}] \\
 & & & & & & \\
 & & & & & & \\
 & & & & & & \\
 & & & & & & \\
[K_{N1}] & [K_{N2}] & [K_{N3}] & & & & [K_{NN}]
\end{bmatrix}
$$

Figure 3.7. Partitioning of tangent stiffness matrix

where I, J = 1, 2, ..., N.

A regular, symmetric, non-hyper matrix [k] can be expressed in product form as:

$$[k] = [t]^T [d][t] \tag{3.44}$$

where [t] is an upper triangular matrix which has unit entries on the diagonals, and [d] is a diagonal matrix. The above decomposition procedure can be effectively performed in the following way (77).

With $d_{11} = k_{11}$ , for the $t_{ij}$ in the jth column (j = 2,...,n), we have

$$t_{m_j,j} = k_{m_j,j} / d_{m_j,m_j} \tag{3.45}$$

and $$t_{ij} = \left( k_{ij} - \sum_{r=m_m}^{i-1} t_{ri} d_{rr} t_{rj} \right) / d_{ii} \quad \text{for } i = m_j+1, \cdots, j-1 \tag{3.46}$$

where $m_j$ is the smallest row number of the non-zero elements in the jth column, and $m_m = \max\{ m_i , m_j \}$ . And

$$d_{jj} = k_{jj} - \sum_{r=m_j}^{j-1} t_{rj} d_{rr} t_{rj} \quad . \tag{3.47}$$

To get the displacement vector $\{\Delta d\}$ in the equation

$$[k]\{\Delta d\} = \{\Delta r\} \quad , \tag{3.48}$$

we have an intermediate vector $\{v\}$ which is obtained by

$$v_1 = \Delta r_1 \quad , \tag{3.49}$$

$$v_i = \Delta r_i - \sum_{r=m_i}^{i-1} t_{ri} v_r \quad \text{for} \quad i = 2, \cdots, n \tag{3.50}$$

where $\Delta r_i$ and $v_i$ are the ith elements of $\{\Delta r\}$ and $\{v\}$. The back-substitution is performed by first having $\{\bar{v}\}$, where

$$\{\bar{v}\} = [d]^{-1}\{v\} \quad . \tag{3.51}$$

Then using $\{\bar{v}\}^{(n)} = \{\bar{v}\}$, we have $\Delta d_n = \bar{v}_n^{(n)}$. For i = n,..., 2,

$$\bar{v}_r^{(i-1)} = \bar{v}_r^{(i)} - t_{ri}\,\Delta d_i \; ; \quad r = m_i, \cdots, i-1 \tag{3.52}$$

$$\Delta d_{i-1} = \bar{v}_{i-1}^{(i-1)} \tag{3.53}$$

where the superscript (i - 1) indicates that the element is calculated in the evaluation of $\Delta d_{i-1}$.

It is usual to apply the above direct solution procedure to the solution of Equation (3.42) which has the hypermatrix in the following fashion (78).

The hypermatrix [K] is decomposed into

$$[K] = [T]^T [D][T] \tag{3.54}$$

where the upper triangular hypermatrix [T] has unit diagonal submatrices, and the diagonal hypermatrix [D] has full submatrices on the diagonals.

With $[D_{11}] = [K_{11}]$, for J = 2, ..., N

$$[T_{M_J,J}] = [D_{M_J,M_J}]^{-1}[K_{M_J,J}] \quad , \tag{3.55}$$

$$[T_{IJ}] = [D_{II}]^{-1}([K_{IJ}] - \sum_{R=M_m}^{I-1}[T_{RI}]^T[D_{RR}][T_{RJ}]) \quad , \tag{3.56}$$

for I = M +1, ..., J-1,

$$[D_{JJ}] = [K_{JJ}] - \sum_{R=M_J}^{J-1}[T_{RJ}]^T[D_{RR}][T_{RJ}] \tag{3.57}$$

where $M_J$ is the smallest row partition number of the nonzero submatrices in the Jth column partition, and $M_m = \max\{M_I, M_J\}$.

Using the [T] and [D], we have the following reduced load vector {V}:

$$\{V_1\} = \{\Delta R_1\} \tag{3.58}$$

$$\{V_I\} = \{\Delta R_I\} - \sum_{R=M_I}^{I-1}[T_{RI}]^T\{V_R\} \quad \text{for} \quad I=2,\cdots,N \tag{3.59}$$

where the subscript I of the vector indicates that the vector is a subvector corresponding to the Ith row partition of the hypervector {V}. The back-substitution is performed by first having

$$\{\bar{V}_I\} = [D_{II}]^{-1}\{V_I\} \qquad \text{for } I = 1, \ldots, N \qquad (3.60)$$

Then using $\{\bar{v}\}^{(N)} = \{\bar{v}\}$, we have

$$\{\Delta D_N\} = \{\bar{V}_N\}^{(N)} \qquad . \qquad (3.61)$$

For I = N, ..., 2

$$\{\bar{V}_R\}^{(I-1)} = \{\bar{V}_R\}^{(I)} - [T_{RI}]\{\Delta D_I\} \quad ; \; R = M_I, \cdots, I-1 \qquad (3.62)$$

$$\{\Delta D_{I-1}\} = \{\bar{V}_{I-1}\}^{(I-1)} \qquad (3.63)$$

where the superscript (I-1) indicates that the vector is calculated in the evaluation of $\{\Delta D_{I-1}\}$.

An alternative solution procedure for the system of linear equations involving the hypermatrix concept is developed in this study. The main idea is to decompose the hypermatrix [K] into the diagonal and triangular hypermatrices which are identical to the diagonal and triangular matrices obtained by decomposing the matrix [K] without partitions. Namely,

$$[K] = [\bar{T}]^T[\bar{D}][\bar{T}] \qquad (3.64)$$

where the upper triangular hypermatrix $[\bar{T}]$ has diagonal submatrices having unit diagonal elements and non-zero upper off-diagonal elements, and the diagonal submatrices of the

diagonal hypermatrix $[\bar{D}]$ consist of non-zero diagonal elements and all zero off-diagonal elements. Therefore, the diagonal hypermatrix can be considered as a vector quantity and stored in the form of a vector.

In the solution procedure, the following recursive formula are utilized. To get $[\bar{T}_{IJ}]$ of the Jth column partition, with

$$[G_{11}] = [K_{11}] \quad , \tag{3.65}$$

for J = 2, ..., N, we have

$$[G_{IJ}] = [K_{IJ}] - \sum_{R=M_m}^{I-1} [\bar{T}_{RI}]^T [\bar{D}_{RR}] [\bar{T}_{RJ}] \quad ; I = M_{J+1}, \cdots, J-1 \; . \tag{3.66}$$

This intermediate matrix $[G_{IJ}]$ is reduced to yield $[\bar{T}_{IJ}]$ whose size is m by n. For j= 1,....n, the components of $[\bar{T}_{IJ}]$ are computed by using

$$t_{1j} = g_{1j} / d_{11} \quad , \tag{3.67}$$

$$t_{ij} = (g_{ij} - \sum_{r=1}^{i-1} \bar{t}_{ri} d_{rr} t_{rj}) / d_{ii} \quad \text{for} \quad i = 2, \cdots, m \tag{3.68}$$

where $t_{ij}$ , $g_{ij}$ , $\bar{t}_{ri}$ and $d_{rr}$ are the components of the submatrices $[\bar{T}_{IJ}]$ , $[G_{IJ}]$ , $[\bar{T}_{II}]$ and $[\bar{D}_{II}]$ respectively. The diagonal submatrices are computed from

$$[G_{JJ}] = [K_{JJ}] - \sum_{R=M_J}^{J-1} [\bar{T}_{RJ}]^T [\bar{D}_{RR}] [\bar{T}_{RJ}] \quad , \tag{3.69}$$

and with $d_{11} = g_{11}$ , for j = 2, ..., n,

$$t_{1j} = g_{1j} / d_{11} \quad , \tag{3.70}$$

$$t_{ij} = (g_{ij} - \sum_{r=1}^{i-1} t_{ri}\, d_{rr}\, t_{rj})/d_{ii} \quad \text{for } i = 1,\cdots,j-1 \quad , \tag{3.71}$$

$$d_{jj} = g_{jj} - \sum_{r=1}^{j-1} t_{rj}\, d_{rr}\, t_{rj} \quad , \tag{3.72}$$

$$t_{jj} = 1 \quad , \tag{3.73}$$

where $t_{ij}$ , $g_{ij}$ and $d_{rr}$ are the components of the submatrices $[\bar{T}_{JJ}]$ , $[G_{JJ}]$ and $[\bar{D}_{RR}]$ respectively.

The forward reduction of the load vector is done by

$$\{V_1\} = \{\Delta R_1\} \quad , \tag{3.74}$$

$$\{V_I\} = \{\Delta R_I\} - \sum_{R=M_I}^{I-1} [\bar{T}_{RI}]^T \{\bar{V}_R\} \quad \text{for } I=2,\cdots,N \quad , \tag{3.75}$$

and $$\bar{v}_1 = v_1 \quad , \tag{3.76}$$

$$\bar{v}_i = v_i - \sum_{r=1}^{i-1} \bar{t}_{ri}\, \bar{v}_r \qquad \text{for } i = 2,\cdots,m \tag{3.77}$$

where $\bar{v}_i$ , $v_i$ and $\bar{t}_{ri}$ are the components of $\{\bar{V}_I\}$ , $\{V_I\}$ and $[\bar{T}_{II}]$ .

The back substitution is initiated by

$$\{\quad\} = [\bar{D}]^{-1}\{\bar{V}\} \tag{3.78}$$

or $u_i = \bar{v}_i / d_{ii}$ $\quad i = 1, \ldots$ , (size of load vector) (3.79)

where $u_i$ , $\bar{v}_i$ and $d_{ii}$ are the components of $\{U\}$, $\{\bar{V}\}$ and $[\bar{D}]$. With

$$\{U\}^{(N)} = \{U\} \quad \text{and} \quad \{\Delta\bar{D}_N\} = \{U_N\}^{(N)} \quad , \text{ for } I=N,\ldots,2$$

$$\{U_R\}^{(I-1)} = \{U_R\}^{(I)} - [\bar{T}_{RI}]\{\Delta D_I\} \quad ; \qquad (3.80)$$

$$R=M \ , \ \ldots, \ I-1$$

$$\{\Delta\bar{D}_{I-1}\} = \{U_{I-1}\}^{(I-1)} \qquad (3.81)$$

The subvector $\{\Delta\bar{D}_{I-1}\}$ whose size is m is reduced to yield the subvector $\{\Delta D_{I-1}\}$ for displacements. With $\{\Delta\bar{D}_{I-1}\}^{(m)} = \{\Delta\bar{D}_{I-1}\}$ and $\Delta d_m = \Delta\bar{d}_m$, for i = m, ..., 2

$$\Delta\bar{d}_r^{(i-1)} = \Delta\bar{d}_r^{(i)} - \bar{t}_{ri}\,\Delta d_i \quad ; \quad r = 1, \cdots, i-1 \qquad (3.82)$$

$$\Delta d_{i-1} = \Delta\bar{d}_{i-1}^{(i-1)} \qquad (3.83)$$

where $\Delta d_i$ , $\Delta\bar{d}_i$ and $\bar{t}_{ri}$ are the components of $\{\Delta D_{I-1}\}$ , $\{\Delta\bar{D}_{I-1}\}$ and $[\bar{T}_{(I-1),(I-1)}]$ respectively.

A comparison of the two solution procedures is shown in Table 3.1. In decomposition, the alternative solution procedure takes less than half of the total number of matrix-matrix multiplications needed for the conventional procedure. With additional efforts for Equations (3.67) and (3.68), the alternative procedure excludes the need to compute and store the inverses of the diagonal submatrices. In computing the

Table 3.1. Comparison of two solution procedures for system of linear equations

| | Formula | | Number of major operations | |
|---|---|---|---|---|
| | Conventional Algorithm | Alternative Algorithm | Conventional Algorithm | Alternative Algorithm |
| Decomposition | $[T_{IJ}] = [D_{II}]^{-1}\left([K_{IJ}] - \sum_{R=M_m}^{I-1}[T_{RI}]^T[D_{RR}][T_{RJ}]\right)$<br>for $I = (M_J+1), \cdots, (J-1)$<br>$J = 1, 2, \cdots, N$ | $[G_{IJ}] = [K_{IJ}] - \sum_{R=M_m}^{I-1}[\bar{T}_{RI}]^T(\bar{D}_{RR})[\bar{T}_{RJ}]$<br>$t_{ij} = (g_{ij} - \sum_{r=1}^{i-1}\bar{t}_{ri}\, d_{rr}\, t_{rj})/d_{ii}$<br>for $I = (M_J+1), \cdots, (J-1)$<br>$J = 1, 2, \cdots, N$ | 2 matrix-matrix multiplications for each R<br>1 matrix-matrix multiplication for each I | 1 matrix-matrix multiplication for each R<br>1 operation equivalent to matrix-vector multiplication for each R<br>1 forward reduction of $[G_{IJ}]$ for each I |
| | $[D_{JJ}] = [K_{JJ}] - \sum_{R=M_J}^{J-1}[T_{RJ}]^T[D_{RR}][T_{RJ}]$<br>Compute $[D_{JJ}]^{-1}$<br>for $J = 1, 2, \cdots, N$ | $[G_{JJ}] = [K_{JJ}] - \sum_{R=M_J}^{J-1}[\bar{T}_{RJ}]^T(\bar{D}_{RR})[\bar{T}_{RJ}]$<br>$t_{ij} = (g_{ij} - \sum_{r=1}^{i-1}t_{ri}\, d_{rr}\, t_{rj})/d_{ii}$<br>$d_{jj} = g_{jj} - \sum_{r=1}^{j-1}t_{rj}\, d_{rr}\, t_{rj}$<br>for $J = 1, 2, \cdots, N$ | 2 matrix-matrix multiplications for each R<br>1 matrix inverse for each J | 1 matrix-matrix multiplication and 1 operation equivalent to matrix-vector multiplication for each R<br>1 forward reduction of $[G_{JJ}]$ for each J |
| Forward reduction of load vector | $\{V_I\} = \{\Delta R_I\} - \sum_{R=M_I}^{I-1}[T_{RI}]^T\{V_R\}$<br>for $I = 1, 2, \cdots, N$ | $\{V_I\} = \{\Delta R_I\} - \sum_{R=M_I}^{I-1}[\bar{T}_{RI}]^T\{\bar{V}_R\}$<br>$\bar{v}_i = v_i - \sum_{r=1}^{i-1}\bar{t}_{ri}\bar{v}_r$, for $I = 1, 2, \cdots, N$ | 1 matrix-vector multiplication for each R | 1 matrix-vector multiplication for each R<br>1 forward reduction of $\{V_I\}$ for each I |
| Back-substitution | $\{\bar{V}_I\} = [D_{II}]^{-1}\{V_I\}$ | $U_i = \bar{v}_i / d_{ii}$ | 1 matrix-vector multiplication for each I | 1 vector division through whole solution procedure |
| | For $I = N, \cdots, 2$<br>$\{V_R\}^{(I-1)} = \{\bar{V}_R\}^{(I)} - [T_{RI}]\{\Delta D_I\}$<br>; $R = M_I, \cdots, (I-1)$<br>$\{\Delta D_{I-1}\} = \{\bar{V}_{I-1}\}^{(I-1)}$ | For $I = N, \cdots, 2$<br>$\{U_R\}^{(I-1)} = \{U_R\}^{(I)} - [\bar{T}_{RI}]\{\Delta D_I\}$<br>; $R = M_I, \cdots, (I-1)$<br>$\{\Delta \bar{D}_{I-1}\} = \{U_{I-1}\}^{(I-1)}$<br>For $i = n, \cdots, 2$<br>$\Delta \bar{d}_r^{(i-1)} = \Delta \bar{d}_r^{(i)} - \bar{t}_{ri}\Delta d_i$<br>; $r = 1, 2, \cdots, (i-1)$<br>$\Delta d_{i-1} = \Delta \bar{d}_{i-1}^{(i-1)}$ | 1 matrix-vector multiplication for each R | 1 matrix-vector multiplication for each R<br>1 back-substitution of $\{\Delta \bar{D}_I\}$ for each I |

displacement vector, inverse matrix-vector multiplications are not required for the alternative solution procedure. Instead, additional efforts are required for Equations (3.77), (3.82) and (3.83).

Counting the number of major operations and the storage requirements makes us believe that the alternative solution procedure is nearly two times faster than the conventional solution procedure in decomposition. However, it is believed that the times for computing the displacement vector after decomposition are almost the same for both procedures. Therefore, the benefit from the use of the alternative procedure with an ordinary digital computer should be high. On the other hand, when an attached array processor is used for the solution, the conventional algorighm is preferred unless we develop software implementing the operations specially needed for the alternative procedure to be suitable for computation on the array processor.

Another important advantage of using the alternative algorithm is in computing the determinant of the tangent stiffness matrix. The determinant of the tangent stiffness matrix is easily computed in the alternative procedure as the product of diagonal elements of the diagonal hypermatrix stored in a vector form, while it is computed as the product of the determinants of the diagonal submatrices of the diagonal hypermatrix in the conventional procedure.

(5) Numerical Integration

In evaluating the nonlinear strain incremental stiffness matrices and the internal force vectors of the beam element, the Newton-Cotes numerical integration scheme (70,77) is employed with the selection of four integration points in each direction. Therefore, sixty-four integration points are needed for each beam element.

The Newton-Cotes integration formula for a one-dimensional problem is given by

$$I = \int_a^b f(x)\,dx$$

$$\approx \frac{L}{8}\left[ f(x_0) + 3f(x_1) + 3f(x_2) + f(x_3) \right] \qquad (3.84)$$

where $L = b - a$, and the four integration points are evenly spaced. The application of Equation (3.84) to our three-dimensional beam problem yields

$$I = \int_{-\frac{B}{2}}^{\frac{B}{2}} \int_{-\frac{D}{2}}^{\frac{D}{2}} \int_0^L F(r,s,t)\,dr\,ds\,dt$$

$$\approx \frac{BDL}{512}\left[ \left\{ F(0,-\tfrac{D}{2},-\tfrac{B}{2}) + F(L,-\tfrac{D}{2},-\tfrac{B}{2}) + F(0,\tfrac{D}{2},-\tfrac{B}{2}) \right.\right.$$
$$+ F(L,\tfrac{D}{2},-\tfrac{B}{2}) + F(0,-\tfrac{D}{2},\tfrac{B}{2}) + F(L,-\tfrac{D}{2},\tfrac{B}{2})$$
$$\left.\left. + F(0,\tfrac{D}{2},\tfrac{B}{2}) + F(L,\tfrac{D}{2},\tfrac{B}{2}) \right\} + 3\left\{ F(\tfrac{L}{3},-\tfrac{D}{2},-\tfrac{B}{2}) \right.$$
$$\left. + F(\tfrac{2}{3}L,-\tfrac{D}{2},-\tfrac{B}{2}) + F(0,-\tfrac{D}{6},-\tfrac{B}{2}) + F(L,-\tfrac{D}{6},-\tfrac{B}{2}) \right.$$

$$+ F\left(0, \frac{D}{6}, -\frac{B}{2}\right) + F\left(L, \frac{D}{6}, -\frac{B}{2}\right) + F\left(\frac{L}{3}, \frac{D}{2}, -\frac{B}{2}\right) + F\left(\frac{2}{3}L, \frac{D}{2}, -\frac{B}{2}\right)$$

$$+ F\left(0, -\frac{D}{2}, -\frac{B}{6}\right) + F\left(L, -\frac{D}{2}, -\frac{B}{6}\right) + F\left(0, \frac{D}{2}, -\frac{B}{6}\right) + F\left(L, \frac{D}{2}, -\frac{B}{6}\right)$$

$$+ F\left(0, -\frac{D}{2}, \frac{B}{6}\right) + F\left(L, -\frac{D}{2}, \frac{B}{6}\right) + F\left(0, \frac{D}{2}, \frac{B}{6}\right) + F\left(L, \frac{D}{2}, \frac{B}{6}\right)$$

$$+ F\left(\frac{L}{3}, -\frac{D}{2}, \frac{B}{2}\right) + F\left(\frac{2}{3}L, -\frac{D}{2}, \frac{B}{2}\right) + F\left(0, -\frac{D}{6}, \frac{B}{2}\right) + F\left(L, -\frac{D}{6}, \frac{B}{2}\right)$$

$$+ F\left(0, \frac{D}{6}, \frac{B}{2}\right) + F\left(L, \frac{D}{6}, \frac{B}{2}\right) + F\left(\frac{L}{3}, \frac{D}{2}, \frac{B}{2}\right) + F\left(\frac{2}{3}L, \frac{D}{2}, \frac{B}{2}\right)\Big\}$$

$$+ 9\Big\{F\left(\frac{L}{3}, -\frac{D}{6}, -\frac{B}{2}\right) + F\left(\frac{2}{3}L, -\frac{D}{6}, -\frac{B}{2}\right) + F\left(\frac{L}{3}, \frac{D}{6}, -\frac{B}{2}\right) + F\left(\frac{2}{3}L, \frac{D}{6}, -\frac{B}{2}\right)$$

$$+ F\left(\frac{L}{3}, -\frac{D}{2}, -\frac{B}{6}\right) + F\left(\frac{2}{3}L, -\frac{D}{2}, -\frac{B}{6}\right) + F\left(0, -\frac{D}{6}, -\frac{B}{6}\right) + F\left(L, -\frac{D}{6}, -\frac{B}{6}\right)$$

$$+ F\left(0, \frac{D}{6}, -\frac{B}{6}\right) + F\left(L, \frac{D}{6}, -\frac{B}{6}\right) + F\left(\frac{L}{3}, \frac{D}{2}, -\frac{B}{6}\right) + F\left(\frac{2}{3}L, \frac{D}{2}, -\frac{B}{6}\right)$$

$$+ F\left(\frac{L}{3}, -\frac{D}{2}, \frac{B}{6}\right) + F\left(\frac{2}{3}L, -\frac{D}{2}, \frac{B}{6}\right) + F\left(0, -\frac{D}{6}, \frac{B}{6}\right) + F\left(L, -\frac{D}{6}, \frac{B}{6}\right)$$

$$+ F\left(0, \frac{D}{6}, \frac{B}{6}\right) + F\left(L, \frac{D}{6}, \frac{B}{6}\right) + F\left(\frac{L}{3}, \frac{D}{2}, \frac{B}{6}\right) + F\left(\frac{2}{3}L, \frac{D}{2}, \frac{B}{6}\right)$$

$$+ F\left(\frac{L}{3}, -\frac{D}{6}, \frac{B}{2}\right) + F\left(\frac{2}{3}L, -\frac{D}{6}, \frac{B}{2}\right) + F\left(\frac{L}{3}, \frac{D}{6}, \frac{B}{2}\right) + F\left(\frac{2}{3}L, \frac{D}{6}, \frac{B}{2}\right)\Big\}$$

$$+ 27\Big\{F\left(\frac{L}{3}, -\frac{D}{6}, -\frac{B}{6}\right) + F\left(\frac{2}{3}L, -\frac{D}{6}, -\frac{B}{6}\right) + F\left(\frac{L}{3}, \frac{D}{6}, -\frac{B}{6}\right) + F\left(\frac{2}{3}L, \frac{D}{6}, -\frac{B}{6}\right)$$

$$+ F\left(\frac{L}{3}, -\frac{D}{6}, \frac{B}{6}\right) + F\left(\frac{2}{3}L, -\frac{D}{6}, \frac{B}{6}\right) + F\left(\frac{L}{3}, \frac{D}{6}, \frac{B}{6}\right) + F\left(\frac{2}{3}L, \frac{D}{6}, \frac{B}{6}\right)\Big\}\Big] .$$

# CHAPTER 4

## SOFTWARE DESIGN

In this study, computer software was designed in FORTRAN 77 (86) for the 32 bit SEL minicomputer. The potential use of an attached 64-bit array processor is considered in the design of the software. The details of the computer configurations are given in (79) and (82).

In order to make it possible to handle large-scale problems, special techniques are employed. Major features of the special techniques are the use of a hypermatrix scheme, the construction of a data base, and the segmentation of the software package into a number of processors which are independent programs. On the other hand, to solve small problems efficiently, a single program is separately designed by combining all processors. This single program can handle problems with up to 1,000 degrees of freedom.

### (1) The Hypermatrix Scheme

The use of the finite element method in solving structural problems frequently yields large matrices which may easily exceed the main memory capacity of typical computer hardware, which makes completely in-core operations impossible. As a solution for this problem, the large-scale matrices are par-

titioned into smaller submatrices, and out-of-core operations are allowed.

Due to the core limitation on the given hardware system, the maximum allowable submatrix size and the maximum number of non-zero submatrices are limited to 50 by 50 and 3,000 respectively. The system allows a maximum of 200 partitions, which permits hypermatrices of the order of 10,000 by 10,000.

Each hypermatrix is identified by a unique name consisting of four characters and is stored on two disk files: a sequential file for directory information and a random access file for storing non-zero submatrices. The directory information includes the hypermatrix name, the number of row and column partitions, the total number of rows and columns, and a list of the number of rows/columns per row/column partition, the number of the first row/column within a row/column partition relative to the complete matrix, and the number of non-zero submatrices per row partition. Also, information on the location of each non-zero submatrix within the matrix and the record number where it is stored in the random access file are provided in the sequential file.

(2) Processors

According to the major steps of the finite element solution procedure employed in this study, eleven processors (programs) were developed. The processors share common library

subroutines and the common data through a central data base. A brief description of each processor is given below:

DATA - Reads data including geometry, boundary conditions, material properties and loads, creates disk files, and initializes the data base.

LOAD - Updates the current external nodal point load vector and adjusts the residual force vector corresponding to the load increment.

STIFF- Computes the tangent stiffness matrices for beam elements and assembles them into a global tangent stiffness hypermatrix.

DECOM- Decomposes the tangent stiffness hypermatrix into a triangular hypermatrix and a diagonal hypermatrix and computes the determinant of the tangent stiffness hypermatrix.

FRDBST-By using the triangular hypermatrix and diagonal hypermatrix obtained in DECOM, solves for the displacement vector corresponding to the known load vector.

STRESS-Updates the nodal coordinates, displacement vectors, coordinate transformation matrices corresponding to the current deformed configuration and computes the stresses, internal forces and residual forces.

CONV - Checks convergence by computing maximum norm.

OUTPUT - Prints out the job data and the nodal point displacements.

PRINTM - Prints out directory information and sub-matrices of a hypermatrix.

PRINTMD- Prints out the directory information for a hypermatrix.

PRINTV - Prints out a vector.

(3) Data Base

A data base was designed with many things in mind, amongst which are considerations of data types and the efficiency in data handling and file management. Each data group is stored in a disk file and can be accessed by each processor. In every processor using specific data stored in a specific disk file, a standard COMMON block is provided for the storage of the data. Whenever the data are needed during execution, they are transferred into core and the updated data are written back on the disk file after modification.

Each data file has a unique eight character name: four characters for the job name, one ".", and three for extension. Therefore for the same job name, each file is identified by its unique three-character extension. The descriptions of the files are given below:

.JOB - Sequential file containing the job name, number of points, number of elements, number of degrees of freedom, solution algorithm number, number

of increments, number of iterations, current load parameter, and the reference norms for convergence check.

.DIV - Sequential file containing the total displacement vector.

.IDV - Sequential file containing the incremental displacement vector corresponding to the residual force vector.

.ID0 - Sequential file containing the incremental displacement vector corresponding to the incremental loads at each increment step. This is needed for the constant-arc-length method.

.ID2 - Sequential file containing the displacement vector corresponding to the reference load at each iteration step. This information is needed for the constant-arc-length method.

.CLV - Sequential file containing the current load vector.

.RFV - Sequential file containing the residual force vector.

.RLV - Sequential file containing the reference load vector.

.DIR - Sequential file containing the directory information of the tangent stiffness hypermatrix.

.PTS - Random access file containing the initial and current coordinates and freedom pattern of each nodal point.

.ELT - Random access file containing two nodal point numbers, reference point number, area, width, depth, Young's modulus, Poisson's ratio, initial length, current length, length increment, and incremental displacements corresponding to the nodal degrees of freedom of each element.

.LDS - Random access file containing the discretized nodal point loads.

.STR - Random access file containing the stresses at 64 points of each beam element.

.BNL - Random access file containing the strain-displacement transformation matrix evaluated at 64 points of each beam element.

.TRN - Random access file containing the coordinate transformation matrices for global to initial local, initial local to current local, and global to current local coordinate systems for each beam element.

.NUM - Random access file containing the nonzero submatrices of the tangent stiffness hypermatrix.

(4) Implementation of Solution Algorithms

In this study four nonlinear solution algorithms were implemented. They are the Newton-Raphson (NR) method, the modified Newton-Raphson (MNR) method and the modified constant-arc-length methods associated with the NR and MNR procedures respectively.

The flow chart in Figure 3.1 shows the typical NR and MNR procedures, and is employed in this study. To accelerate the convergence of the MNR method, the tangent stiffness matrix is updated twice within each increment step: at the beginning of the increment step and at the time of the first iteration step.

The modified constant-arc-length methods are implemented as shown in Figure 4.1. The scaled arc-length is kept constant through the entire solution when it is used with NR procedure while it varies according to Equation (3.29) with the MNR procedure.

The useful convergence criteria for the iterative solution procedures in nonlinear structural procedures can be classified in one of the following groups: force criteria, displacement criteria, and stress criteria. Bergan and Clough (80) advocates that in many cases it is most efficient and accurate to base the convergence criterion merely on displacement quantities. In this study, the following so called maximum norm of the displacement increments is implemented:

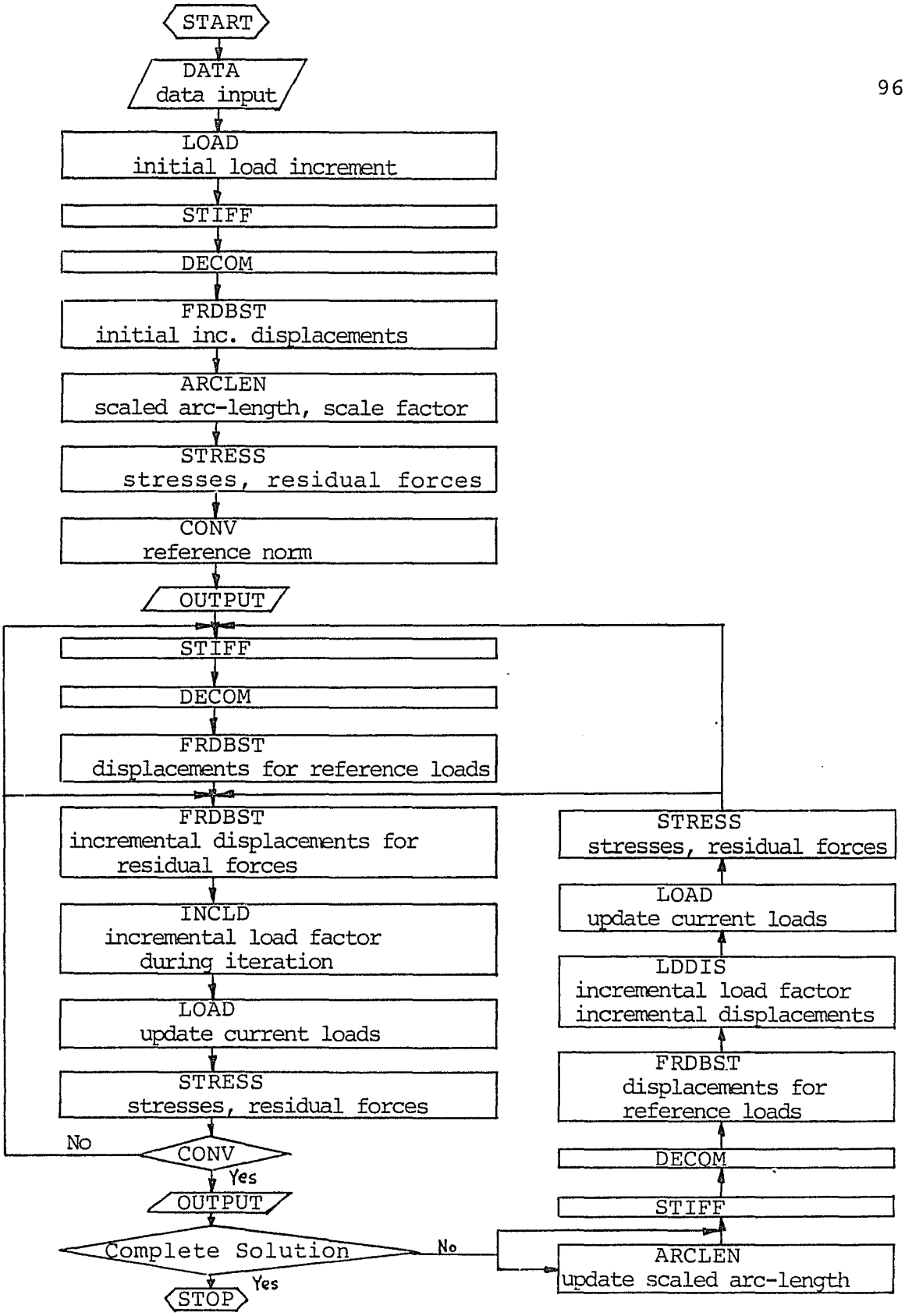


Figure 4.1. Flow-chart of modified constant-arc-length methods

$$\|\varepsilon\| = \max_i \left| \frac{\Delta d_i}{d_{i,ref}} \right| \tag{4.1}$$

where $\Delta d_i$ is the change in displacement component i during the iteration cycle, and $d_{i,ref}$ is a reference displacement quantity for the component i. The maximum translational displacement and the maximum rotational displacement taken from the linear solution for the reference loads are used for the reference displacement quantities for translational displacement components and rotational displacement components respectively. To stop the iterations, the norm should satisfy

$$\|\varepsilon\| < \alpha \tag{4.2}$$

$\alpha$ = 0.001 is used for this study

(5) Performance of Array Processor

Even though we have software designed to overcome the core limitation problem of the given system, the use of the software for large-scale problems with the minicomputer alone can still be impractical because of the extra-ordinary computer time needed for the execution.

Recent studies (81, 82, 83, 84) show that the use of an array processor for the solution of nonlinear finite element structural problems can be very effective. The array pro-

cessor is a special purpose digital computer attached to a minicomputer. It is relatively inexpensive, and can perform the arithmetic operations involving large-scale arrays considerably faster than the minicomputer. In this study a 64-bit array processor attached to a 32-bit minicomputer is considered.

To measure the performance of the array processor on the current 3-D frame structural analysis program, simulators are designed for the use of the minicomputer alone and the use of the array processor with the minicomputer. The simulators are constructed by measuring the CPU and elapsed times for basic arithmetic operations for vectors and matrices, I/O operations, and other time consuming parts in each program. In executing the simulators, the I/O or computational operations are not executed unless they are indispensably needed to correctly simulate the actual executions.

For the time measurements, a basic 3-D frame model as shown in Figure 4.2 was selected. Three different configurations of that model, described in Table 4.1, are considered, and the relative performance of the software for each case is listed in Tables 4.2, 4.3 and 4.4. In the tables, HC32 and HC32 + AP 64 represent the 32-bit minicomputer and the combination of the 32-bit minicomputer and the 64-bit minicomputer respectively. The tables indicate that one can best benefit from using the array processor in the decomposition procedures. A speed-up factor of 15 to 23 is obtained for decomposition by using the

Table 4.1. Description of structural model for three cases

| | CASE 1 | CASE 2 | CASE 3 |
|---|---|---|---|
| Number of nodes | 315 | 642 | 1436 |
| Number of elements | 378 | 783 | 1800 |
| Number of degrees of freedom | 1890 | 3852 | 8736 |
| Half-bandwith | 240 | 336 | 432 |

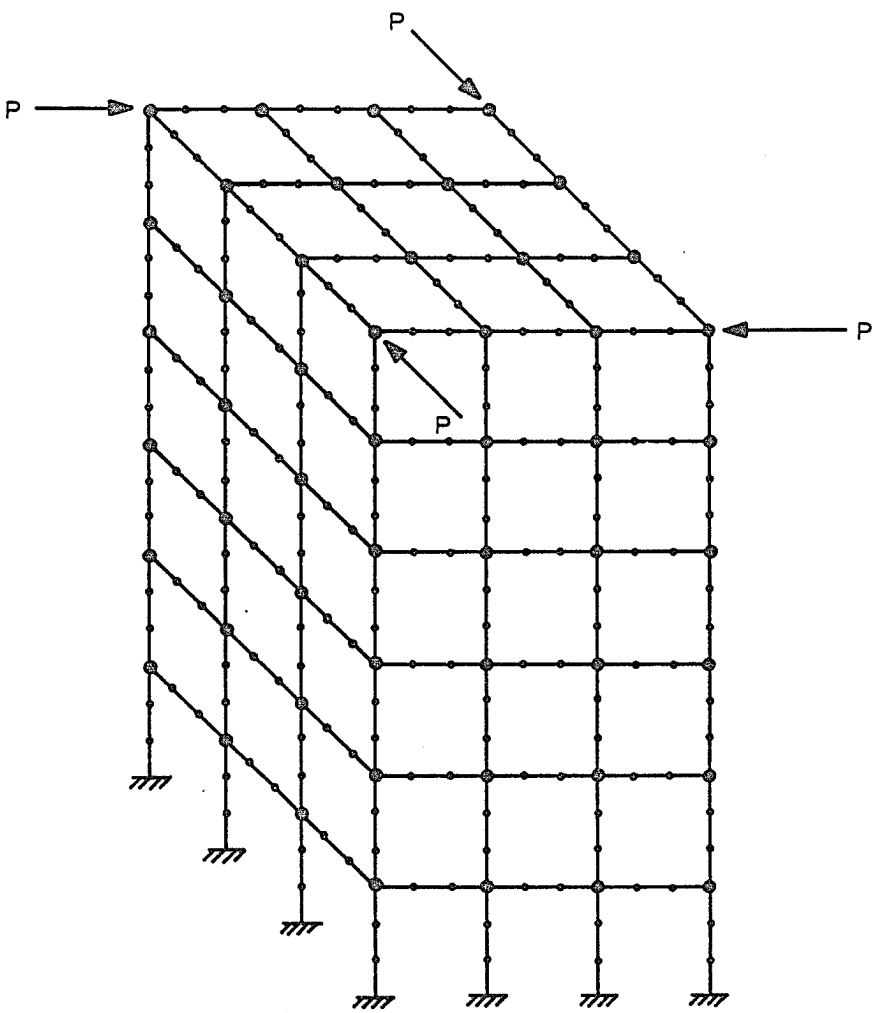


Figure 4.2. 3-D frame structural model

Table 4.2. Relative performance of Case 1

time: secs

| Processors | CPU time | | | Elapsed time | | |
|---|---|---|---|---|---|---|
| | HC32 | HC32 + AP64 | Speed-up factor | HC32 | HC32 + AP64 | Speed-up factor |
| DATA | 158 | 158 | 1.0 | 224 | 224 | 1.0 |
| LOAD | 2 | 2 | 1.0 | 6 | 6 | 1.0 |
| STIFF | 283 | 283 | 1.0 | 357 | 357 | 1.0 |
| DECOM | 3145 | 150 | 21.0 | 3202 | 205 | 15.6 |
| FRDBST | 556 | 81 | 6.9 | 606 | 131 | 4.6 |
| STRESS | 128 | 128 | 1.0 | 240 | 240 | 1.0 |
| CONV | 1 | 1 | 1.0 | 2 | 2 | 1.0 |
| OUTPUT | 1 | 1 | 1.0 | 5 | 5 | 1.0 |

Table 4.3. Relative performance of Case 2

time: secs

| Processors | CPU time | | | Elapsed time | | |
|---|---|---|---|---|---|---|
| | HC32 | HC32 + AP64 | Speed-up factor | HC32 | HC32 + AP64 | speed-up factor |
| DATA | 324 | 324 | 1.0 | 453 | 453 | 1.0 |
| LOAD | 3 | 3 | 1.0 | 8 | 8 | 1.0 |
| STIFF | 584 | 584 | 1.0 | 733 | 733 | 1.0 |
| DECOM | 10041 | 418 | 24.0 | 10162 | 537 | 18.9 |
| FRDBST | 1182 | 207 | 5.7 | 1305 | 330 | 4.0 |
| STRESS | 265 | 265 | 1.0 | 493 | 493 | 1.0 |
| CONV | 1 | 1 | 1.0 | 3 | 3 | 1.0 |
| OUTPUT | 2 | 2 | 1.0 | 10 | 10 | 1.0 |

Table 4.4. Relative performance of Case 3

time: secs

| Processors | CPU time | | | Elapsed time | | |
|---|---|---|---|---|---|---|
| | HC32 | HC32 + AP64 | speed-up factor | HC32 | HC32 + AP64 | speed-up factor |
| DATA | 741 | 741 | 1.0 | 1031 | 1031 | 1.0 |
| LOAD | 7 | 6 | 1.2 | 15 | 13 | 1.2 |
| STIFF | 1317 | 1317 | 1.0 | 1642 | 1642 | 1.0 |
| DECOM | 34879 | 1273 | 27.4 | 35161 | 1558 | 22.6 |
| FRDBST | 2804 | 579 | 4.8 | 3139 | 913 | 3.4 |
| STRESS | 608 | 608 | 1.0 | 1127 | 1127 | 1.0 |
| CONV | 2 | 2 | 1.0 | 5 | 5 | 1.0 |
| OUTPUT | 5 | 5 | 1.0 | 20 | 20 | 1.0 |

array processor, and the factor increases with the size of the problem. On the other hand, the speed-up factor for the forward and back substitution procedures to get the displacement vector, decreases with the problem size, from 4.6 to 3.4.

The estimated CPU times needed for the execution of one load increment step in the NR procedure and one equilibrium step in the MNR procedure are listed in Table 4.5 for each case. The speed-up factors for the increment loop are 6.4, 8.2, and 10.5 for the cases 1, 2, and 3 respectively. One iteration loop is speeded up by 3.3, 3.1, and 2.9 respectively for the corresponding cases.

If we breakdown the operations within the decomposition processor as shown in Table 4.6, we realize that a substantial speed up of the I/O operations may cause a significant additional speed-up. While the time for I/O operations is 2 to 4 percent of the total time on the minicomputer alone, it increases to 47 to 62 percent of the total time with the attached processor.

Therefore, in order to increase the benefit from using the attached array processor, improvements in the solution algorithms and the software design, as well as an optimization of the I/O transfer speed should be performed. More detailed investigations are presented in (79).

Table 4.5. Speed-up factors in CPU time gained by using an array processor

(1) Load increment loop of Newton Raphson procedure

time: secs

| Processors | Case 1 | | | Case 2 | | | Case 3 | | |
|---|---|---|---|---|---|---|---|---|---|
| | HC32 | HC32+ AP64 | Spd-up factor | HC32 | HC32+ AP64 | Spd-up factor | HC32 | HC32+ AP64 | Spd-up factor |
| LOAD | 2 | 2 | 1.0 | 3 | 3 | 1.0 | 7 | 6 | 1.2 |
| STIFF | 283 | 283 | 1.0 | 584 | 584 | 1.0 | 1317 | 1317 | 1.0 |
| DECOM | 3145 | 150 | 21.0 | 10041 | 418 | 24.0 | 34879 | 1273 | 27.4 |
| FRDBST | 556 | 81 | 6.9 | 1182 | 207 | 5.7 | 2804 | 579 | 4.8 |
| STRESS | 128 | 128 | 1.0 | 265 | 265 | 1.0 | 608 | 608 | 1.0 |
| CONV | 1 | 1 | 1.0 | 1 | 1 | 1.0 | 2 | 2 | 1.0 |
| Total | 4115 | 645 | 6.4 | 12076 | 1478 | 8.2 | 39617 | 3785 | 10.5 |

(2) Equilibrium iteration loop of modified Newton-Raphson procedure

time: secs

| Processors | Case 1 | | | Case 2 | | | Case 3 | | |
|---|---|---|---|---|---|---|---|---|---|
| | HC32 | HC32+ AP64 | Spd-up factor | HC32 | HC32+ AP64 | Spd-up factor | HC32 | HC32+ AP64 | Spd-up factor |
| FRDBST | 556 | 81 | 6.9 | 1182 | 207 | 5.7 | 2804 | 579 | 4.8 |
| STRESS | 128 | 128 | 1.0 | 265 | 265 | 1.0 | 608 | 608 | 1.0 |
| CONV | 1 | 1 | 1.0 | 1 | 1 | 1.0 | 2 | 2 | 1.0 |
| Total | 685 | 210 | 3.3 | 1448 | 473 | 3.1 | 3414 | 1189 | 2.9 |

Table 4.6. Distribution of elapsed time in decomposition

time: secs

| Type of operations | Time per operation | | Number of operations | | | Total time | | | | | |
|---|---|---|---|---|---|---|---|---|---|---|---|
| | | | | | | Case 1 | | Case 2 | | Case 3 | |
| | HC32 | HC32+ AP64 | Case 1 | Case 2 | Case 3 | HC32 | HC32+ AP64 | HC32 | HC32+ AP64 | HC32 | HC32+ AP64 |
| Matrix reads | 0.470 | 0.470 | 130 | 271 | 551 | 61 | 61 | 127 | 127 | 259 | 259 |
| Matrix writes | 0.470 | 0.470 | 143 | 364 | 1008 | 67 | 67 | 171 | 171 | 474 | 474 |
| Matrix-matrix multiplications | 5.173 | 0.125 | 505 | 1725 | 6246 | 2612 | 63 | 8923 | 215 | 32311 | 781 |
| Matrix inversions | 11.491 | 0.141 | 39 | 80 | 181 | 448 | 5 | 919 | 11 | 2080 | 26 |
| Others | | | | | | 14 | 9 | 22 | 13 | 37 | 18 |
| Total | | | | | | 3202 | 205 | 10162 | 537 | 35161 | 1558 |

# CHAPTER 5

# NUMERICAL EXAMPLES

In order to verify the performance of the finite element formulations and the solution algorithms employed in this study, several numerical experiments were performed. Even for small problems, tracing the complete nonlinear solution path is a very time-consuming and costly task. Due to the lack of proper array processor software, the array processor cannot be utilized at this time, which makes it impractical to solve a large problem even though the program has been designed to handle large models. Therefore, in this study only relatively small and well-known two-and three-dimensional frame problems are selected.

To reduce computing costs, relatively large step sizes are taken in tracing the solution path. In this case, the modified constant-arc-length method associated with the NR procedure is preferred to the method with the MNR procedure because of its faster convergence rate.

## (1) A Cantilever Beam

To evaluate the performance of the NR and MNR solution procedure, the cantilever beam shown in Figure 5.1 was considered. Only four beam elements were used. Figure 5.1 shows the load-deflection curves for horizontal and vertical displacements. Also the results are compared to the linear

solution and an analytical solution. Table 5.1 shows the load increment steps and number of iterations taken for each increment step. The time measurements for both procedures give almost identical values.

(2) A Toggle Frame

The toggle frame shown in Figure 5.2 was analyzed by employing five beam elements for half of the structure. The problem was initially investigated by Williams (8) experimentally and analytically.

In tracing the solution path nine increment steps were taken, and two to five iterations are required for each increment step. The results obtained in this study are in very good agreement with the results of Williams' experiment and the finite element solutions by Wood and Zienkiewicz (51) and Papadrakakis (60).

(3) A Shallow Arch

A shallow arch under a concentrated load as shown in Figure 5.3 was investigated by taking half of the structure and using six beam elements. A total of 19 increment steps were taken, and the number of iterations needed for each increment was 2 to 4.

Mallet and Berke (29) also solved the same problem up to the limit point by using four "equilibrium-based" elements. Good agreement between the two solutions is observed.

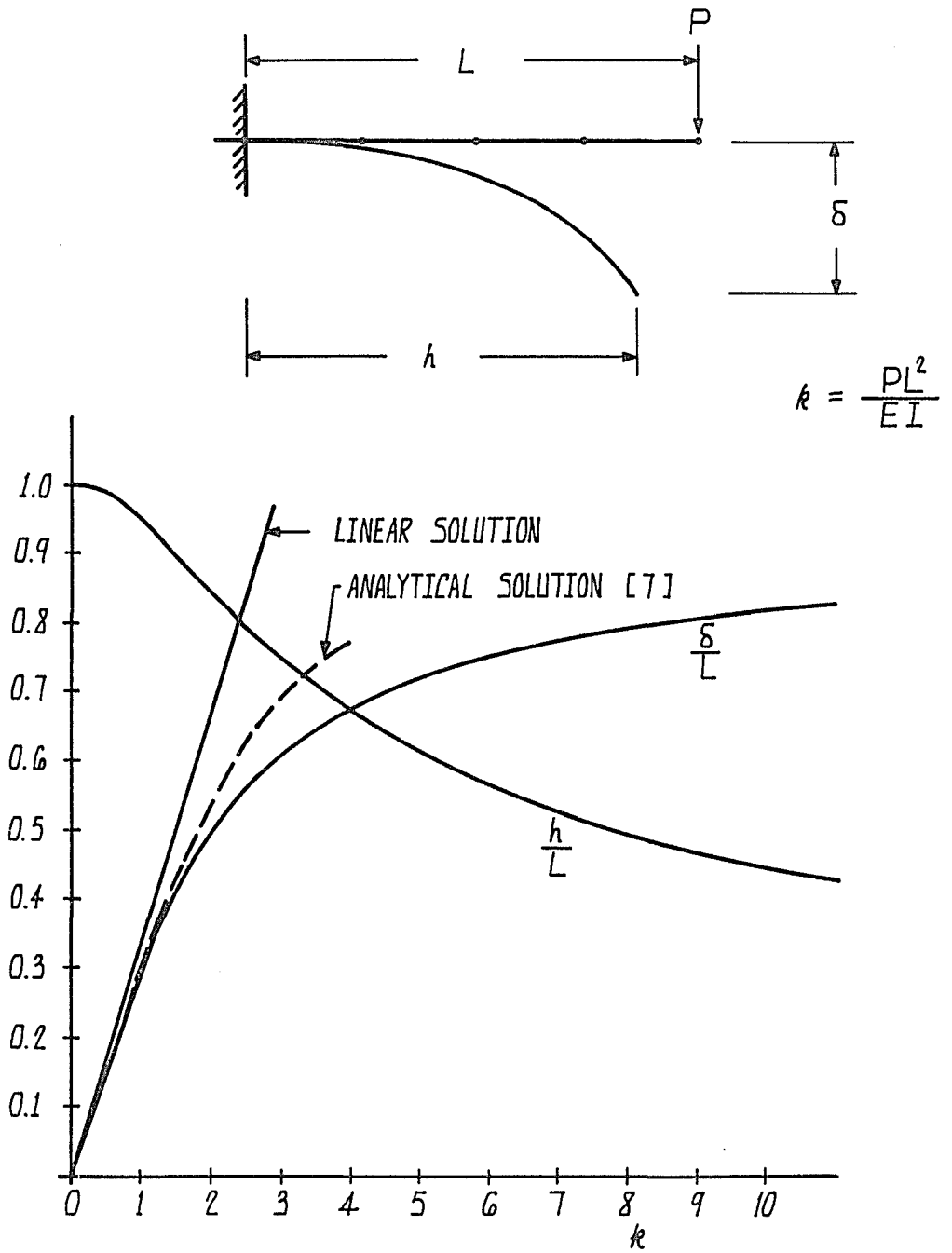


Figure 5.1. Large deflection analysis of a cantilever beam subjected to a concentrated load

Table 5.1. Performance of NR and MNR solution procedures for a cantilever beam.

L = 12"
E = $1.0 \times 10^7$ psi
A = 1 $in^2$
I = 0.0833 $in^4$
P = 2500 lbs.

| Load Level | $k$ $(\frac{PL^2}{EI})$ | No. of iterations | | Horizontal Displacement at 5 (h) | $\frac{L-h}{L}$ | Vertical Displacements | | | | $\frac{\delta}{L}$ |
|---|---|---|---|---|---|---|---|---|---|---|
| | | NR | MNR | | | at 2 | at 3 | at 4 | at 5 ($\delta$) | |
| 1 (linear) | .432 | 0 | 0 | 0 | 1.0 | 0.148 | 0.540 | 1.093 | 1.728 | 0.144 |
| 1 | .432 | 3 | 4 | 0.139 | 0.988 | 0.146 | 0.529 | 1.065 | 1.676 | 0.140 |
| 2 | .864 | 3 | 20 | 0.508 | 0.958 | 0.283 | 1.014 | 2.029 | 3.178 | 0.265 |
| 3 | 1.296 | 3 | 18 | 1.007 | 0.916 | 0.403 | 1.433 | 2.840 | 4.422 | 0.369 |
| 4 | 1.728 | 3 | 14 | 1.548 | 0.871 | 0.508 | 1.784 | 3.500 | 5.411 | 0.451 |
| 5 | 2.160 | 3 | 10 | 2.080 | 0.827 | 0.599 | 2.076 | 4.032 | 6.190 | 0.516 |
| 6 | 2.592 | 3 | 8 | 2.577 | 0.785 | 0.677 | 2.321 | 4.463 | 6.804 | 0.567 |
| 7 | 3.024 | 3 | 6 | 3.031 | 0.747 | 0.747 | 2.529 | 4.815 | 7.295 | 0.608 |
| 8 | 3.456 | 3 | 5 | 3.442 | 0.713 | 0.809 | 2.707 | 5.108 | 7.692 | 0.641 |
| 10 | 4.320 | 3 | 10 | 4.145 | 0.655 | 0.915 | 2.997 | 5.563 | 8.292 | 0.691 |
| 12 | 5.184 | 3 | 6 | 4.720 | 0.607 | 1.004 | 3.224 | 5.902 | 8.721 | 0.727 |
| 14 | 6.048 | 3 | 4 | 5.197 | 0.567 | 1.081 | 3.409 | 6.165 | 9.042 | 0.754 |
| 16 | 6.912 | 3 | 3 | 5.598 | 0.534 | 1.149 | 3.564 | 6.377 | 9.292 | 0.774 |
| 18 | 7.776 | 3 | 3 | 5.939 | 0.505 | 1.210 | 3.696 | 6.551 | 9.493 | 0.791 |
| 20 | 8.640 | 3 | 3 | 6.234 | 0.481 | 1.265 | 3.811 | 6.697 | 9.660 | 0.805 |
| 25 | 10.800 | 3 | 4 | 6.823 | 0.431 | 1.385 | 4.044 | 6.984 | 9.976 | 0.831 |
| 30 | 12.960 | 3 | 3 | 7.266 | 0.395 | 1.485 | 4.225 | 7.196 | 10.204 | 0.850 |

CPU time: NR 592.5 secs MNR 593.5 secs

Elapsed time: NR 1292 secs MNR 1333 secs

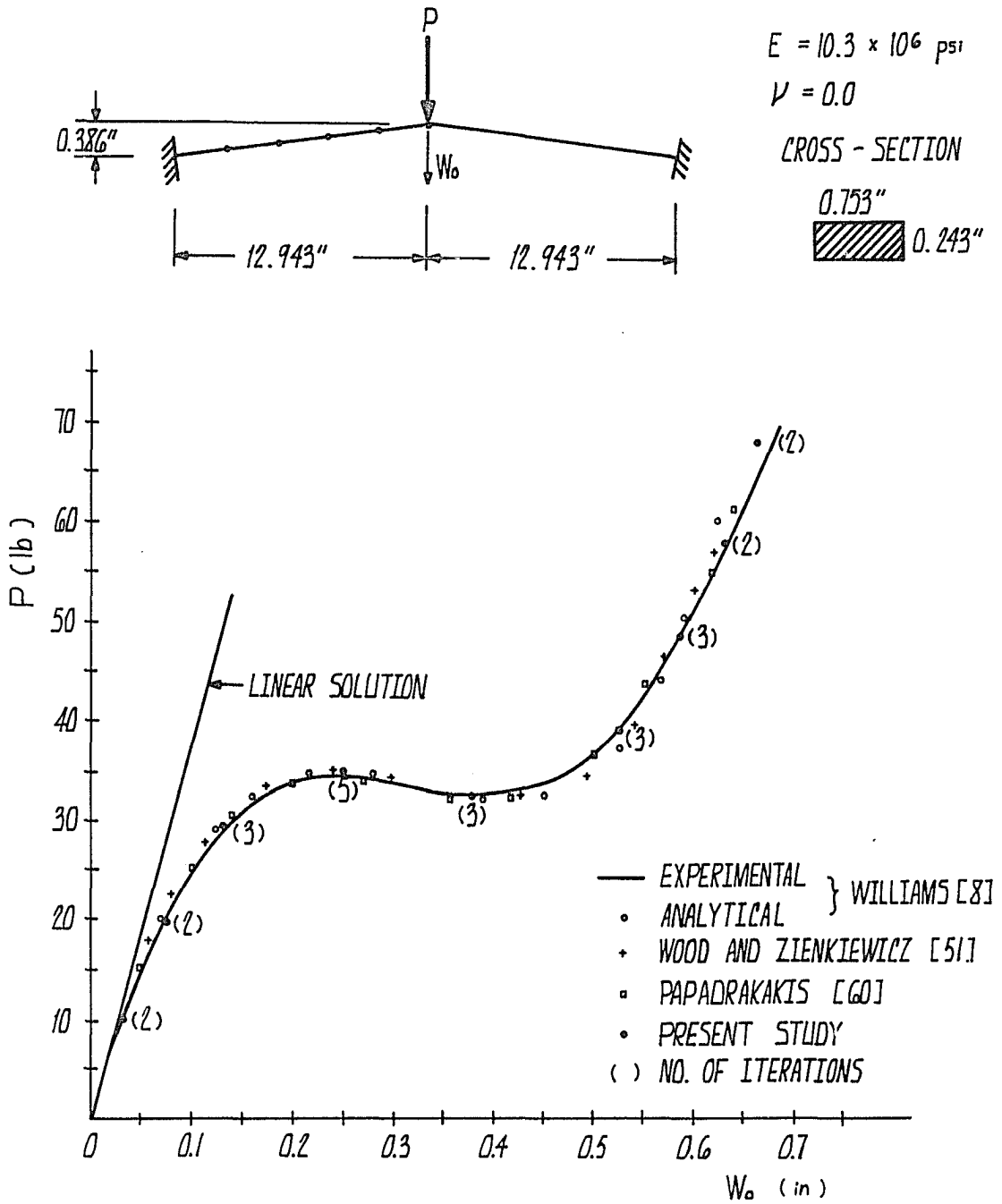


Figure 5.2. Load-deflection curve of Williams' toggle frame

(4) A Deep Arch

A two-hinged deep arch whose geometry and loading conditions are shown in Figure 5.4 was analyzed. This problem had been solved by Huddleston (20) and DaDeppo and Schmidt (27) analytically and by Wood and Ziemkiewicz (51) using paralinear isoparametric elements. It is known that the lowest buckling load occurs in an asymmetric mode characterized by a bifurcation in the load-deflection curve.

First, the symmetric deformations were investigated by analyzing half of the arch with six beam elements. The symmetric buckling load of 15.86 $EI/R^2$ compares well with the value of the 15.23 $EI/R^2$ obtained by Huddleston (20).

The asymmetric buckling is usually initiated by introducing a small perturbation on either geometry or loads. Here, to the half of the arch the following perturbation on the radius is applied:

$$R = R_o + \frac{t}{1000} \sin\left(\frac{\pi r}{\theta}\right) \tag{5.1}$$

where the variables are the same as defined in Figure 5.4. Therefore, the maximum radius is greater than the original radius by only 1/1000 times the thickness. The asymmetric buckling load of 13.36 $EI/R^2$ is close to 13.0 $EI/R^2$ obtained by Huddleston (20) and DaDeppo and Schmidt (27).

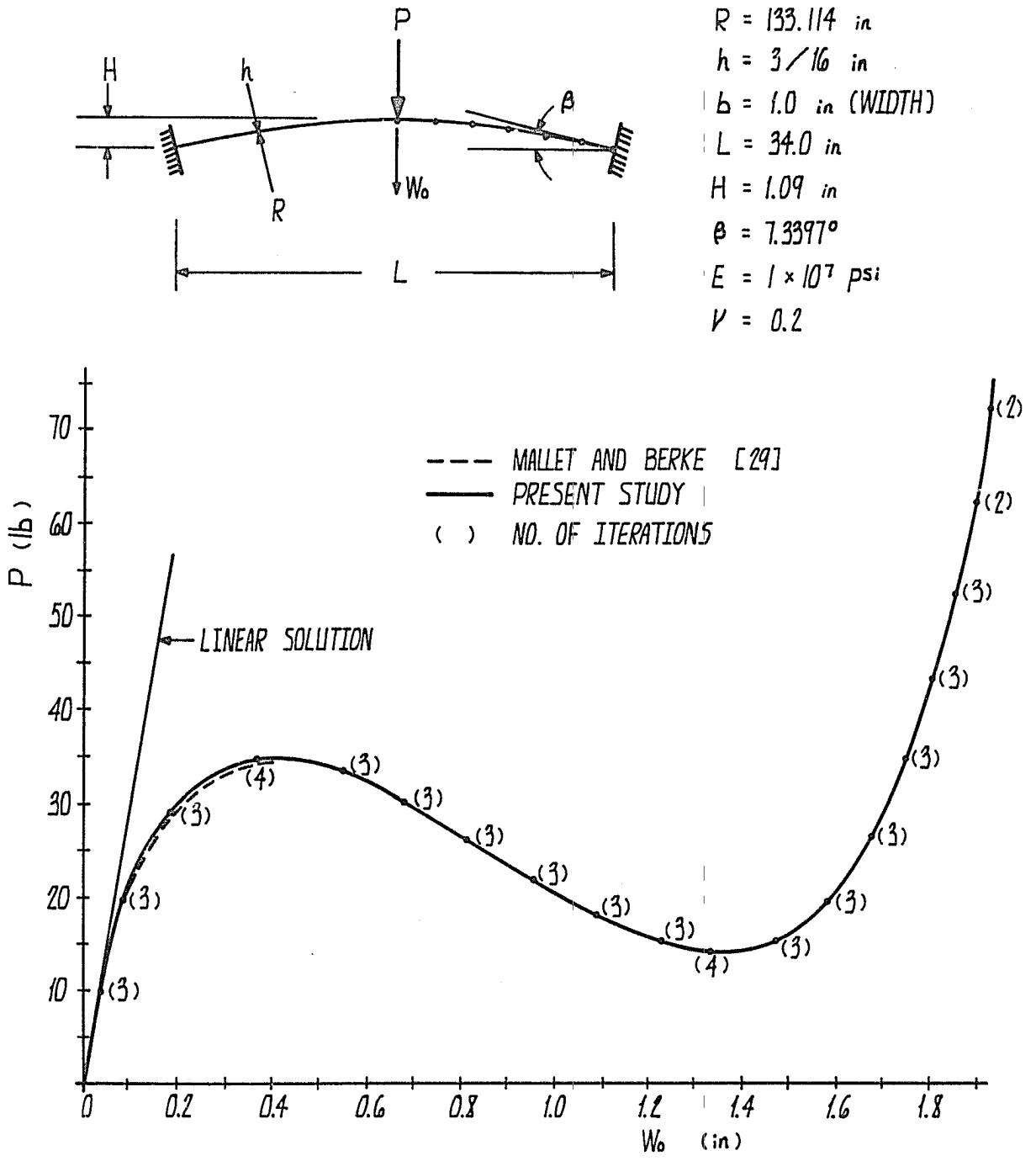


Figure 5.3. Load-deflection curve of shallow arch under a concentrated load

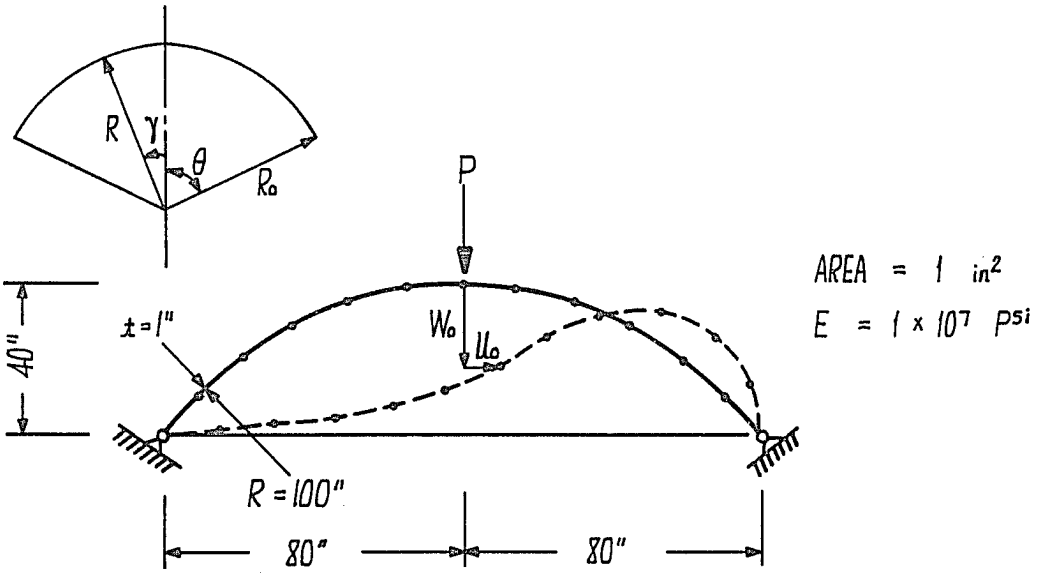


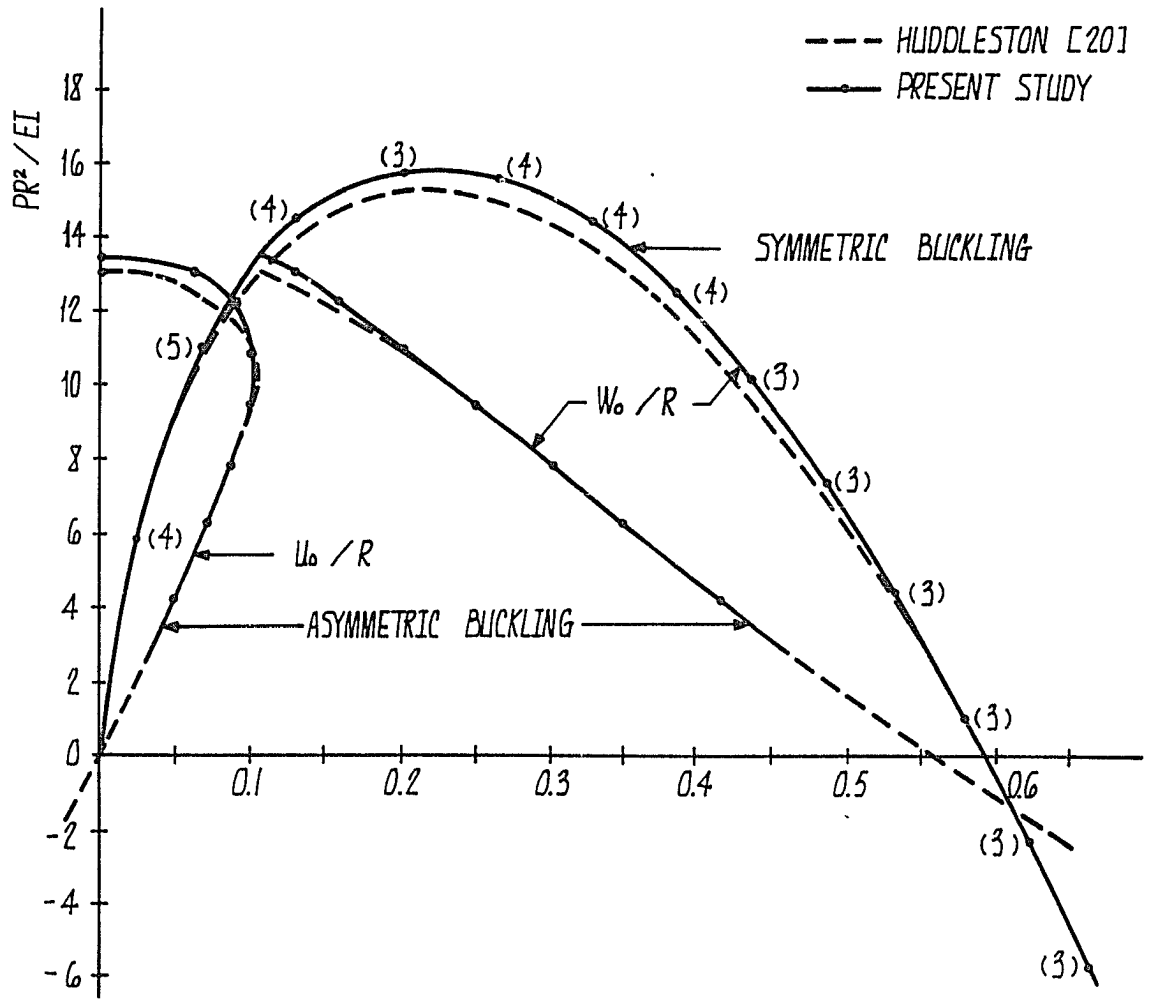


Figure 5.4. Load-deflection curve of a two-hinged deep arch under a concentrated load

(5) A Two-Member Frame

A large deflection analysis of a two-member frame as shown in Figure 5.5 has been performed analytically by Lee et al (55). The postbuckling path is characterized by its snap-back phenomenon. In this study, two trials with different initial load increments were made. The increment steps and the number of iterations taken for each step are shown for both cases in Figure 5.5. It is observed that to pass the vertical limit points a large number of iterations are needed.

The buckling load of 19.4 $EI/L^2$ compares well with 18.55 $EI/L^2$ obtained by Lee (55). The deflected shapes corresponding to five different equilibrium configurations are shown in Figure 5.6.

(6) A 12-Member Space Frame

Half of the structure is modeled to analyze the 12-member space frame shown in Figure 5.7. Four beam elements are employed for each member. The central load-deflection curve constructed from 30 load increment steps is shown with the finite element solution by Papadrakakis (60) in Figure 5.7.

The buckling load 60.7 pounds is identical to that of the analytical solution by Chu et al and compared well with the experimental value of 56.5 pounds obtained by Griggs (28).

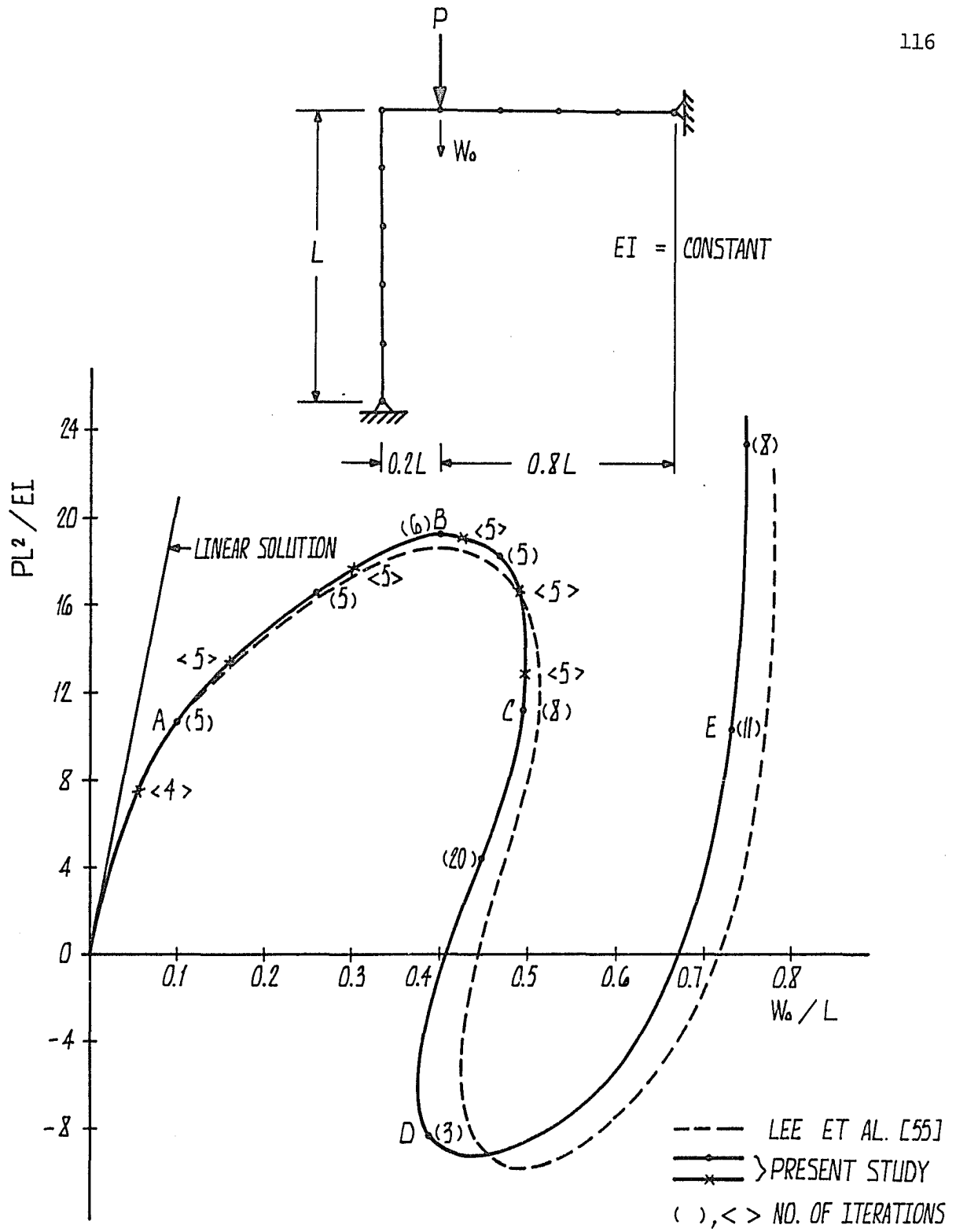


Figure 5.5. Load-deflection curve of a 2-member frame

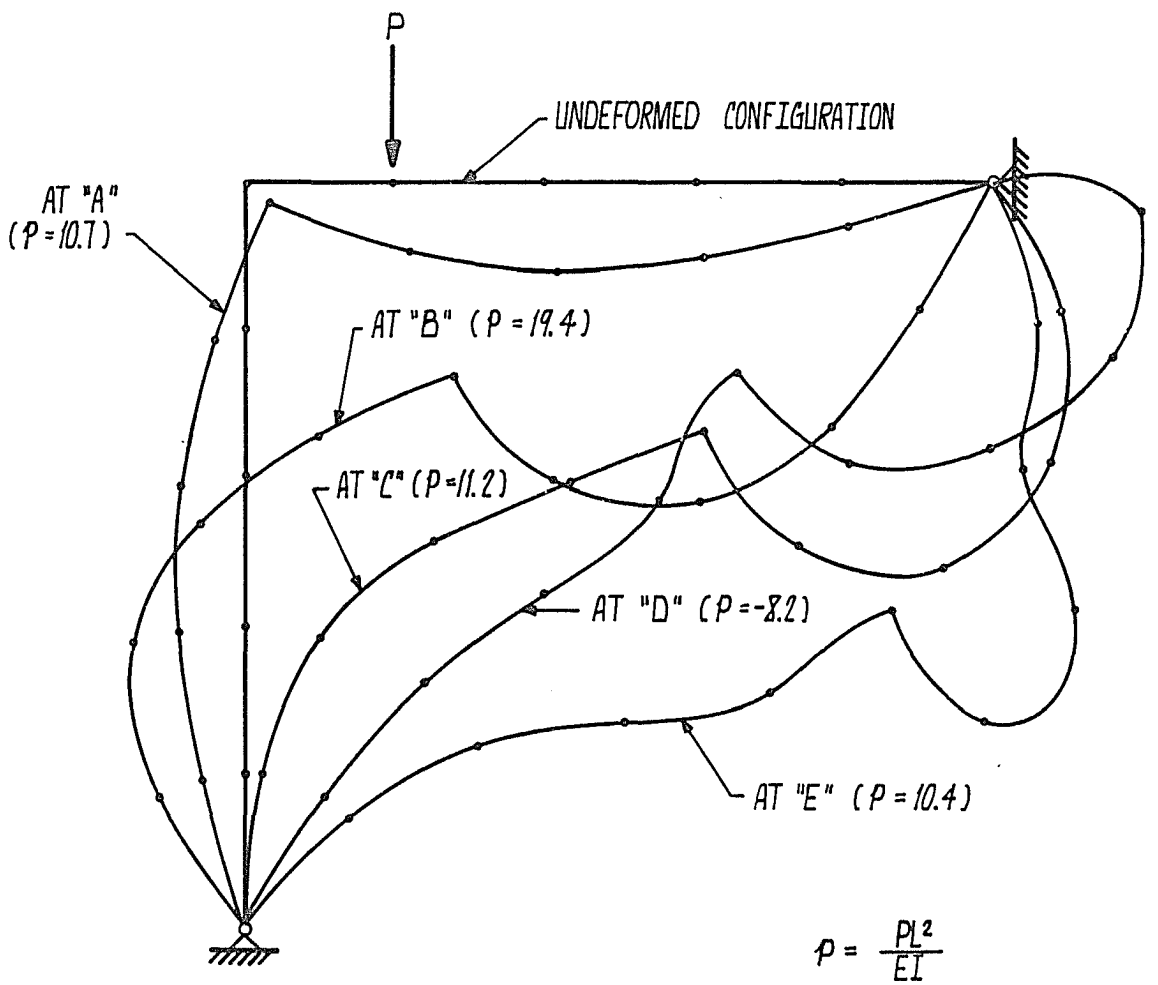


Figure 5.6. Deflected shapes of a 2-member frame

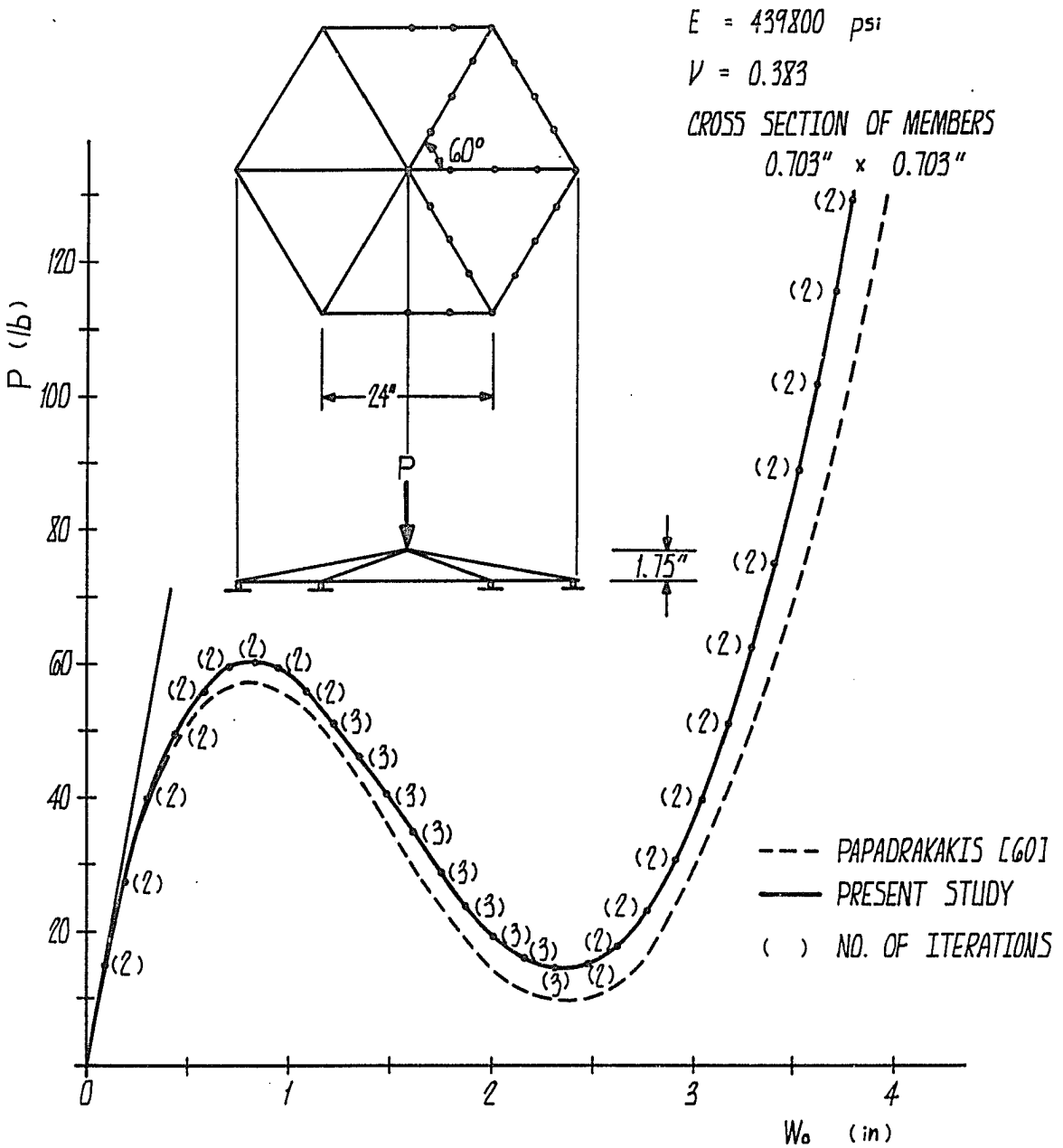


Figure 5.7. Load-deflection curve of a 12-member frame under a concentrated load

# CHAPTER 6

# CONCLUSION

An updated Lagrangian finite element formulation for the analysis of large deformation problem of three-dimensional elastic frame structures has been developed in this study by employing conventional two node-twelve degree of freedom beam elements. In order to trace out the postbuckling path, a modified constant-arc-length method has been proposed. The accuracy of the formulation and the effectiveness of the non-linear solution algorithm have been demonstrated in application to selected two- and three-dimensional structural examples. The numerical experiments have shown that by using the solution scheme the limit points and befurcation points of the equilibrium path can be passed. However, to make the solution scheme more reliable, additional research should be done for improvements in tracing the bifurcation type buckling path and in passing the vertical limit points without an excessively large number of iterations. The efficiency of the solution algorithm may be increased by using it with other nonlinear solution procedures such as an accelerated modified Newton-Raphson method or a quasi-Newton method.

Software has been designed to make it possible to solve large-scale problems on a minicomputer by adopting the hyper-matrix scheme and the segmentation of the code into a number of processors which are independent programs. A study of the

performance of the software using a combined minicomputer/ array processor system has shown that large-scale problems can be practically solved by using the system. Also it has been observed that in order to further reduce the execution time on the system, improvements on solution algorithms, task distribution, and the optimization of input/output transfer speeds are very important.

With the use of the hypermatrix scheme, an alternative solution algorithm for the system of linear equations has been proposed. It is believed that for most of finite element structural problems the algorithm can reduce the time needed by the conventional algorithm to nearly half on a minicomputer. However, to achieve the similar improvement with an array processor we should develop additional array processor software for some special arithmetic operations needed for the alternative solution procedure.

Extensions of this study should include the implementation of structural element of various cross-sectional types, the consideration of material nonlinearity, and the introduction of non-proportional and dynamic loadings. Further extension of the study includes the implementation of other types of finite elements and may lead to the completion of a general purpose nonlinear structural analysis program.

## REFERENCES


1. Stricklin, J. A. and Haiser, W. E., "Formulations and Solution Procedures for Nonlinear Structural Analysis," Computers & Structures, 7, 1977, pp. 125-136.

2. Mondkar, D. P. and Powell, G. H., "Finite Element Analysis of Nonlinear Static and Dynamic Response," Int. J. for Num. Meth. in Eng., 11, 1977, pp. 499-520.

3. Cescotto, S., Frey, F. and Fonder G., "Total and Updated Lagrangian Descriptions in Nonlinear Structural Analysis: A Unified Approach," Energy Methods in Finite Element Analysis, (eds) R. Glowinski et al., John Wiley & Sons, 1979, pp. 283-296.

4. Mitchell, A. R. and Wait, R., The Finite Element Method in Partial Differential Equations, John Wiley & Sons, 1977.

5. Patterson, C., "Finite-element Analysis of Large Displacement and Stability Problems: An Introduction", Stability Problems in Engineering Structures and Computers, (eds) T.H. Richards & P. Stanley, Applied Science Publishers Ltd: London, 1979, pp. 101-114.

6. Crisfield, M.A., "Finite Element Analysis for Combined Material and Geometric Nonlinearities", Nonlinear Finite Element Analysis in Structural Mechanics, (eds) Wunderlich et al, Springer-Verlag, 1981, pp. 325-338.

7. Holden, J. T., "On the Finite Deflections of Thin Beams," International Journal of Solids and Structures, 1972, pp. 1051-1055.

8. Williams, F. W., "An Approach to the Nonlinear Behavior of the Members of a Rigid Jointed Plane Framework with Finite Deflections", Quarterly Journal of Mechanics and Applied Mathematics, 17, 1964, pp. 451-469.

9. Almroth, B.O., Stern, P. and Brogan, F.A., "Future Trends in Nonlinear Structural Analysis", Computors & Structures, 10, 1979, pp. 369-374.

10. Crisfield, M.A., "A Fast Incremental/Iterative Solution Procedure that Handles "Snap-Through"," Computers & Structures, 13, 1981, pp. 55-62.

11. Geradin M., Idelsohn, S. and Hogge, M., "Computational Strategies for the Solution of Large Nonlinear Problems via Quasi-Newton Methods," Computers & Structures, 13, 1981, pp. 73-81.

12. Kamat, M. P., Watson, L. T. and Vanden Brink, D. J., "An Assessment of Quasi-Newton Sparce Update Techniques for Nonlinear Structural Analysis," Computer Methods in Applied Mechanics & Engineering, 26-3, 1981, pp. 363-375.

13. Matthies, H. and Strang G., "The Solution of Nonlinear Finite Element Equations," Int. J. for Num. Meth. in Eng., 14, 1979, pp. 1613-1626.

14. Crisfield, M. A., "A Faster Modified Newton-Raphson Iteration," Computer Methods in Applied Mechanics and Engineering, 20, 1979, pp. 267-278.

15. Bergan, P. G., Horrigmore, G., Krakeland, B. and Soreide, T. H., "Solution Techniques for Nonlinear Finite Element Problems," Int. J. for Num. Meth. in Eng., 12, 1978, pp. 1677-1696.

16. Bergan, P. G., "Solution Algorithms for Nonlinear Structural Problems," Computers & Structures 12, 1980, pp. 497-509.

17. Bergan, P. G. and Soreide, T. H., "Solution of Large Displacement and Instability Problems Using the Current Stiffness Parameter," International Conference on Finite Elements in Nonlinear Solid and Structural Mechanics, Trandheim: Tapir, 1978, pp. 647-669.

18. Row, D. G., Powell, G. H. and Mondkar, D. P., "Solution of Progressively Changing Equilibrium Equations for Nonlinear Structures," Computers & Structures, 7, 1977, pp. 659-665.

19. Powell, G. and Simons, J., "Improved Iteration Strategy for Nonlinear Structures," Int. J. for Num. Meth. in Eng., 17, 1981, pp. 1455-1467.

20. Huddleston, J. V., "Finite Deflections and Snap-Through of High Circular Arches," Journal of Applied Mechanics, 1968, pp. 763-769.

21. Irons, B. and Elsawaf, A.F., "The Conjugate Newton Algorithms for Solving Finite Element Equations," Formulations and Computational Algorithms in Finite Element Analysis, (eds) K. J. Bathe, J. T. Oden and W. Wunderlich, 1977, pp. 655-672.

22. Wellford Jr., L. C. and Vahdani, B., "A Block Iteration Scheme for the Solution of Systems of Equations Resulting from Linear and Nonlinear Finite Element Models," Computer Methods in Applied Mechanics and Engineering, 26, 1981, pp. 33-52.

23. Taylor, R. L., Wilson, E. L. and Sackett, S. J., "Direct Solution of Equations by Frontal and Variable Band, Active Column Methods," Nonlinear Finite Element Analysis in Structural Mechanics, (eds) Wunderlich, Stein and Bathe, Springer-Verlag, 1981, pp. 521-552.

24. Nayak, G. C. and Zienkiewicz, O. C., "Note on the 'Alpha'-Constant Stiffness Method for the Analysis of Non-linear Problems," Int. J. for Num. Mech. in Eng., 4, 1972, pp. 579-582.

25. Riks, E., "An Incremental Approach to the Solution of Snapping and Buckling Problems," International Journal of Solids and Structures, 15, 1979, pp. 529-551.

26. Bathe, K. J. and Cimento, A.P., "Some Practical Procedures for the Solution of Nonlinear Finite Element Equations," Computer Methods in Applied Mechanics and Engineering, 22, 1980, pp. 59-85.

27. DaDeppo, D. A. and Schmidt, R., "Sidesway Buckling of Deep Circular Arches Under a Concentrated Load," Journal of Applied Mechanics, 1969, pp. 325-327.

28. Griggs, H. P., "Experimental Study of Instability in Elements of Shallow Space Frames," Res. Rep., Dept. of Civil Engineering, MIT, Cambridge, Mass., September 1966.

29. Mallet, R. H. and Berke, L., "Automated Method for the Large Deflection and Instability Analysis of Three-Dimensional Truss and Frame Assemblies," AFFDL-TR-66-102, 1966.

30. Argyris, J. H. and Dunne, P. C., "Nonlinear and Post-buckling Analysis of Structures," Formulations and Computational Algorithms in Finite Element Analysis, (eds) K. J. Bathe, J. T. Oden and W. Wunderlich, MIT Press, 1977, pp. 525-571.

31. Wellford Jr., L. C. and Dib, G. M., "Post-Buckling Behavior of Structures Using a Finite Element-Nonlinear Eigenvalue Technique," Int. J. for Num. Meth. in Eng., 15, 1980, pp. 955-980.

32. Holzer, S. M., "Static and Dynamic Stability of Reticulated Shells," International Colloquium on Stability of Structures under Static and Dynamic Loads, Washington, D.C., 1977, pp. 27-39.

33. Koiter, W. T., "Elastic Stability and Post-Buckling Behavior," Nonlinear Problems, (ed) R. E. Langer, University of Wisconsin Press, 1963, pp. 257-275.

34. Hutchinson, J. W. and Koiter, W. T., "Postbuckling Theory," Applied Mechanics Reviews, 23, 1970, pp. 1353-1366.

35. Fuchs, G. von, Roy, J. R. and Schrem, E., "Hypermatrix Solution of Large Sets of Symmetric Positive-Definite Linear Equations," Computer Methods in Applied Mechanics and Engineering, 1, 1972, pp. 197-216.

36. Banovec, J., "An Efficient Finite Element Method for Elastic-Plastic Analysis of Plane Frames," Nonlinear Finite Element Analysis in Structural Mechanics, (eds) Wunderlich, Stein and Bathe, Springer-Verlag, 1981, pp. 385-402.

37. Bagchi, D. K., "Inelastic Bending of Beam Including Transverse Shear," Int. J. for Num. Meth. in Eng., 14, 1979, pp. 1323-1333.

38. Uzgider, E. A., "Inelastic Response of Space Frames to Dynamic Loads," Computers & Structures, 11, 1980, pp. 97-112.

39. Noor, A. K. and Peters J. M., "Bifurcation and Post-Buckling Analysis of Laminated Composite Plates via Reduced Basis Technique," Computer Methods in Applied Mechanics and Engineering, 29, 1981, pp. 271-295.

40. Mazzolani, F. M., Di Carlo, A. and Pignatro, M., "Post-Buckling Behavior of Multistory Steel Frames," International Colloquim on Stability of Structures under Static and Dynamic Loads, Washington, D. C., 1977, pp.194-211.

41. Gallagher, R. H., "Perturbation Procedures in Nonlinear Finite Element Structural Analysis," Computational Mechanics, Lecture Notes in Mathematics 461, (eds) J. T. Oden, Springer: New York, 1975, pp. 75-89.

42. Oleson, J. F. and Byskov, E., "Accurate Determination of Asymptotic Postbuckling Stress by the Finite Element Method," Computers & Structures, 15, 1982, pp. 157-163.

43. Haftka, R. T., Mallett, R. H. and Nachbar, W., "Adaption of Koiter's Method to Finite Element Analysis of Snap-Through Buckling Behavior," International Journal of Solids and Structures, 7, 1971, pp. 1427-1445.

44. Casciaro, R. and Aristodemo, M., "Perturbation Analysis of Geometrically Nonlinear Structures," Finite Elements in Nonlinear Mechanics, (eds) P. Bergan et al, Trondheim: Tapir, 1978, pp. 433-452.

45. Carnoy, E. G., "Asymptotic Study of the Elastic Post-buckling Behavior of Structures by the Finite Element Method," Computer Methods in Applied Mechanics and Engineering, 29, 1981, pp. 147-173.

46. Akay, H. U., Johnson, C. P. and Will, K. M., "Lateral and Local Buckling of Beams and Frames," Journal of the Structural Division, Proceedings of ASCE, 103, ST9, 1977, pp. 1821-1832.

47. Bathe, K. J. and Bolourchi, S., "Large Displacement Analysis of Three-Dimensional Beam Structures," Int. J. for Num. Meth. in Eng., 14, 1979, pp. 961-986.

48. Belytschko, T., Schwer, L. and Klein, M. J., "Large Displacement Transient Analysis of Space Frames," Int. J. for Num. Mech. in Eng., 11, 1977, pp. 65-84.

49. Chu, K. H. and Rampetsreiter, R. H., "Large Deflection Buckling of Space Frames," Journal of the Structural Division, Proceedings of ASCE, 98, ST12, 1972, pp. 2701-2722.

50. Remseth, S. N., "Nonlinear Static and Dynamic Analysis of Framed Structures," Computers & Structures, 10,1979, pp. 879-897.

51. Wood, R. D. and Zienkiewicz, O. C., "Geometrically Nonlinear Finite Element Analysis of Beams, Frames, Arches and Axisymmetric Shells," Computers & Structures, 7, 1977, pp. 725-735.

52. Karamanlidis, D., Honecker, A. and Knothe, K., "Large Deflection Finite Element Analysis of Pre- and Postcritical Response of Thin Elastic Frames," Nonlinear Finite Element Analysis in Structural Mechanics, (eds) Wunderlich, Stein and Bathe, Springer-Verlag, 1981, pp. 217-235.

53. Bagci, C., "Elastic Stability and Buckling Loads of Multi-Span Nonuniform Beams, Shafts and Frames on Rigid or Elastic Supports by Finite Element Method Using Planar Uniform Line Elements," Computers & Structures, 12, 1980, pp. 233-243.

54. Connor Jr., J. J., Logcher, R. D. and Chan, S. C., "Nonlinear Analysis of Elastic Framed Structures," Journal of the Structural Division, Proceedings of ASCE, 94, ST6, 1968, pp. 1525-1547.

55. Lee, S. L., Manuel, F. S. and Rossaw, E. C., "Large Deflections and Stability of Elastic Frames," Journal of the Engineering Mechanics Division, Proceedings of ASCE, 94, EM 2, 1968, pp. 521-547.

56. Noor, A. K., "Survey of Computer Programs for Solution of Nonlinear Structural and Solid Mechanics Problems," Computers & Structures, 13, 1981, pp. 425-465.

57. Zhang, L. and Owen, D. R. J., "A Modified Secant Newton Method for Nonlinear Problems," Computers & Structures, 15, 1982, pp. 543-547.

58. Park, K. C., "A Family of Solution Algorithms for Nonlinear Structural Analysis Based on Relaxation Equations," Int. J. for Num. Method in Eng., 18, 1982, pp. 1337-1347.

59. Padovan, J. and Tovichakchaikul, S., "Self-Adaptive Predictor-Corrector Algorithm for Static Nonlinear Structural Analysis," Computers & Structures, 15, 1982, pp. 365-377.

60. Papadrakakis, M., "Post-Buckling Analysis of Spatial Structures by Vector Iteration Methods," Computers & Structures, 14, No. 5-6, 1981, pp. 393-402.

61. Bergan, P. G., "Solution by Iteration in Displacement and Load Spaces," Nonlinear Finite Element Analysis in Structural Mechanics, (eds) Wunderlich, Stein and Bathe, Springer-Verlag, 1981, pp. 553-571.

62. Ramm, E., "Strategies for Tracing the Nonlinear Response Near Limit Points," Nonlinear Finite Element Analysis in Structural Mechanics, (eds) Wunderlich, Stein and Bathe, Springer-Verlag, 1981, pp. 63-89.

63. Nour-Omid, B., Parlett, B. N. and Taylor, L. R., "A Newton-Lanczos Method for Solution of Nonlinear Finite Element Equations," Computers & Structures, 16, 1983, pp. 241-252.

64. Argyris, J. H., Boni, B., Hindenlang, U. and Kleiber, M., "Finite Element Analysis of Two-and Three-Dimensional Elasto-Plastic Frames--The Natural Approach," Computer Methods in Applied Mechanics and Engineering, 35, 1982, pp. 221-248.

65. Qashu, R. K., "Finite Deformation and Stability of non-rectangular Elastic Rigid Frame Structures," Doctoral Dissertation, University of Arizona, 1980.

66. Switzky, H. and Wang, P. C., "Design and Analysis of Frames for Stability," Journal of the Structural Division, Proceedings of ASCE, 95, ST 4, 1969, pp. 695-713.

67. Bathe, K. J., Ramm, E. and Wilson, E. L., "Finite Element Formulations for Large Deformation Dynamic Analysis," Int. J. for Num. Mech. in Eng., 9, 1975, pp. 353-386.

68. Oran, C. and Kassimali, A., "Large Deformations of Framed Structures under Static and Dynamic Loads," Computers & Structures, 6, 1976, pp. 539-547.

69. Fung, Y. C., Foundation of Solid Mechanics, Prentice-Hall: Englewood Cliffs, N. J., 1965.

70. Atkinson, K. E., An Introduction to Numerical Analysis, John Wiley & Sons, 1978.

71. Zienkiewicz, O. C., The Finite Element Method in Engineering Science, 3 rd ed., McGraw-Hill: London, 1977.

72. Lovelock, D. and Rund H., Tensors, Differential Forms, & Variational Principles, John Wiley & Sons, 1975.

73. Gallagher, R. H., Finite Element Analysis Fundamentals, Prentice-Hall: Englewood Cliffs, N. J., 1975.

74. Cook, R. D., Concepts and Applications of Finite Element Analysis, John Wiley & Sons, 1974.

75. Batoz, J. L. and Dhatt, G., "Incremental Displacement Algorithms for Nonlinear Problems," Int. J. for Num. Meth. in Eng., 11, 1977, pp. 1262-1267.

76. Shariffi, P. and Popov, E. P., "Nonlinear Buckling Analysis of Sandwich Arches," Journal of the Engineering Mechanics Division, Proceedings of ASCE, 97, 1971, pp. 1397-1412.

77. Bathe, K. J. and Wilson, E. L., Numerical Methods in Finite Element Analysis, Prentice-Hall: Englewood Cliffs, N. J., 1976.

78. Kamel, H. A. and McCabe, M. W., GIFTS 5 Theoretical Manual, University of Arizona, 1979.

79. Sarigul, N., Jin, M., Kolar, R. and Kamel, H. A., "Design of Array Processor Software for Nonlinear Structural Analysis," presented at the ASME Winter Annual Meeting, Boston, November 13-18, 1983.

80. Bergan, P. G. and Clough, R. W., "Convergence Criteria for Iterative Processes," AIAA Journal, 10, 1972, pp. 1107-1108.

81. Kamel, H. A. and Maitan, J., "Performance of Finite Element Algorithms on an Array Processor-Minicomputer Based System," Nonlinear Finite Element Analysis in Structural Mechanics, (eds) Wunderlich, Stein and Bathe, Springer-Verlag, 1981, pp. 742-757.

82. Sarigul, N., Maitan, J. and Kamel, H.A., "Solution of Nonlinear Structural Problems Using Array Processor," Computer Methods in Applied Mechanics and Engineering, 34, 1982, pp. 939-954.

83. Swanson, J. A., Cameron, G. R. and Hoberland, J. C., "Adapting the ANSYS Finite Element Analysis Program to an Attached Processor," Computer, June 1983, pp. 85-91.

84. Strohkorb, G. A. and Noor, A. K., "Potential of Mini-computer/Array Processor System for Nonlinear Finite Element Analysis," NASA T.M. 84566, 1983.

85. Kamel, H. A. and McCabe, M. W., "Direct Numerical Solution of Large Sets of Simultaneous Equations," ONR Technical Report No. 3, University of Arizona, 1978.

86. Reference Manual FORTRAN-77+, Release 3.0, Systems Engineering Laboratories, Inc., October 1981.

87. Key, J. E., "Computer Program for Solution of Large, Sparse, Unsymmetric Systems of Linear Equations," Int. J. for Num. Meth. in Eng., 6, 1973, pp. 497-509.

88. Calahan, D. A., "A Vectorized General Sparsity Solver," Systems Engineering Laboratory Report No. 168, The University of Michigan, 1982.

89. Calahan, D. A., Buning, P. G. and Joy, W. N., "Vectorized General Sparsity Algorithms with Backing Store," Systems Engineering Laboratory Report No. 96, The University of Michigan, 1977.

90. Evans, D. J., "New Parallel Algorithms in Numerical Algebra," E.D.F. Bulletin de la Direction des Etudes et Recherches, Série C., Mathématiques, Informatique, n° 1, 1983, pp. 61-70.

91. Gentzsch, W., "How to Maintain the Efficiency of Highly Serial Algorithms Involving Recursions on Vector Computers," E.D.F. Bulletin de la Direction des Etudes et Recherches, Série C, Mathématiques, Informatique, n° 1, 1983, pp. 79-86.

92. Verprat, M. and Thomas, J. M., "Implementation of Some Algorithms and Their Performances on a Vector Computer," E.D.F. Bulletin de la Direction des Etudes et Recherches, Série C, Mathématiques, Informatique, n° 1, 1983, pp. 163-166.